Foaming Behavior of Aqueous Solutions of a Zwitterionic Surfactant in the Presence of Salts: Analysis of Specific Ion Effect and Synergism

A thesis submitted in

partial fulfillment of the requirement for the degree of

DOCTOR OF PHILOSOPHY

by

Shailesh Ravi Varade

Department of Chemical Engineering

Indian Institute of Technology Guwahati

Guwahati – 781039, Assam, India

July 2020

Foaming Behavior of Aqueous Solutions of a Zwitterionic Surfactant in the Presence of Salts: Analysis of Specific Ion Effect and Synergism

A thesis submitted in

partial fulfillment of the requirement for the degree of

DOCTOR OF PHILOSOPHY

by

Shailesh Ravi Varade

Department of Chemical Engineering

Indian Institute of Technology Guwahati

Guwahati – 781039, Assam, India

July 2020

To my parents and friends

Indian Institute of Technology Guwahati

Department of Chemical Engineering

STATEMENT

I, hereby declare that the content embodied in this thesis entitled **"Foaming Behavior of Aqueous Solutions of a Zwitterionic Surfactant in the Presence of Salts: Analysis of Specific Ion Effect and Synergism"** is the result of investigations carried out by me at the Department of Chemical Engineering, Indian Institute of Technology Guwahati, Guwahati, India, under the supervision of **Prof. Pallab Ghosh**.

In keeping with the general practice of reporting scientific observations, due acknowledgments have been made wherever the work described is based on the findings of other investigators.

Guwahati,
July 2020

Shailesh Ravi Varade

Indian Institute of Technology Guwahati

Department of Chemical Engineering

CERTIFICATE

It is certified that the work described in this thesis entitled **"Foaming Behavior of Aqueous Solutions of a Zwitterionic Surfactant in the Presence of Salts: Analysis of Specific Ion Effect and Synergism"** by Mr. Shailesh Ravi Varade for the award of degree of Doctor of Philosophy is an authentic record of the results obtained from research work carried out under my supervision at the Department of Chemical Engineering, Indian Institute of Technology Guwahati, Guwahati, India, and this work has not been submitted elsewhere for a degree.

Prof. Pallab Ghosh
Professor
Department of Chemical Engineering
IIT Guwahati, Guwahati – 781039
Assam, India

ACKNOWLEDGMENTS

I would like to thank several people who have contributed in some way to the work described in this thesis and supported me to complete my Ph.D.

First and foremost, I would like to express my sincere gratitude to my Ph.D. supervisor, **Prof. Pallab Ghosh**, for introducing me to work in such a fascinating area of research. I am grateful to my supervisor for his continuous guidance, scientific discussions, important bits of advice, and most importantly allowing me the freedom to work in my way. It was an honor to work under him.

I would also like to thank my Doctoral Committee members, **Dr. S Senthilmurugan** and **Dr. Partho Sarathi Gooh Pattader** from Department of Chemical Engineering and **Prof. K.S.R Krishna Murthy** from Department of Mechanical Engineering, for their valuable suggestions and constructive criticism during the project evaluations, which helped me to make necessary improvements in various stages of my research.

I would also like to thank **Prof. Dipankar Bandyopadhyay** and **Prof. Nanda Kishore**, for their research-oriented teaching during my coursework. I also thank **Prof. Bishnupada Mandal and Prof. Anugrah Singh**, Head, Department of Chemical Engineering, for their administrative support. Furthermore, I would like to thank other Faculty members of the Department of Chemical Engineering for their valuable support during my research.

I must thank to all the technical staffs of my department specially, **Mr. Ariful Hoque**, **Mrs. Ritumani Kalita**, **Mr. Harsaraj Biswanath**, **Mr. Deepak Barman**, **Mr.**

Pankaj Baruah, **Mr. Prasun Bhattacharjee**, **Mr. Debajit Borah**, **Dr. Kaustavmoni Deka**, **Dr. Lukumani Borah** and **Mr. Pankaj Kumar**.

I would like to thank my colleagues and friends at IIT Guwahati for helping me out on several occasions. I deeply acknowledge my research group members Dr. Meneka, Dr. Singdha, Dr. Badri, Sainath, Jinesh, Manas, Venu, Shashank, Ananya, Neha, Nipu, Awadh, Anurag, Sandeep, and Dr. Rima. I would also like to thank my friends Ms. Rajashree, Ms. Jayeeta, Ms. Urbashi, Ms. Lhingcy, Sohan Bir Singh, Pranav, Harshad, Venkatesh, Viswanath, Dr. Machhindra, Pravin, Abhik, Dr. Mohan, Dr. Kamal, Dr. Poddar, Pankaj, Pradeep, Dr. Debashish, and Dr. Rahul in who have made my stay pleasant in IIT Guwahati.

Saving the best for the last, I am forever indebted to my parents, **Mrs. Mahananda Varade** and **Mr. Ravi Varade,** who are the reason I have received a great education. They have been a source of love and encouragement for me, and without their emotional support, it would have been impossible to stay away from home all this time. Also, I would like to thank my sister, brother-in-law, and nephew for their love and support, which kept my morale high during my Ph. D.

Shailesh Ravi Varade

ABSTRACT

Ionic and nonionic surfactants have been widely used during the past few decades. However due to their wide applicability in high-value formulations, the use of zwitterionic surfactants has recently been increased. Zwitterionic surfactants have the unique property of bearing hydrophilic head-groups having both positive and negative charges. The presence of both the head-groups in its structure makes it an interesting molecule to investigate at the air–water interface. Aqueous foams are the dispersion of gas bubbles in water containing stabilizing surface-active species, such as surfactants and particles. Surfactants constitute the primary materials required in almost all the foaming processes. Foam can be formed using a surfactant solution by dispersing gas within an aqueous phase. Foaming plays a significant role in personal care products, enhanced oil recovery, mineral processing, processing of textiles, and firefighting. Although aqueous foams are frequently applied in daily life and several industrial processes, a general understanding of how to manipulate foam stabilities is often missing.

The presence of salts in the surfactant solution influence the foam stability in various ways. Salts in the surfactant solution can compress the electrical double layer associated with the adsorbed surfactant molecules on the two opposite sides of a foam lamella and can alter the foam stabilities. The magnitude of these changes depends on the nature and concentration of the added salts and can help to tune the foaming properties. Thus, a study on the effect of NaCl, $CaCl_2$ and $AlCl_3$ on the stability of foams generated from the aqueous solutions of the zwitterionic surfactant, N-Dodecyl-N,N-dimethyl-3-ammonio-1-propanesulfonate (DDAPS) using the blender test was performed. To

develop insight into the mechanisms of the adsorption of zwitterionic surfactants in absence and presence of salts, surface and interfacial tensions were measured. These tensions and the critical micelle concentration (CMC) decreased upon salt addition, signifying increased adsorption of the surfactant molecules at the interface. The quantity of salt required for reducing the surface tension and CMC was in the sequence: NaCl > $CaCl_2$ > $AlCl_3$. The salts had a remarkable effect on the foaming characteristics of these surfactants. The effectiveness of salts in reducing the foam stability followed the sequence: $AlCl_3$ > $CaCl_2$ > NaCl. The effect of oil (i.e. *n*-hexane) on foam stability was also investigated in the presence of these salts. The presence of oil decreased the foam volume and reduced its stability. The stability of foams in the presence of oil was explained by calculating the entering, bridging, and spreading coefficients.

Electrolyte solutions are ubiquitous and form a vital part of life. The specific nature of electrolytes makes them most suitable to control ionic strength of the solution. A general understanding of specific ion effects at interface is important in many fields of life science and for industrial applications e.g. the disposal of nuclear waste. Furthermore, a thin liquid film constitute a good model for studying interactions in colloidal systems. The specific interaction between electrolytes and surfactant are of significant importance with respect to foam film properties. The stability of foam is linked to the adsorption of ions at the air−water interface and the specific ion effect between the head-groups and ions. Therefore, the specific interactions between the salts (i.e., NaCl, LiCl, and CsCl) and surfactant and its effect on the foamability and foam stability were thus regarded within this thesis. The foams prepared from the aqueous solutions of a DDAPS in the presence of three monovalent salts (i.e. LiCl, NaCl, and CsCl) were characterised using the blender test. Adsorption studies performed showed that addition of salt to the DDAPS

solution increased the adsorption of surfactant at the interface and decreased the CMC. The efficiency of these salts in decreasing the surface and interfacial tension followed the order: CsCl > NaCl > LiCl. Similarly, the efficiency of these salts in decreasing the foam stability followed the above-mentioned order. The hydrated radii of the ions played a significant role in the foaming properties of the surfactant solutions. Furthermore, the zeta potential was also measured and the efficiency of the salts in making the zeta potential more negative followed the same order.

The industrial use of surfactants mostly involves a mixture of two or more surfactant species in order to obtain synergistic effects with respect to surface tension and foam stability studies. Thus, surface tension, foamability and stability of foam for the mixture of zwitterionic (i.e., DDAPS) and cationic [i.e., cetyltrimethylammonium bromide (CTAB)] surfactants at different concentration ratios and in the presence of salt (i.e., NaCl) were thus investigated. The synergism between the surfactants was examined by measuring the surface tension for various compositions of the surfactants and the salt. The interaction occurring between the surfactant molecules adsorbed at the air–water interface influenced the monolayer properties. The mixed surfactant system produced a significant decrease in surface tension as compared to the single surfactant systems. In the presence of salt, the surface tension reduction was larger. The interaction among the surfactant molecules at the air−water interface and the same in the mixed micelles was quantified by the respective interaction parameters. The blender test was used to investigate the foamability and foam stability. The foamability studies showed synergistic behavior inasmuch as higher foam volumes were generated in the mixed surfactant systems as compared to the single surfactant systems. The addition of salt had a remarkable effect on the foaming properties of the mixed surfactant systems. It increased

the stability of foams significantly. Furthermore, the synergism between the surfactant molecules had a notable influence on the zeta potential at the air–water interface.

CONTENTS

LIST OF FIGURES

LIST OF TABLES

NOMENCLATURE

a	distance of closest approach between two head-groups (m)
A	film surface area (m^2)
A_m	Area occupied by a surfactant molecule (m^2)
A_H	Hamaker constant (J)
c	concentration of salt in the solution (mol m^{-3})
c_0	initial bulk concentration of surfactant (mol m^{-3})
c_{12}	solution-phase concentrations of the pure surfactants 1 in the mixture (mol m^{-3})
c_1^0	solution-phase concentrations of the pure surfactants 1
$c_1^{0,CMC}$	concentration of surfactant 1 that is required to yield a surface tension equal to that of a mixture of the two surfactants at its CMC (mol m^{-3})
c_1^M	CMC of surfactant 1 (mol m^{-3})
c_{12}^M	concentration of surfactant 1 in the mixture at its CMC (mol m^{-3})
c_{21}	solution-phase concentrations of the pure surfactants 2 in the mixture (mol m^{-3})
c_2^0	solution-phase concentrations of the pure surfactants 2 (mol m^{-3})
$c_2^{0,CMC}$	concentration of surfactant 2 that is required to yield a surface tension equal to that of a mixture of the two surfactants at its CMC (mol m^{-3})
c_2^M	CMC of surfactant 2 (mol m^{-3})
c_{21}^M	concentration of surfactant 2 in the mixture at its CMC (mol m^{-3})
c_s	concentration of surfactant in the bulk solution (mol m^{-3})
C	London constant (J m^6)
C_1	concentration of surfactant 1 (mol m^{-3})
C_2	concentration of surfactant 2 (mol m^{-3})

d	droplet diameter (m)
D	diffusion coefficient of MNB ($m^2\ s^{-1}$)
D_s	diffusion coefficient of surfactant ($m^2\ s^{-1}$)
e	electronic charge (C)
E	entering coefficient ($N\ m^{-1}$)
E_G	Gibbs elasticity ($N\ m^{-1}$)
F	force (N)
F_d	force of detachment (N)
G	Gibbs free energy (J)
ΔG_{mix}	free energy change upon mixing of the two surfactants (J)
h	thickness of foam film (m)
I	ionic strength of the medium ($mol\ m^{-3}$)
k_B	Boltzmann constant ($J\ K^{-1}$)
k_1, k_2	decay coefficients
K_L	equilibrium constant in the Langmuir adsorption equation ($m^3\ mol^{-1}$)
L	length of surfactant tail (m)
L_w	wetted perimeter of the Wilhelmy plate (m)
N_A	Avogadro's number
P_{atm}	atmospheric pressure (Pa)
P_B	intrinsic pressure in the bulk phase (Pa)
P_{in}	Pressure inside the bubble (Pa)
P_{out}	Pressure outside the bubble (Pa)
P_N	pressure in the film normal to the plane-parallel film surfaces (Pa)
r	distance between two adjacent head-groups (m)
r_w	radius of wire (m)
R_r	radius of the ring (m)

R_1 and R_2	principal radii of curvature (m)
R	gas constant (J mol^{-1} K^{-1})
S	spreading coefficients (N m^{-1})
t	time (s)
T	Temperature (K)
U	electrophoretic mobility (m^2 V^{-1} s^{-1})
V, V_1, V_2	foam volume (cm^3)
V_l	volume of the aqueous solution (cm^3)
V_f	volume of the foam (cm^3)
x_1	mole fraction of surfactant 1 in the mixed monolayer
x_2	mole fraction of surfactant 2 in the mixed monolayer
x_1^{M}	mole fraction of surfactant 1 in the micelle
z, z_1 and z_2	valence of ion

Greek symbols

β	interaction parameter
β^{σ}	interaction parameter that measures the nature and extent of interactions between the two different surfactant molecules in the mixed monolayer
β^{M}	interaction parameter that measures the nature and extent of interactions between the two different surfactant molecules in the mixed micelle
γ	surface tension (mN m^{-1})
γ_{Expt}	experimentally measured value of surface (or interfacial) tension (N m^{-1})
γ_0	surface tension of pure water (N m^{-1})
$\gamma_{A/O}$	interfacial tension between air and oil (N m^{-1})
$\gamma_{A/W}$	interfacial tension between air and the aqueous phase (N m^{-1})
γ_{CMC}	surface tension at the CMC (N m^{-1})
$\gamma_{O/W}$	interfacial tension between oil and the aqueous phase (N m^{-1})

δ	distance between two spherical surfactant head-groups (m)
Γ	surface excess concentration of surfactant (mol m^{-2})
Γ_∞	maximum surface excess concentration in Langmuir adsorption equation (mol m^{-2})
ΔP	excess pressure inside a spherical bubble (Pa)
ε	dielectric constant of the aqueous phase
ε_0	permittivity of free space (C^2 J^{-1} m^{-1})
ζ	zeta potential (V)
θ	θ is the contact angle (degrees)
κ	Debye–Hückel parameter (m^{-1})
μ	viscosity (Pa s)
$\Delta\rho$	density difference between the two fluids (kg m^{-3})
Π	disjoining pressure (Pa)
Π_{vdW}	disjoining pressure due to van der Waals force (Pa)
Π_{EDL}	disjoining pressure due to electrostatic double layer force (Pa)
σ	charge density at air–water interface (C m^{-2})
τ	dummy variable in Equation (1.3) (s)
ϕ	liquid volume fraction in foam
ϕ_A	interaction energy between the parallel hydrophobic chains (J)
ϕ_R	interaction energy between the surfactant head-groups (J)
ψ_0	potential at air–water interface (V)

Abbreviations

ASTM	American Society for Testing and Materials
CBF	common black film
CMC	critical micelle concentration
CTAB	cetyltrimethylammonium bromide
DDAPS	N-dodecyl-N,N-dimethyl-3-ammonio-1-propanesulfonate
DLS	dynamic light scattering
DLVO	Derjaguin–Landau–Verwey–Overbeek
DSB	dodecyl sulfobetaine

EDL	electrical double layer
EPS	exopolysaccharide
IEP	isoelectric point
MNB	Micronanobubble
NBF	Newton black film
NDB	N-dodecyl betaine
NMR	Nuclear Magnetic Resonance
vdW	van der Waals

CHAPTER 1

INTRODUCTION

1.1 General Overview

Colloidal matters and interface science have always been mystical subjects to the scientific community, and they have garnered immense attention since the beginning of scientific research.[1–3] The term *interface* signifies the boundary between two immiscible phases.[4] Interface science deals with the characteristic behavior of the elements on the interface as well as those in the bulk. When one of the phases is a gas, the boundary is termed as *surface*. The physicochemical properties of the interface differ from those of the bulk, which makes them important.[5] Research performed on fluid–fluid and fluid–solid interfaces has helped us to formulate emulsions, dispersions, and foaming and wetting agents, which are used in our daily activities. Therefore, it has made a huge impact on our life.[6] The special properties observed at the interface are primarily due to the atoms and molecules, which experience an asymmetrical environment.[7] The thermodynamic and kinetic properties of the interface differ from their counterparts in the bulk phase due to the different geometrical arrangements and molecular motions.[8,9] Thus, molecular level understanding of the phenomena occurring at the interface is of prime importance.

1.2 Surface active agents

Surface active agents or *surfactants* are a class of materials, which influence the interfacial properties of a system.[10,11] Surfactants exhibit the unique property of adsorption at the interfaces, and hence alter their free energy by a marked degree. They typically act as a building block for a number of assemblies when proper concentration, pH, polarity of the medium, temperature, and the presence of electrolyte are maintained. They are used extensively in various industries manufacturing varied range of products such as food, motor oil, detergent, drilling mud, agricultural spray, coating, catalyst, and

flotation agent. Surfactants also find extensive use in bio-applications such as skin care, bio-lubrication, ophthalmology, and pharmaceuticals.[12–22] During the last decade, surfactants have been used in electronic printing, magnetic recording, and microelectronics.[23–28]

Surfactant molecules are also termed as *amphiphilic* or *amphipathic* based on their unique structure. The molecular structure of a surfactant has two distinct parts. One part has a strong affinity towards the solvent. It is termed as the *lyophilic* group (also known as *head-group*). The other part has very negligible or no attraction towards the solvent. It is termed as the *lyophobic* group (also known as *tail-group)*. When the solvent is water, these groups are termed as *hydrophilic* and *hydrophobic*, respectively. The typical size of a typical amphoteric surfactant monomer is ~1–1.5 nm. The diameter of surfactant head-group lies between 0.1–0.5 nm whereas the hydrophobic tail group lies between 0.7–1.0 nm.[29] The hydrophilic moiety in a surfactant may involve carboxylate, sulfate, sulfonate, quaternary ammonium, hydroxyl, and polyoxyethylene group(s). On the other hand, the hydrophobic moiety of a surfactant usually consists of one or more long hydrocarbon chains, sometimes consisting of fluorocarbon or siloxane as well. Figure 1.1 shows the structure of a typical surfactant molecule.

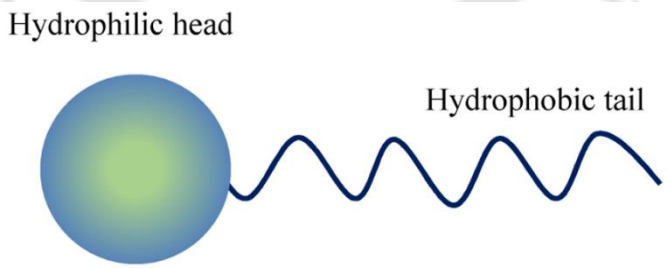

Figure 1.1. Schematic representation of a typical surfactant molecule.

The characteristic feature of the surfactant molecules is their ability to adsorb at

the interfaces and form clusters in the bulk solution by self-assembly. The hydrophilic and hydrophobic moieties of the surfactant molecule establish a unique interaction with water. The hydrophobic group of the surfactant molecule distorts the structure of water. This distortion is caused by the rupture of the hydrogen bond network of the water molecules and their reorientation. This phenomenon causes the free energy of the system to increase. Since, this is a thermodynamically unfavorable condition, some of the surfactant molecules are expelled to the air–water interface from the bulk solution in order to minimize the contact of the tail-groups with the water molecules. The hydrophilic head-groups interact favorably with the aqueous environment via dipole–dipole or ion–dipole interaction and hydrogen bonding. After adsorbing at the air–water interface, the hydrophilic group extends into the aqueous phase, and the tail, due to its hydrophobic nature, extends into the air. The air molecules are essentially non-polar and hydrophobic. The hydrophilic head-group tends to maximize its contact with the water molecules, whereas, the hydrophobic part hides away from it. This unique behavior of the surfactant molecules is the driving force for adsorption at the air–water or oil–water interface. The adsorption of surfactant molecules at the air–water interface causes a decrease in the surface tension of water. The solubility of the surfactant in water depends on the hydrophobicity of its tail and the hydrophilicity of its head-group. William Griffin [56] introduced the *hydrophilic–lipophilic balance* system *(HLB)* as a way to figure out the solubility and surface activity of the non-ionic surfactants in water. He developed the *HLB method* (or scale) on the premise that the surfactant combines the hydrophilic and lipophilic groups in one molecule, and that the proportion between the weight percentages of these two groups for the surfactant molecule gives a valuable source of information on the potential application of the surfactant. The polarity of the head-group determines the hydrophilic character of the surfactant. Typical surfactant head-groups are amine,

quaternary ammonium, ethoxylate, sulfate, sulfonate, phosphate, and carbonate. The polarity of the head-group may be altered in some cases by adjusting the pH of the solution. Increasing the size of the tail group should decrease the HLB. Surfactants having a lipophilic character are assigned a low HLB number, and surfactants having a hydrophilic character are assigned a high HLB number. The surfactants having low HLB values tend to be oil-soluble, and those having high values tend to be water-soluble.

For the surfactants based on polyhydric alcohol fatty acid esters (e.g., glycerol mono-stearate), the HLB can be given by the relationship,

$$\text{HLB} = 20\left(1 - \frac{S}{A}\right) \qquad (1.1)$$

where S is the saponification number of the ester and A is the acid number of the acid. A typical nonionic surfactant of this type, known as Tween 20 [polyoxyethylene (20) sorbitan monolaurate], with $S = 45.5$ and $A = 276$, would have an *HLB* of 16.7. For materials that cannot be saponified, an empirical formula of the following form can be employed.

$$\text{HLB} = \frac{E + P}{5} \qquad (1.2)$$

In eq. (1.2), E is the weight percent of the oxyethylene chains and P is the weight percent of the polyhydric alcohol (i.e., glycol, sorbitan, etc.) in the molecule. An example is given below.

For Atlas G-1441 (a polyoxyethylene sorbitol lanolin derivative), $E = 65.1$ and $P = 6.7$. Therefore, from eq. (1.2),

$$\text{HLB} = \frac{65.1 + 6.7}{5} = 14 \qquad (1.3)$$

These formulae are satisfactory for non-ionic surfactants of many types.

The above simple equations cannot be used for surfactants containing propylene

oxide or butylene oxide. They cannot be applied for ionic surfactants too. Davies[45] devised a method for calculating the HLB number for surfactants from their chemical formula, using empirically determined group numbers. A group number is assigned to various component groups.

$$\text{HLB} = \sum(\text{hydrophilic group numbers}) - \sum(\text{hydrophobic group numbers}) + 7 \quad (1.4)$$

For example, the HLB value of sodium dodecyl sulphate ($C_{12}H_{25}SO_4^-Na^+$) can be computed as shown below.

$$\text{HLB} = \sum(\text{hydrophilic group numbers}) - \sum(\text{group number per } -CH_2 - \text{ group}) + 7$$

$$\sum(\text{hydrophilic group numbers}) = 38.7$$

$$\sum(\text{group number per } -CH_2 - \text{group}) = 12 \times 0.475 = 5.7$$

Thus, $\text{HLB} = 38.7 - 5.7 + 7 = 40$. Therefore, the HLB value of sodium dodecyl sulfate is 40. Similarly, the HLB value of DDAPS can be calculated using Davis's method as follows:

$$\sum(\text{hydrophilic group numbers}) = 11 + 9.4 = 20.4$$

$$\sum(\text{group number per } -CH_2 - \text{group}) = 13 \times 0.475 = 6.175$$

Thus, $\text{HLB} = 20.4 - 6.175 + 7 = 21.225$. Therefore, the HLB value of DDAPS is 21.225.

A few surfactants and their HLB values are given in Table 1.1.

Table 1.1: HLB values of some surfactants

Surfactant	Type	HLB Value
Sorbitan tristearate	Nonionic	2.1
Sodium dodecyl sulphate	Anionic	40.0
N-cetyl N-ethyl morpholinium ethosulphate	Cationic	27.0
N-Dodecyl-N-N-dimethyl-3-3ammonio-1-propane sulfonate	Zwitterionic	21.225

When an interface is completely saturated with the surfactant molecules, additional surfactant molecules present in the bulk aqueous phase form self-assembled structures called *micelles*. The surfactant concentration at which this phenomenon occurs is called *critical micelle concentration* (CMC). It is the lowest concentration at which aggregation in the bulk solution begins. The CMC depends on the structure of the surfactant molecule and the physicochemical conditions such as pH, temperature, and the composition of the solution. A favorable interaction among the surfactant tail-groups by the hydrophobic effect leads to the formation of a hydrophobic core in the bulk solution at the CMC.[29] This process minimizes the unfavorable contact with the water molecules and leads to the formation of micelles. Micelles can have a wide variety of shapes (e.g., spherical, cylindrical, and lamellar) and their size can vary widely (e.g., from a few nanometers to several micrometers). Figure 1.2 depicts the schematic representation of surfactant molecules adsorbed at the air–water interface, and micelles and monomers present in the aqueous solution. If the bulk phase is non-aqueous, reverse micelles may form with polar heads pointing inward into an aqueous core and the hydrophobic tails pointing outward into the oil phase. As more surfactant is added to the solution, micelles may form other structures such as lamellar and bicontinuous.[30]

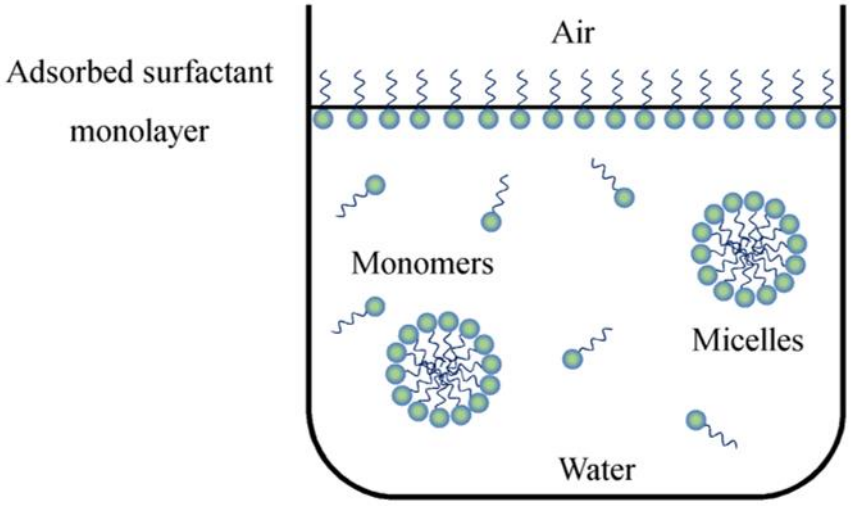

Figure 1.2. Schematic representation of the formation of a surfactant monolayer at the air–water interface, micelles, and surfactant monomers in the bulk phase when surfactant concentration is above the CMC.

1.3 Classification of surfactants

Surfactants are typically classified into five major categories (i.e., anionic, cationic, zwitterionic, nonionic, and gemini) based on their charge and structure.

1.3.1 Anionic surfactants

Anionic surfactants are most commonly used and they account for almost 50% of the world's surfactant production.[31] In these surfactants, the head-group carries a negative charge. The head-group may contain carboxylate, phosphate, sulfate, and sulfonate compounds. Examples of this type of surfactant are sodium and potassium salts of straight-chain fatty acids (i.e., $RCOO^{-}M^{+}$), alkylbenzenesulfonates $\left(RC_6H_4SO_3^{-}Na^{+}\right)$, N-acyl-n-alkylaurates $\left[RCON\left(R'\right)CH_2CH_2SO_3^{-}Na^{+}\right]$, α-olefin sulfonates,

sulfosuccinate esters $\left[ROOCCH_2CH\left(SO_3^-Na^+\right)COOR\right]$, sulfated primary alcohols $\left[ROS_3^-Na^+\right]$, and fatty acid monoethanolamide sulfates $\left[RCONHCH_2CH_2OSO_3^-Na\right]$.

1.3.2 Cationic surfactants

Cationic surfactants bear a positively charged head-group and adsorb strongly onto the negatively charged surfaces. A majority of these surfactants contains nitrogen compounds accompanied by an alkyl chain. Common cationic surfactants include long chain amines and their salts $\left(RNH_3^+X^-\right)$, acylated diamines and polyamines, quaternary ammonium salts, polyoxyethylene (POE) long-chain amines $\left\{RN\left[\left(CH_2CH_2O\right)_x H\right]_2\right\}$, and amine oxides $\left[RN^+\left(CH_3\right)_2 O^-\right]$.

1.3.3 Nonionic surfactants

Nonionic surfactants are the second most widely used surfactants (after the anionics) worldwide. They constitute almost 40% of the overall industrial production of surfactant, and they are usually good dispersing agents for carbon.[32] The hydrophilic entity of the nonionic surfactants is made of groups such as alcohol, phenol, ester, ether, or amide, which do not ionize in the aqueous medium. A few examples of this type of surfactant are POE alkylphenols $\left[RC_6H_4\left(OC_2H_4\right)_x OH\right]$, alcohol ethoxylates $\left[R\left(OC_2H_4\right)_x OH\right]$, POE mercaptans $\left[RS\left(C_2H_4O\right)_x H\right]$, tertiary acetylenic glycols $\left[R_1R_2C\left(OH\right)C\equiv CC\left(OH\right)R_1R_2\right]$, and POE silicones.

1.3.4 Gemini surfactants

Gemini surfactants belong to a relatively new class of surfactants as compared to the conventional surfactants. They have two or three hydrophobic, and usually two hydrophilic groups. The hydrophobic groups are connected by a linkage that is close to the hydrophilic groups. The properties of these surfactants vary greatly depending upon the structure of these three parts of the molecule. The interfacial effects of these surfactants may be such stronger than the surfactants having a single hydrophilic and hydrophobic group. The gemini surfactants can have negative, positive or both types of charges. They can be nonionic as well. Since these surfactants have large number of carbon atoms in their hydrophobic part, they have a penchant for adsorbing at the interface. however, at the same time, their solubility in water may be less. The hydrophilic groups prevent this difficulty. These surfactants require only a small amount to saturate the interface.

1.3.5 Zwitterionic surfactants

Zwitterionic surfactants are manufactured in smaller quantities globally. Their unique capabilities of enhancing the characteristic properties of the surfactant formulations have entitled them a unique position in the surfactant world. The zwitterionic surfactants have a distinctive molecular structure, i.e., both anionic and cationic head-groups are present in it. Thus, it is interesting to investigate their properties at the fluid–fluid interfaces. The typical structure of a zwitterionic surfactant is shown in Figure 1.3.

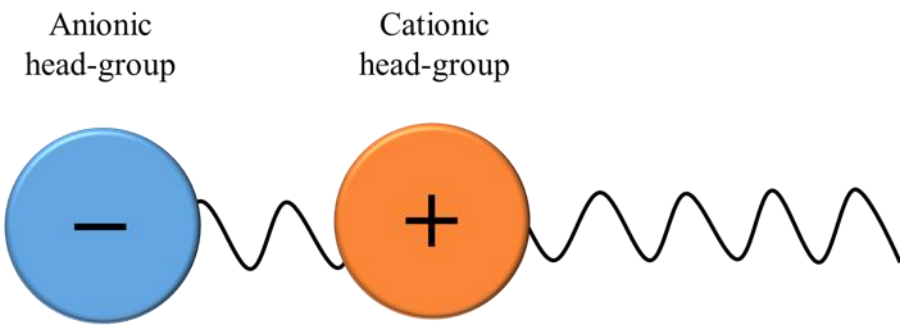

Figure 1.3. A typical zwitterionic surfactant molecule with cationic and anionic head-groups.

These surfactants can adsorb on both positively- and negatively-charged surfaces without significantly altering their charge. The cationic entity of the surfactant is mostly based on ammonium groups whereas the anionic entity may include carboxylic acid, sulfonic acid, and sulfuric acid esters. Also, the tail may consist of groups from hydrocarbon, fluorocarbon, or siloxane. The tail may contain straight or branched chains, or ring structures. Such uniqueness in the molecular structure helps this type of surfactant to exhibit unique interfacial and solution properties with varied practical applications. Hence, the researchers have been encouraged to modify its molecular structure and study its physicochemical behavior.

The structure of these surfactant molecules helps them to self-assemble such that they form three-dimensional structures with distinct regions housing polar and nonpolar parts, barring any contact with one another. As zwitterionic surfactants contain both the anionic and cationic head-groups, they are most suitable for unit operations and processes that involve a wide pH range and alternate use of hard and soft water. The pH of the system determines which group will dominate because the surfactant shows the characteristic properties of the anionics at high pH and those of the cationics at low pH. However, at the isoelectric point, these surfactants show both charges and are amphoteric in nature, with maximum water solubility. The electrically-neutral nature of these

surfactants renders their function similar to the nonionic surfactants, and hence they are compatible with all other types of surfactant. Since they are less irritating towards the skin and eyes, they are ideal for preparing baby care products and "no tears" shampoos. A few examples of the zwitterionic surfactant are β-N-alkylaminopropionic acids $\left[RN^{+}(CH_3)_2 CH_2COO^{-}\right]$, N-alkyl-β-iminodipropionic acids $\left[RNH(C_2H_4COOH)\right]_2$, imidazoline carboxylates $(C_6H_8N_2O_2)$, N-alkylbetaines $\left[RN^{+}(CH_3)CH_2COO^{-}\right]$, amidoamines $\left[RCONH(CH_2)_n NRCOO\right]$, amine oxides $\left[RN^{+}(CH_3)_2 O\right]$, sulfobetaines $(C_5H_{11}NO_5S)$, and sultaines $\left[RN^{+}(CH_3)_2(CH_2)_x SO_3^{-}\right]$.

1.4 Foams

1.4.1 Definition and applications

Foams are colloidal dispersions of gas bubbles generated from an aqueous solution containing one or more surfactants.[33,34] Aqueous foams are ubiquitous and they are present in our everyday life. They play a significant role in many applications such as fire-fighting,[35,36] deliquification of natural gas,[37] enhanced oil recovery,[38,39] mineral flotation,[40,41] cosmetics[42,43], and detergents.[44] Foams are broadly classified as solid foams (e.g., polyurethane, ceramic, and metallic) and aqueous foams (e.g., beer and laundry).[45,46] Solid foams are commonly used in lightweight structures, upholstery, thermal insulation, sound absorption, and vibration. The aqueous foams play a significant role in detergency, cosmetics, food engineering, and pharmaceutics.[42,46] Foams also commonly occur in the environment (e.g., lake, river, and sea). These foams are produced due to the agitation of water, which contains algae containing a high amount of dissolved organic matter and surface active chemicals that can act as foam-forming agents.

Surfactants are widely used to produce foams in almost all industrial processes. Aqueous foams produced from surfactant solutions exhibit low density, large surface area, and exhibit both the solid- and liquid-like behavior. Foams may be desirable or undesirable in the unit operations. For example, foams are desirable in the petroleum extraction processes such as drilling, fracturing, acidizing, and controlling the gas mobility. However, during the production of oil from the oil-well and well-head, oil floatation, distillation and fractionation tower, and in fuel oil and jet fuel tanks, foams are undesirable. The combination of surfactant solution and foam has been employed in the petroleum industry for the past few decades in order to improve the efficiency of crude oil recovery.[34,47] Their use has been successful in the environmental remediation while removing the hydrocarbons and other contaminants from the soil.[27]

1.4.2 Foam morphology

Foams formed in a vertical column usually contain spherical bubbles at the bottom, whereas, they have a polyhedral structure at the top.[48] The spherical bubbles formed at the bottom of the column are called *kugelschaum* and their liquid content is considerably high. These foams are also known as "wet" foams. However, with time, the liquid drains from these foams as several forces start to act on them, and the polyhedral structures with many faces are developed. This foam is known as *polyederschaum* and has a minimum liquid content.[49,50] They are also called "dry" foams. Figure 1.4 illustrates these two types of foam.

The shape of the foam network is dependent on the liquid volume fraction (ϕ) in it, i.e., the ratio of the liquid volume to the foam volume. It is given by, $\phi = V_l / V_f$, where V_l is the volume of the aqueous solution and V_f is the volume of the foam. Usually ϕ lies between 0.01 and 0.3. The value of ϕ for wet foams is generally above 0.05, and

these foams stay mostly towards the bottom of the foam column. However, for dry foams, the liquid volume fraction is < 0.05, and these foams are polyhedral with well-defined edges and slightly curved faces.[51-54] The liquid volume fraction can significantly affect the thermodynamic and rheological properties of the foams. In the case of the dry foams, there is a wide space between the cells, whereas, for the wet foams a close-packing of spheres is observed. Easy handling, reproducible preparation, and well-defined geometry have made them a suitable tool for studying the interactions between the surfaces.

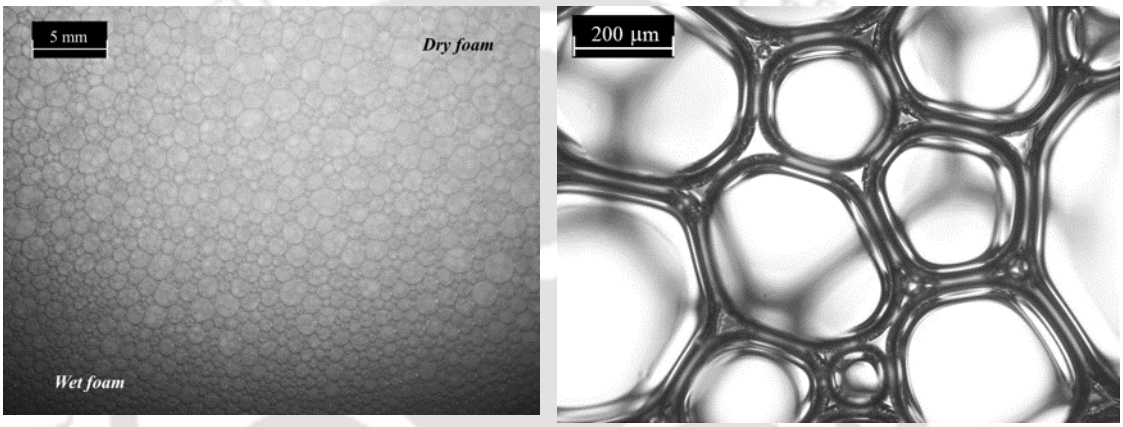

(a) (b)

Figure 1.4. (a) Dry and wet foams dispersed in an aqueous surfactant solution and (b) a photograph of an aqueous polyhedral foam.

Formation of foam is a complex process, which occurs at both microscopic and macroscopic scales. Many properties of liquid foams are direct consequences of their structure. There is a large difference in size along the lateral and normal directions inside the foam. The typical foam structure involves three main components i.e., thin liquid film (termed as *lamella*), Plateau border, and node.[51,55] The details of these parts of foam are discussed in Section 1.5.

1.5. Foam lamella, Plateau border, and Node

1.5.1 Foam Lamella

The aqueous foam films have two air–water interfaces on each side. The thickness of this film varies between a few micrometers and several nanometers, which is much smaller than the bubble diameter. The thickness of the film decreases with time as liquid drainage takes place. The age of the foam films depends upon several factors such as the concentration of surfactant, surface diffusion, surface tension gradient, and external perturbations caused by the system disturbances.[56] The film thickness influences foam drainage and foam stability. A typical foam film is shown in Figure 1.5.

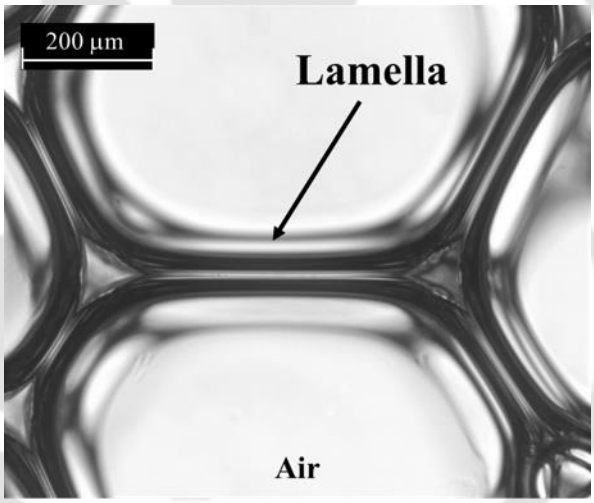

Figure 1.5. Typical foam lamella developed from an aqueous surfactant solution.

1.5.2 Plateau border

When three foam films meet symmetrically at an angle of 120°, the junction of these films is known as *Plateau border*. This angle is known as *Steiner angle*. The Plateau border is a major component of foam with a wide channel network forming the interstitial space among the foam bubbles. It holds the majority of liquid present in foam, and most of the drainage under gravity occurs through this network. The opacity of foam is caused by the

diffusive light scattering from the films and the Plateau borders. Figure 1.6 depicts the typical image of a Plateau border.

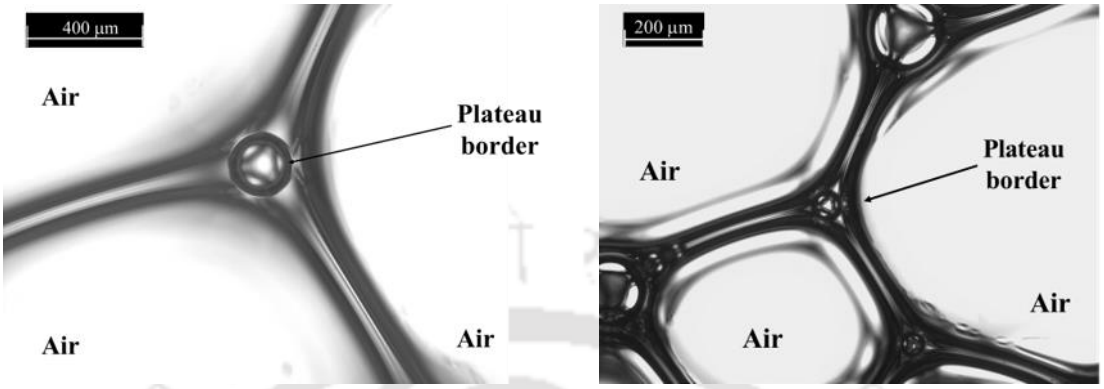

Figure 1.6. Plateau border in foam.

The Plateau borders transmit the mechanical force applied on foam through them.[57] The shape of the air–water interface is described by the Young–Laplace equation. This equation gives the pressure difference between the inside and the outside of a curved interface.[58] It is given by

$$\Delta P = \gamma\left(\frac{1}{R_1}+\frac{1}{R_2}\right) \tag{1.5}$$

where ΔP is the pressure difference, γ is the surface tension, and R_1 and R_2 are the principal radii of curvature. The pressure inside a bubble is always greater than that outside. In the case of a spherical bubble, $R_1 = R_2 = R$, and Equation (1.5) becomes

$$\Delta P = \frac{2\gamma}{R} \tag{1.6}$$

Equations (1.5) and (1.6) relate the pressure difference across the bubble surface to the size of the bubble.[57] Equation (1.6) signifies that the pressure difference across the bubble surface is inversely proportional to radius of the bubble. Thus, the pressure inside a smaller bubble is higher than that inside a larger bubble.

1.5.3 Node

Nodes are the points of intersection of at least four Plateau borders forming a network of foam structure that runs through the entire foam channel (see Figure 1.7). Nodes are formed when four Plateau borders meet symmetrically at a junction at an angle of 109.47°. The flow of liquid through the nodes is more complex than that through the Plateau borders as a result of the merger of the Plateau borders at the junction.

During the foam formation process, the surfactant molecules are transported from the bulk solution to the air–water interface. This phenomenon depends on the surface activity and bulk concentration of the surfactant, and the interaction between the surfactant molecules at the interface. Surface tension of the aqueous solution plays a significant role in foam formation. During the formation of foam, air is entrapped. The bubble, when isolated, tries to occupy the smallest surface area, and hence it assumes a spherical shape. When two bubbles come into contact, they spontaneously change the shape and reduce the total interfacial area. The resulting shape of the foam is due to the competitive interaction between the two bubbles.

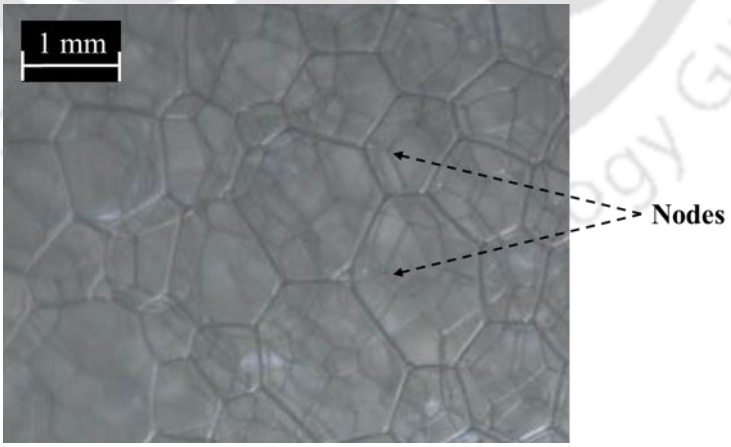

Figure 1.7. Nodes in a foam channel.

1.5.4 Structure of foam bubbles

The properties of liquid foams are direct consequences of their structure. Lord Kelvin[67] showed that tetrakaidecahedron is the ideal cell in a dry, polyhedral, and monodisperse foam. This polyhedron has eight non-planar hexagonal faces and six planar quadrilateral faces with curved edges. The curved surfaces are required for the minimization of surface energy and they also satisfy the Plateau's condition. However, the statistical distribution of polygon faces on the packed foam bubbles differs markedly from Kelvin's tetrakaidecahedron, and the bubbles show a predominance of the pentagonal faces. Weaire and Phelan[94] found that the common films in foams are pentagonal in most cases. They constructed a collection of eight polyhedral bubbles, which contained many pentagonal faces and possessed a fractionally-less surface area (i.e., 0.3%) than a Kelvin cell.

A catenoid is a surface, which is constructed by rotating a catenary curve about an axis. The catenoid is a minimal surface that spans two coaxial circular rings. It occupies the least area when bounded by a closed space. A soap film attached to twin circular rings will take the shape of a catenoid, which has the equation, $r = \cosh(z)$ in the cylindrical coordinates (see Figure 1.8). If the rings are pulled further apart, the neck will narrow until the critical separation is reached, and then the catenoid will pop into two disks. In case of soap films, the film is an infinitesimally-thin two-dimensional surface.

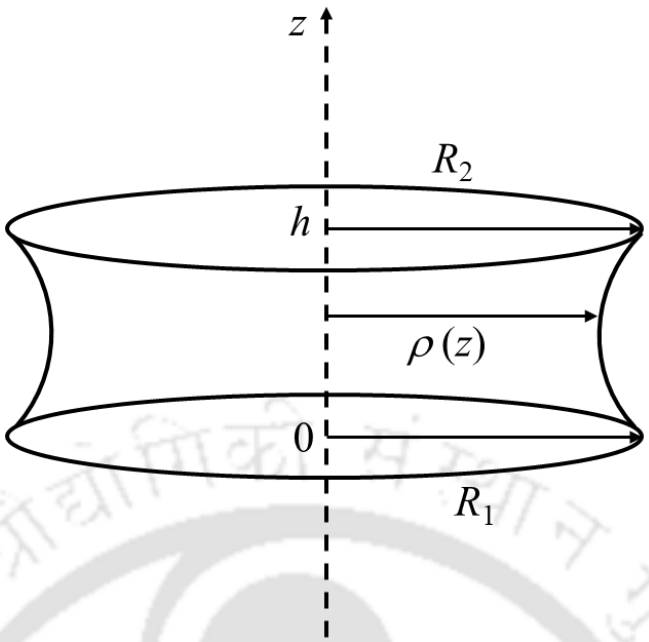

Figure 1.8. A schematic sketch of a foam film stretched between two parallel circular rings.

The foam film, at equilibrium, should have zero mean curvature everywhere, which can be explained by the Young–Laplace equation [i.e., eq. (1.5)]. $\Delta P = P_{in} - P_{out}$, where P_{in} and P_{out} are the pressures inside and outside, respectively. In a catenoidal shape, the film does not enclose any volume. Therefore, the pressure on both sides of the film are equal to the atmospheric pressure. If we assume that the film has a constant thickness, and treat the inside of the film as the inner fluid, then one side of the film has a positive curvature, while the other side has a negative curvature. Therefore, if we apply the Young–Laplace equation to the positive curvature, it would imply $P_{in} > P_{atm}$. On the other hand, if we apply it to the negative curvature, we would get $P_{in} < P_{atm}$, which is a contradiction. Thus, for a constant thickness film, the mean curvature will be equal to zero everywhere.

1.6 Foam formation

Aqueous foams are thermodynamically unstable due to their high interfacial free energy. They eventually break and disappear.[59,60] Surfactants significantly influence the properties of foam. The characteristic property of the surfactant is to adsorb at the air–water interface and alter the interfacial properties, such as reduction of the surface and interfacial tension. These features have made them interesting and useful with respect to the foams. Foam formation is a dynamic process. It involves dynamic adsorption of surfactant molecules at the air–water interface. The interfacial region of a typical foam film can be divided into two parts (see Figure 1.9). Adsorption of surfactant molecules occurs in the upper surface layer of this region. The subsurface region is located just below the surface layer. The thickness of this layer is about a few molecular diameters. Adsorption of surfactant molecules in the foam film is a two-step process. The first step involves the adsorption of surfactant molecules from the subsurface region of the foam film to its surface.[61] In the initial phase, the surfactant molecules get adsorbed in the lamellae and Plateau border. However, at longer times, desorption may take place. The second step involves the irreversible movement of the surfactant molecules from the bulk solution to the surface by diffusion. The diffusion may be accompanied by convection. Diffusion of surfactant occurs in an extensively larger domain as compared to the thickness of the adsorption layer.

In the initial stages of foam formation, a fresh surface forms where the surfactant concentration is negligibly small. The surfactant molecules from the subsurface region begin to adsorb on the air–water interface, thus reducing the surfactant concentration in the subsurface. This depletion of surfactant molecules in the subsurface region is balanced by the diffusion of molecules from the bulk region to the subsurface region, which restores the subsurface concentration. Accordingly, the adsorption of surfactant

molecules at the air–water interface and the transport of surfactant molecules from the bulk solution to the subsurface play an important role in

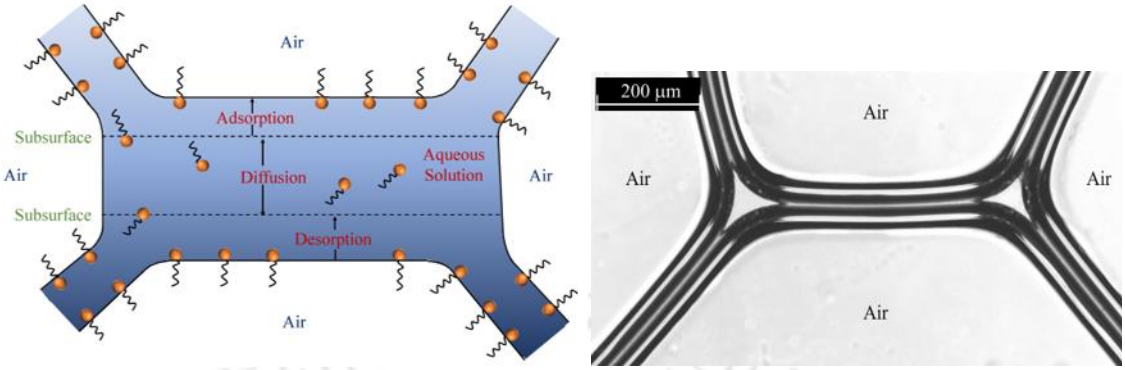

(a) (b)

Figure 1.9 (a) Schematic diagram of the dynamic adsorption of the surfactant molecules in the lamella during foam formation. The thickness of the subsurface region is exaggerated for illustration. The actual thickness is of the order of a few molecular diameters only; (b) photograph of the foam lamella.

foam formation and the initial foam volume. Ward and Tordai[62] explained the dynamic adsorption of the surfactant molecules at the air−water interface. Their equation is given by

$$\Gamma(t) = 2c_0\left(\frac{D_s t}{\pi}\right)^{1/2} - \left(\frac{D_s}{\pi}\right)^{1/2}\int_0^t \frac{c_s(0,t)}{(t-\tau)^{1/2}}\,d\tau \qquad (1.7)$$

where Γ is the surface excess concentration of the surfactant, c_0 is the initial bulk concentration of the surfactant, D_s is the diffusion coefficient of surfactant, t is the time, c_s is the concentration of surfactant in the bulk solution, and τ is a dummy variable. The second term on the right side of equation (1.7) represents the "back diffusion", which occurs when the diffusion process slows down due to the increase in the subsurface concentration. If $c_s(0,t) = 0$, i.e., the surface has an extensive ability for surfactant

adsorption, the second term in equation (1.7) becomes zero, and therefore, $\Gamma(t) \alpha \sqrt{t}$.

1.7 Foamability and foam stability

Foams are usually characterized by *foamability* and *foam stability*. A surfactant solution's ability to produce foam is determined by its foamability or foam generation capacity. It is a quantitative assessment in terms of the initial foam volume or initial foam height, measured within seconds after the foam formation. On the other hand, foam stability is defined as the lifetime of foam after its formation. The stability of foams is important in their performance in various industries. Therefore, researchers and product manufacturers have developed a deep interest in the investigation of foam stability. The foamability and foam stability are significantly influenced by the foam formation method, and these two parameters often define the effectiveness of the surfactant.

1.8 Foam stabilizing mechanisms

Formation of foam depends on the concentration of surfactant, type of liquid, and the gas. The foam can be short-lived, fragile, and disappear rapidly. The stability of foam depends on the ability of the surfactant solution to form a strong, flexible, and cohesive film, which can reduce gas permeability and hinder the coalescence of the bubbles. Foam stabilizing mechanism involves film elasticity, Marangoni effect, gas diffusion through the lamellae, interfacial rheology, and intermolecular and surface forces.

1.8.1 Film elasticity

Elasticity, in general, is defined as the ratio of stress to strain. It is a measure of the propensity of the material to restore its initial state following deformation. In foams, it represents the "self-healing" capacity of foam films against any external disturbance. The elasticity in foams depends on how the surface tension changes with the film surface area.

The Gibbs elasticity $\left(E_G\right)$ is defined as

$$E_G = 2A\frac{d\gamma}{dA} \tag{1.8}$$

where $d\gamma$ is the change in the surface tension and dA is the change in the film surface area. The Gibbs elasticity refers to the increase in the film surface tension resulting from a decrease in the surfactant concentration within the interlamellar solution caused by the small extension of the film relative to the film size.[63] The foam film elasticity is affected by the redistribution of the surfactant between the bulk of the film and its two surfaces, which takes place after stretching.[64] Gibbs elasticity is often useful for explaining the stability of static foam, whereas, for dynamic foam, the elasticity due to Marangoni effect is more appropriate.[65]

1.8.2 Marangoni effect

In an active foam channel, under dynamic conditions, transport of surfactant molecules occurs as the foam film drains from the center of the film towards the Plateau border. The flow occurs from a region of high surfactant concentration to a region of low surfactant concentration near the film edges.[66,67] In an aqueous foam, the surfactant concentration gradient across the foam film causes the Marangoni effect.[68] Figure 1.10 shows the schematic representation of the Marangoni effect occurring in a foam film. The Marangoni effect plays a significant role in stabilizing the thick foam film since it operates on both expanding and contracting foam films. For a thin foam film susceptible to rupture, this effect helps to stabilize it, and tries to resist the sudden expansion and contraction of the surfaces. However, at a low surfactant concentration, the Marangoni effect is not strong. This is due to a small surface tension gradient, low diffusion rate of the surfactant molecules at the air–water interface, and less diffusion of the surfactant

molecules from the center of the film towards the Plateau borders. Hence, the Marangoni effect does not affect the film drainage significantly at low surfactant concentrations.[69,70] However, at high surfactant concentrations, the density of the surfactant molecules at the interface is high, which causes the movement of the molecules from the surfactant-rich region to the surfactant-lean region of the film. This causes a strong surface tension gradient at the air–water interface and draws the surfactant molecules back to the interface and the liquid into the film. This leads to a strong Marangoni effect, which stabilizes the foam film. In this way, the possibility of film rupture is hindered.

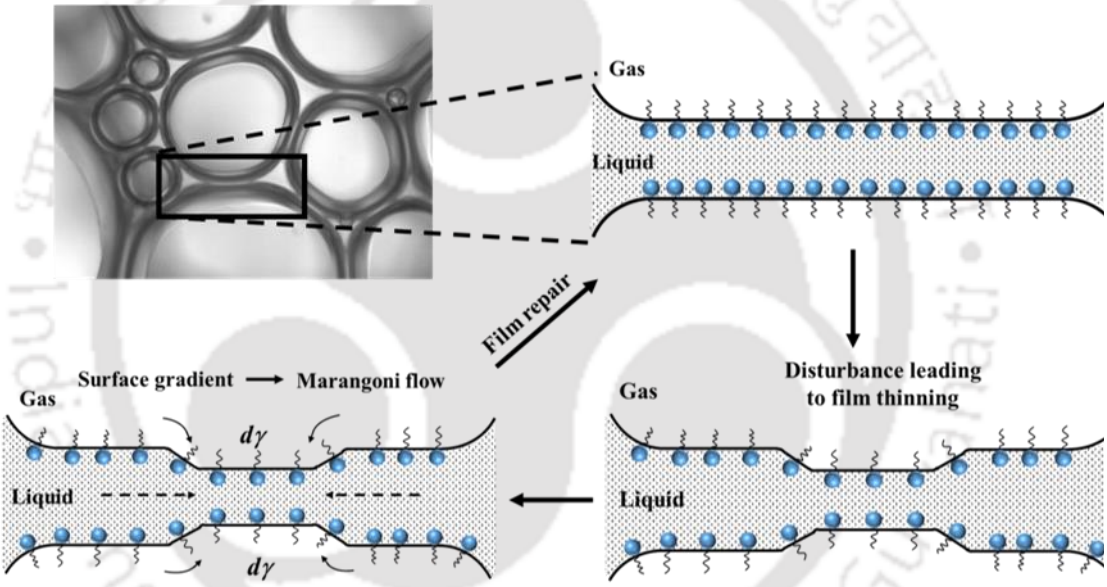

Figure 1.10. Schematic representation of Marangoni flow at the air–water interface caused by the surface surfactant gradient, and the film repair mechanism.

1.8.3 Gas diffusion through foam lamellae

Several researchers have studied the diffusion of gas through the foam lamella in the presence of adsorbed surfactant molecules.[71–73] The overlapping structure of the two monolayers constituting the foam lamella imposes a significant resistance to mass transfer

of the gas. The dynamics of the surface, particularly the effective area of the surfactants, is also important in gas diffusion. Two mechanisms have been proposed to describe the diffusion. If the surfactant monolayer behaves like a homogeneous phase, the gas molecules would encounter a resistance, which is the sum of the diffusional resistances in the gas phase, across the monolayer, and through the liquid. On the other hand, if the surfactant monolayer is not necessarily homogeneous, it may act as an energy barrier to the gas molecules striking the interface. The magnitude of this barrier is a measure of the physical interaction between the gas and the surfactant molecules in the monolayer.[74,75]

The diffusion of gas in the foam network may lead to morphological deformation of the foam films leading to the shrinkage of foam. This deformation due to gas diffusion may result in the instability of the interface and unsteady film thickness, which would affect the stability of the foam. The process in which diffusion of gas between the bubbles occurs is termed as *coarsening*. This is very important for a variety of foam-based products e.g., food and beverage foams. Coarsening may lead to the formation of a less number of foam bubbles (Figure 1.11). The pressure difference between the two bubbles drives the coarsening. The bubbles within foam choose the shortest path to diffuse. The parameters, which influence coarsening depend on gas diffusivity, liquid volume fraction, thickness of the foam film, surface tension of the solution, and the initial diameter of the bubble.[76,77] Other factors which influence coarsening include foam film permeability and the bubble size.[76]

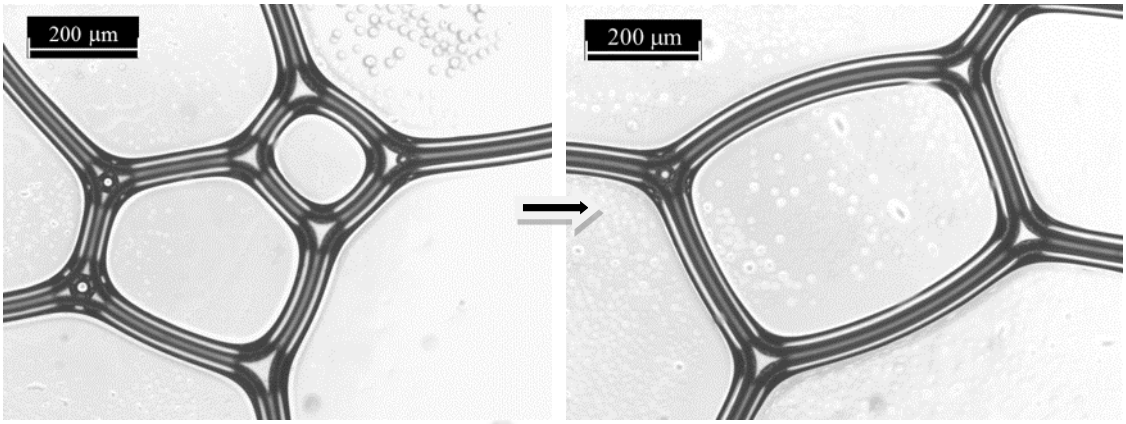

Figure 1.11. Merger of a smaller bubble with a larger one leading to the coarsening of foam.

1.8.4 Interfacial rheology

The main driving force behind the formation of foam is the reduction in surface tension. However, the rheological properties of the air–water interface also play a significant role in its formation and stability. The adsorption of surfactant molecules at the air–water interface forms a monolayer, which gives rise to interfacial viscoelasticity. The formation of foam involves expansion and contraction of the air–water interface under strong dynamic conditions. During this process, the initial equilibrium state becomes distorted inasmuch as the surfactant molecules dynamically adsorb at the air–water interface. Two types of interfacial rheology (i.e., shear and dilatational) characterize the response of the interface to the shear and extensional stresses, respectively. The interfacial shear rheology involves a constant interfacial area but the shape of the interface is altered. On the other hand, dilatational rheology involves an increase or decrease of the interfacial area, while the shape of the concerned area remains constant. These phenomena are explained in Figure 1.12.

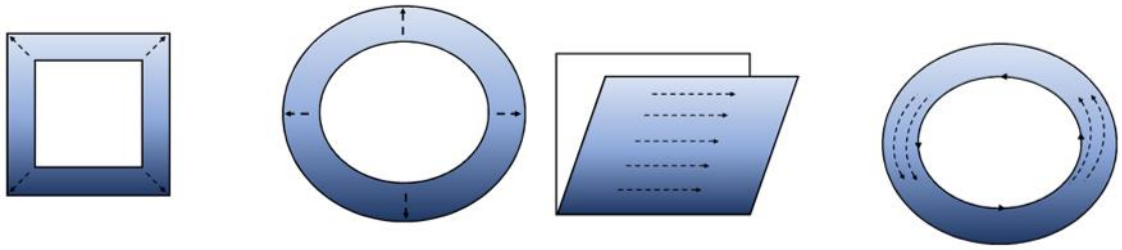

(a) (b)

Figure 1.12 (a) Dilatational and (b) shear rheology of the interface.[78]

The surface dilatational modulus, is defined as the ratio of the surface tension change, to the area change, under dilatational deformation. The surface dilatational modulus has two components, i.e., surface dilatational elasticity (which measures the capacity of the air–water interface to resist a dilatational deformation) and surface dilatational viscosity (which measures the speed of the relaxation processes restoring the equilibrium after the disturbance). High values of the surface viscoelasticity can potentially lead to the suppression of marginal regeneration (which is important in vertical aqueous foam films) and a reduced rate of foam film drainage, which enhance foam stability.

1.8.5 Intermolecular and surface forces

Intermolecular and surface forces play a significant role in the stability of thin foam films. Thus, the link between these forces and the stability of the foam film is critical in understanding the stability of foam. When the foam film becomes thin, interfacial forces begin to act between the two air–water interfaces. The DLVO and the non-DLVO theories have been used to interpret the forces operating in the thin foam films. These forces determine the stability of the film.

The concept of disjoining pressure (Π) was introduced by Derjaguin to explain

the forces between the two surfaces of a thin foam film.[79,80] The disjoining pressure comprises of the attractive and repulsive interactions between these air–water interfaces. The DLVO theory is based on these interactions.[41,79,81-84] The disjoining pressure in the thin liquid film of thickness h is equal to the difference between the pressure in the film normal to the plane-parallel film surfaces $\left(P_N\right)$ and the intrinsic pressure in the bulk phase $\left(P_B\right)$,[85] i.e.,

$$\Pi\left(h\right) = P_N - P_B \tag{1.9}$$

The thermodynamic definition of disjoining pressure for a thin liquid film is given in terms of the change in the Gibbs free energy (G) with the film thickness (h), i.e.,

$$\Pi\left(h\right) = -\left(\frac{dG}{dh}\right)_{T,P,A,N_i} \tag{1.10}$$

where T, P, N_i, and A represent temperature, overall pressure, number of moles of the substances, and cross-sectional area of the film, respectively.

There are two major forces [i.e., electrostatic double layer (EDL) and van der Waals] in the thin foam films. The electrostatic interaction occurs when the interfaces are electrically charged due to the adsorption of ionic surfactants. The electrostatic component of the disjoining pressure $\left(\Pi_{\mathrm{EDL}}\right)$ originates due to the overlapping of the diffuse double layers of the two film surfaces at a small distance. This repulsive force is essentially due to the confinement of the counterions (which neutralize a charged interface) in a narrow region. This repulsion stabilizes the foam films. The presence of salt (e.g., NaCl) screens this repulsion. According to the Debye–Hückel theory, the thickness of the diffuse ionic atmosphere $\left(\kappa^{-1}\right)$ is given by[85]

$$\kappa^{-1} = \left(\frac{\varepsilon \varepsilon_0 k_B T}{e^2 N_A \sum z_i^2 c_i} \right)^{1/2} \tag{1.11}$$

where κ^{-1} is termed as *Debye length*, ε is the dielectric constant of the medium, ε_0 is the permittivity of free space, k_B is the Boltzmann constant, T is the temperature, e is the elementary charge, N_A is the Avogadro's number, and z is the valence of the electrolyte. Equation (1.11) indicates that the Debye length decreases with increasing electrolyte concentration i.e., the interaction occurs at a shorter range due to ionic screening. The *ionic strength* (I) of the medium is defined as

$$I = \frac{1}{2} \sum z_i^2 c_i \tag{1.12}$$

An increase in the ionic strength of the aqueous solution results in a decrease in the Debye length. The contribution of EDL to the disjoining pressure in a thin flat foam film is given by[86,87]

$$\Pi_{\text{EDL}} = 64RTc \tanh^2 \left(\frac{ze\psi_0}{4k_B T} \right) \exp(-\kappa h) \tag{1.13}$$

where ψ_0 is to the potential at the surface. The identically-charged film surfaces repel each other, and hence Π_{EDL} is positive.

The van der Waals interaction is the other significant force in the thin foam films. The attractive van der Waals disjoining pressure (Π_{vdW}) originates from the electromagnetic fields between two dipoles. It is rather insensitive to the variation in the electrolyte concentration and pH. Its magnitude can exceed the double layer repulsion at a small film thickness.[86] Like the EDL force, the van der Waals disjoining pressure is also distance dependent. For two flat surfaces, the disjoining pressure is given by[88,89]

$$\Pi_{\mathrm{vdW}} = -\frac{A_H}{6\pi h^3} \tag{1.14}$$

where A_H represents the Hamaker constant and h is the film thickness. For the air–water–air system (i.e., aqueous foam film), the value of A_H is about 3.7×10^{-20} J .[86,90] The attractive van der Waals attraction tends to destabilize the foam films. Therefore, repulsive force generated by the surfactant molecules is necessary to overcome the attractive force for stabilizing the foam film.

The DLVO theory assumed that the interaction between two surfaces could be well-approximated by a superposition of the electrostatic double layer and the van der Waals forces, i.e.,

$$\Pi(h) = \Pi_{\mathrm{EDL}} + \Pi_{\mathrm{vdW}} \tag{1.15}$$

This theory proposed that an energy barrier due to the repulsive force tends to prevent the rupture of the thin film. If this energy barrier is overcome, the van der Waals attractive force would rupture the film. If the EDL repulsion is strong enough, the films would be stable and prevent the collapse of the foam. The van der Waals force operates at the small separations between the surfaces, whereas, the EDL force dominates at the larger separations. The DLVO theory is based on the assumptions that the solvent can be treated as a continuum characterized by a dielectric constant, ions can be treated as point charges, and EDL and van der Waals forces can be treated as independent and additive.

In the initial stages of foam formation, a thick non-equilibrium film is formed. Various forces such as capillary pressure, gravity, and surface forces act on this film to form a much thinner film with time.[91-93] At equilibrium, a foam film of uniform thickness is formed, which depends on the thermodynamic conditions of the foam system (i.e., surfactant and salt concentrations, temperature and pressure). However, if the thinning process continues further, it may form a very thin film, which appears black in reflected

light. These films are termed as *black films*. The black film can be categorized as *common black film* (CBF), which is thicker, and *Newton black film* (NBF), which is thinner. The repulsive EDL force controls the stability of CBF, and the same agrees well with the classical DLVO theory (Figure 1.13). The thickness of the CBF typically ranges between 20 and 30 nm. At high electrolyte concentration, the EDL repulsion is suppressed and the thickness is reduced to form a very thin NBF. The thickness of the NBF is smaller than 10 nm. The film thickness depends on the salt concentration. It also depends on the interaction between the adsorbed surfactant layers by the short-range (i.e., van der Waals) forces. Formation and stability of these thin foam films decide the efficiency of the entire foam system.

In addition to the disjoining pressures due to the DLVO forces, non-DLVO forces such as steric, hydration, and hydrophobic may also act on the foam films. Steric and hydration forces are repulsive whereas, the hydrophobic forces are attractive. The DLVO theory sometimes fails to describe the interactions at short-ranges, i.e., a few nanometers. This is due to the presence of non-DLVO forces. These forces may be attractive, repulsive, and can be stronger than the DLVO forces. The disjoining pressure due to the short range force (i.e., Π_{sr}) is sometimes included as the third term in equation (1.15).[94]

Therefore, the formation and evolution of foam are governed by several mechanisms occurring at the microscopic level inside the foam film. These mechanisms collectively determine the foam stability. They have their own characteristic length- and time-scales, and they depend on the liquid fraction and the bubble size.

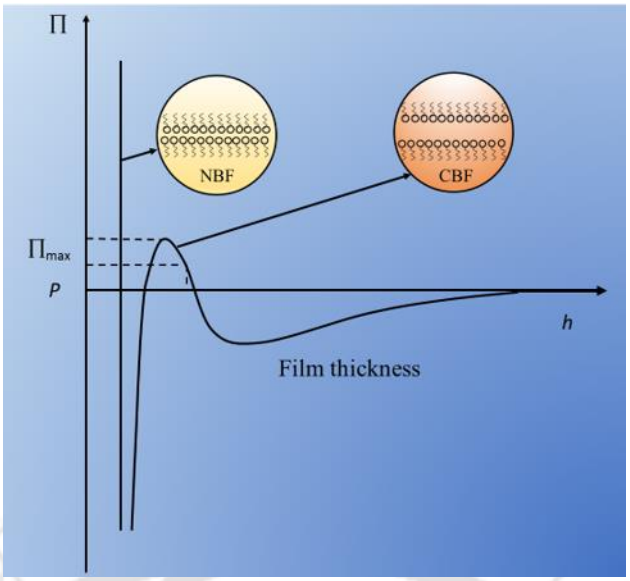

Figure 1.13. Disjoining pressure versus film thickness showing the transition from CBF to NBF.

1.9 Foam Decay

The decay of foam starts immediately after its formation. The decay of foam may be slow or rapid and it usually depends on a number of factors involving structural changes of the bubbles (i.e., from spherical to polyhedral). The decay of foam involves the interplay of different mechanisms, which lead to thinning of the foam film due to drainage, coalescence, coarsening, and external vibrations (see Figure 1.14). Other factors contributing to the decay includes evaporation, temperature gradients, and humidity.

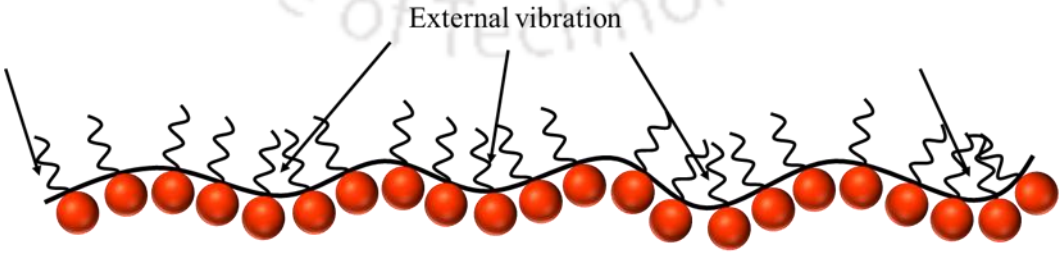

Figure 1.14. Foam film experiencing external vibrations.

1.9.1 Foam drainage

Foam drainage involves the irreversible flow of the aqueous solution through the foam network via the lamellae and the Plateau borders due to the gravity and capillary forces. Drainage has a significant role in foam film stability, and hence the stability of the entire foam system. Figure 1.15 shows the drainage of liquid under the influence of gravity. There is a continuous interplay between drainage and collapse of the foam film.[56,95] The Marangoni effect and hydrostatic forces influence the drainage. For a premicellar aqueous surfactant solution, the Marangoni effect plays an important role. However, for surfactant concentrations above the CMC, the interaction between the adsorbed surfactant layer and the micelles governs the stability of the foam. The foam films formed from the micellar surfactant solutions exhibit step-wise thinning, called *stratification*. It involves a layer-by-layer destruction of the micellar structures inside the film. Stratification depends on several factors such as film area, temperature, concentration of added electrolyte, surfactant concentration, and interaction between the micelles and their concertation in the solution.[96] Drainage may also result in a non-uniform coverage of the surfactant molecules in the foam film.[97] Drainage converts the spherical foam to the polyhedral foam upon aging. The films in the polyhedral foam are more susceptible to rupture by shock, vibration, or temperature gradient. In case of low stability foams, drainage begins immediately after foam formation and induces a significant surface tension gradient at the surfaces of the foam films. This gradient retards the drainage, and hence the rate of foam decay is reduced significantly.

1.9.2 Coalescence of foam bubbles

Coalescence is the merger of adjacent foam cells (or bubbles) due to the rupture of the thin liquid film that separates them. It results in a decrease in the number of bubbles and

an increase in the mean bubble volume in the foam. Coalescence in the foam evolves through a cascade of breaking events. It involves stretching and dilatation of the film, which is followed by its rupture.

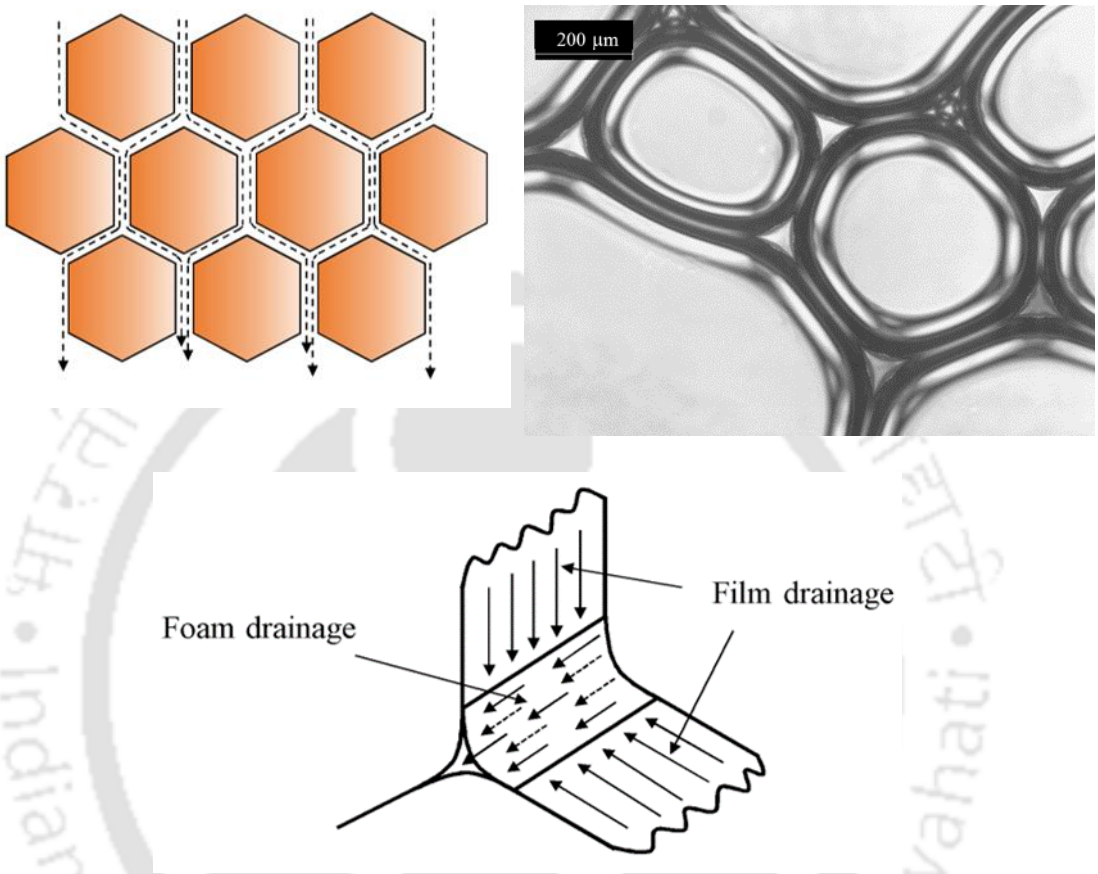

Figure 1.15. Flow of liquid through the foam network under gravity.

A significant parameter affecting the coalescence is *critical liquid fraction*. In freshly formed foam, the initial liquid fraction is nearly the same throughout the system. For smaller foam bubbles, the decrease in liquid fraction is much slower during the drainage. This may be due to the slower velocity of the aqueous solution in the Plateau border or nodes in the foam. This explains the frequently-observed fact that foams with small bubbles are more stable. However, an opposite phenomenon is observed for the large bubbles, where a sudden decrease in the liquid fraction is observed, which

corresponds to the onset of the rupture point. Coalescence of the large bubbles results in avalanches, whereas a decrease in the height of fine foams is nearly continuous. Coalescence is dramatically enhanced below a critical liquid fraction, which depends on the nature of the surfactant and its concentration. Bubble coalescence may occur due to the non-uniformity in the size and shape of the films, which form the faces of the polyhedral bubbles. Eventually, this leads to a nonuniformity in the film-drainage rate, and hence in the film thickness within any volume element of the foam.

1.10 Specific ion effect

In almost all chemical, physical, atmospheric, and biological applications, aqueous foam systems contain various types of ions. The specific ion phenomena are observed when ions of the same valence behave distinctly in the bulk liquid and at the interface.[98] The hydration of the ions and the interactions of these ions with the surfactant molecules play a significant role in many natural and technological processes. Ion specificity plays a pivotal role in electrode and corrosion processes,[99,100] interaction among colloid particles and electrolytes,[101] and the stability of aggregates of amphiphilic species (e.g., vesicles and micelles).[102,103] They also play a significant role in atmospheric chemistry that includes ocean surfaces and seawater aerosols along with the arctic snow packs covered by the sea spray.[104-110] The specific ion effect helps us understand the interaction of these ions with proteins, colloidal particles, and surfactant systems.

Specific ion effect has been investigated over the past 130 years, commencing after the pioneering work of Franz Hofmeister.[111-114] His seminal work at the University of Prague investigated the precipitation efficiency of the proteins. Hofmeister developed a series based on the efficiency of the ions to precipitate the proteins at the critical electrolyte concentration (i.e., the minimum concentration of an electrolyte required to

precipitate a given protein from the solution). This series is called "Hofmeister series" (see Figure 1.16). It is independent of the protein involved.[115,116] Specific ion effect influences many biological processes that fall within the Hofmeister paradigm, and the strength of action of the anions and cations follow a well-defined order, independent of the co-ion. In addition, it has been observed that the relative effect of the ions on the surface tension followed closely with the Hofmeister series.[117]

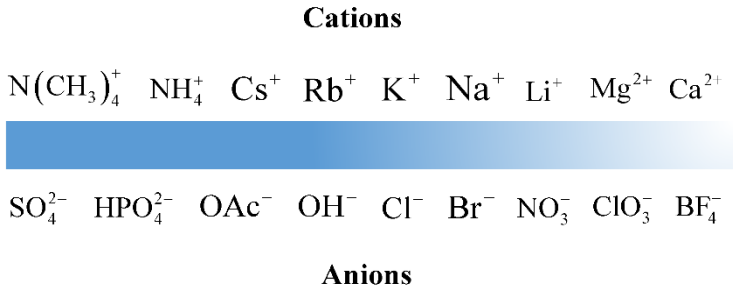

Figure 1.16. Order of cations and anions in the Hofmeister series.[98]

The specific ion effect has been studied by several renowned scientists.[118–141] Several experimental works have validated the pioneering work of Hofmeister. However, the significance of the Hofmeister series is not limited to the proteins. Kunz[142] has reviewed this effect in the biochemical systems, in aqueous solutions, in colloidal dispersions, and at the air–water interface. Jones and Dole,[118] and Cox and Wolfenden[143] have further refined and explained this effect. The former examined it with respect to the viscosity and computed the viscosity B coefficient (which is known by their names), whereas the latter evaluated this coefficient for various uni-univalent electrolytes in the aqueous solution. Frank and Evans[144] derived the expressions for 'water-structure maker' and 'water-structure breaker', and introduced a relationship between the viscosity and the entropy of dilution. The common question often raised regarding this effect is the

origin of interaction beyond the electrostatic interactions of the simple ions with water and other solutes. Furthermore, the role of the size of the ions, geometry, charge density, charge distribution, and the dispersion forces are often analyzed to explain the specific ion effect.

Collins[38] introduced the concept of "matching water affinities" to elucidate the Hofmeister series. He showed that the effect of an ion on the structure of water depends to a large extent on its charge density, and whether the water–water interactions in the bulk solution are comparable to the ion–water interactions. In Collins' concept, each ion is considered as a sphere with a point charge at its center. The adjacent water molecules are tightly bound around the small ions owing to their high charge density. These ions are referred to as kosmotropic or hard ions. Large ions have a loose hydration shell, and they are referred to as chaotropic or soft ions. Owing to the strong electrostatic attraction, they tend to pair due to their loose hydration shells. The situation is different when it comes to the small–large pair of ions of opposite charge. In this case, the electrostatic attraction by the large ion is not sufficient enough that the hard ion loses its hydration shell. Therefore, a small–large or (kosmotropic–chaotropic) ion pair tends to remain apart in the aqueous solutions.

Although Collins' concept of "matching water affinities" allows one to understand the general effect of salts on bubble coalescence, it does not explain the observations concerning the inhibiting effect of all salts on bubble coalescence. For example, NaF (as a kosmotrope–kosmotrope salt with matching affinities) has a stronger effect on bubble coalescence as compared to NaI or NaCl (as kosmotrope–chaotrope salts). NaF and KI are kosmotrope–kosmotrope and chaotrope–chaotrope salts, respectively. Based on the concept of matching affinities, both of them should have a more substantial effect than

the kosmotrope–chaotrope salts such as NaI or NaCl. However, this contrasts with the experimental observations on the effect of these salts on bubble coalescence.

Powale and Bhagat[145] studied the influence of various electrolytes on the foamability of aqueous solutions of commercial grade sodium dodecyl sulfate. The addition of NaCl increased the foaming efficiency whereas the foaming effectiveness was increased only marginally. Here foaming effectiveness is a maximum value of foamability attained by the surfactant solution, whereas foaming efficiency is a concentration of surfactant required to achieve certain foamability value. The effect of cations on foaming efficiency and effectiveness was found to be in the following order: $Li^+ < Na^+ < Cs^+$. They explained this phenomenon in terms of the hydrated size of the cations, which follows the reverse order, i.e., $Li^+ > Na^+ > Cs^+$. Warszyński and coworkers[146–148] measured the specific ion effect on the adsorption of ionic surfactants and calculated their adsorption constant. Their investigation involved the measurement of surface tension of aqueous solutions of sodium dodecyl sulfate in the presence of cations and anions.

The specific ion effect can be studied by adding different electrolytes (e.g., NaCl. KCl, LiCl, and CsCl) to a surfactant solution. The film thickness and stability of foams are linked to the interaction between the surfactant head-groups and the ions. The impact of these ions on the foam film properties can be observed by replacing the inorganic ions by organic electrolytes. The impact of the cations and anions on the properties of the foam are dominated by the electrostatic and/or ion specific interactions. Although the specific ion effects in foam films are of high significance for many applications, the amount of research performed on this topic is rather negligible. This works aims to study the influence of various 1:1 salts on the adsorption of a zwitterionic surfactant at the air–water

interface, and the formation and stability of foams.

1.11 Mixed surfactant systems

Mixed surfactant systems are used in many industrial applications.[149,150] These surfactant systems sometimes occur as a result of nonhomogeneous raw materials, which have mixed chain lengths. The surface activity in the mixed surfactant system can be significantly enhanced than the single surfactant system. It can considerably reduce the surface tension and lower the CMC as compared to the single surfactant system. This useful feature of the mixed surfactant system makes it preferred in commercial and industrial applications. Mixed surfactants, even at low concentrations can display significant modifications of the interfacial properties.

When a purposeful mixing of different types of surfactant yields a greater decrease in the surface tension and CMC than that attainable with any of the individual surfactants, the interaction is termed as *synergistic* and the mixture exhibits synergism. However, when a higher concentration of mixed surfactant is required than any of the individual surfactants, the mixture is said to exhibit *antagonism*. The synergistic interactions between a few surfactants have been observed for many years and the quantitative investigation on synergism has been studied since the last 3 – 4 decades.[151] The nature and strength of the interaction between two different surfactant molecules adsorbed at the interface is indicated by the interaction parameter (β), which is related to the free energy change upon mixing of the two surfactants (ΔG_{mix}) by the following equation:

$$\Delta G_{mix} = \beta x(1-x)RT \qquad (1.16)$$

where x is the mole fraction of the first surfactant and $(1-x)$ is the mole fraction of the second surfactant in the mixture adsorbed at the interface. β is significantly influenced

by the steric effects, inasmuch as its value depends on the variation in the size of the hydrophilic head-groups, or in a few cases, on the branching of the hydrophobic tails of the two surfactants.[152] In a mixed surfactant system, the CMC of the solution depends on the composition of the mixture and the CMCs of the individual surfactants. The CMC of a mixed system depends on the interactions occurring among the head-groups of the surfactants, which may lead to a non-ideal mixing in the micelle.

1.11.1 Interactions in the mixed surfactant monolayer and in the mixed micelle

Several works have investigated the interactions between the surfactants in the monolayer and in the micelle in the mixed surfactant systems. Rosen and Hua[151] developed a procedure for quantitatively evaluating the interaction between two different surfactants in a mixed system. Let us denote the two surfactants by the subscripts 1 and 2. The mole fraction of surfactant 1 in the mixed monolayer (x_1) and the interaction parameter (β^σ) can be calculated by solving the following equations:

$$\frac{x_1^2 \ln\left[c_{12}/\left(x_1 c_1^0\right)\right]}{\left(1-x_1\right)^2 \ln\left[c_{12}/\left\{\left(1-x_1\right)c_2^0\right\}\right]} = 1 \qquad (1.17)$$

$$\beta^\sigma = \frac{\ln\left[c_{12}/\left(x_1 c_1^0\right)\right]}{\left(1-x_1\right)^2} \qquad (1.18)$$

where c_1^0 and c_2^0 are the solution-phase concentrations of the pure surfactants 1 and 2, respectively, and c_{12} and c_{21} are the corresponding solution-phase concentrations of these surfactants in their mixture required to produce a specific surface tension. x_1 is the mole fraction of surfactant 1 in the mixture (on a surfactant-only basis) adsorbed at the interface. β^σ indicates the strength and nature of the molecular interaction between the two types of surfactant at the air–water interface, and its value signifies the deviation of

the mixture from ideality. This interaction parameter can be estimated from the surface tension data.

A few assumptions were made while deriving equations (1.17) and (1.18). The electrostatic effects were ignored. The surfactants were assumed to be molecularly homogenous, without any surface active impurity. It was also assumed that the area occupied by a surfactant molecule in the monolayer is not significantly different from that in the mixed monolayer. This assumption is valid for weak interactions only.[153] However, researchers have used these equations for systems where strong interactions were present (and the interaction parameters were large).[152,154] These equations are best suited for the surfactant systems in which low to moderate interactions are present. The ratios of the activity coefficients of the surfactants in the mixture and in the pure form in the solution have been assumed to be unity. This is correct when the surfactant concentrations are low (e.g., < 10 mol m^{-3}).

β^{σ} is proportional to the free energy change occurring in the mixed surfactant system, and depends on the size of the hydrophilic head-groups and branching in them.[152] The values of the interaction parameter can be used to predict the feasibility of synergism among the surfactants. A negative value of β^{σ} indicates either a greater attraction or a less repulsion between the two surfactants upon mixing. On the other hand, a positive value of β^{σ} has the opposite interpretation inasmuch as it signifies a less attraction or a greater repulsion between the two surfactants upon mixing. The value of β^{σ} is zero when the mixing is ideal.

The mole fraction of surfactant 1 in the micelle $\left(x_1^{\mathrm{M}}\right)$ can be computed by using the following equation:

$$\frac{\left(x_1^{\mathrm{M}}\right)^2 \ln\left[c_{12}^{\mathrm{M}}/\left(x_1^{\mathrm{M}}c_1^{\mathrm{M}}\right)\right]}{\left(1-x_1^{\mathrm{M}}\right)^2 \ln\left[c_{21}^{\mathrm{M}}/\left\{\left(1-x_1^{\mathrm{M}}\right)c_2^{\mathrm{M}}\right\}\right]} = 1 \qquad (1.19)$$

where c_1^{M} and c_2^{M} are the CMCs of the individual surfactants 1 and 2, respectively, and c_{12}^{M} and c_{21}^{M} are the corresponding concentrations of these surfactants in the mixture at the CMC. The interaction parameter that measures the nature and extent of the interaction between the two-surfactant molecules in the mixed micelle $\left(\beta^{\mathrm{M}}\right)$ is given by the following equation:

$$\beta^{\mathrm{M}} = \frac{\ln\left(c_{12}^{\mathrm{M}}/x_1^{\mathrm{M}}c_1^{\mathrm{M}}\right)}{\left(1-x_1^{\mathrm{M}}\right)^2} \qquad (1.20)$$

The value of β^{M} does not vary much upon changing the ratio of the surfactant concentrations in the solution.

Equations (1.17) – (1.20) have been employed widely for investigating the interactions in the surfactant mixtures.[153,154] Addition of salt alters the value of the interaction parameter due to the change in electrostatic interaction. A complex may be formed in the monolayer in the surfactant–salt mixture, which can change the monolayer structure.[153] Equations (1.17) and (1.19) contain the terms $\left[\left(x_1\right)^2/\left(1-x_1\right)^2\right]$ and $\left[\left(x_1^{\mathrm{M}}\right)^2/\left(1-x_1^{\mathrm{M}}\right)^2\right]$, respectively, which change rapidly when x_1 or x_1^{M} approaches either zero or unity. Therefore, these equations are sensitive to error, and they are suitable when the values of x_1 and x_1^{M} lie between 0.2 and 0.8. Thus, while calculating the interaction parameters, the surfactant concentrations should be selected such that these limits are not approached.

For any mixed surfactant system, the values of β^{σ} and β^{M} are usually different.

Generally, a stronger interaction exists in the mixed monolayer than that in the mixed micelle. Type I synergism is perhaps the most desirable synergism for a mixed surfactant system. The conditions necessary for Type I synergism are

$$\beta^{\sigma} - \beta^{\mathrm{M}} < 0 \tag{1.21}$$

and

$$\left|\beta^{\sigma} - \beta^{\mathrm{M}}\right| > \left|\ln\left(\frac{c_1^{0,\mathrm{CMC}} c_2^{0,\mathrm{M}}}{c_2^{0,\mathrm{CMC}} c_1^{0,\mathrm{M}}}\right)\right| \tag{1.22}$$

where $c_1^{0,\mathrm{CMC}}$ and $c_2^{0,\mathrm{CMC}}$ are the concentrations of surfactants 1 and 2, respectively, required to yield a surface tension equal to that of the mixture at its CMC. These quantities are determined by extrapolation of the surface tension versus concentration profiles of the pure surfactants.[5]

1.12 Objectives of research

The main aim of this work was to investigate the foamability and foam stability in the presence of a zwitterionic surfactant (i.e., DDAPS) and various salts, the specific ion effect, and synergism (in the presence of a cationic surfactant). The main objectives are as follows:

[1] Investigate the adsorption of DDAPS at the air–water and hexane–water interfaces, and foaming of its aqueous solutions in the presence and absence of hexane.

[2] Study the effects of NaCl, $CaCl_2$, and $AlCl_3$ on foamability and foam stability.

[3] Study the electrical properties of air–water and hexane–water interfaces in the presence of the salts mentioned above.

[4] Investigate the specific ion effect in the presence of three 1:1 salts (i.e., NaCl, CsCl, and LiCl).

[5] Study foamability and foam stability in the presence of the salts mentioned above.

[6] Study synergism with a cationic surfactant (i.e., CTAB) in the presence of NaCl.

[7] Investigate the role of the synergism mentioned above in foamability and foam stability.

[8] Study the interactions in the mixed surfactant monolayer and mixed micelle for the CTAB–DDAPS system in the presence of NaCl.

[9] Measure the zeta potential at the air–water interface in the mixed surfactant systems and analyze its role in foam stability.

1.13 Outline of the thesis

This thesis deals with the specific characteristics, which are pivotal to foam stability in the presence of a zwitterionic surfactant, inorganic salt, and in the mixture of the zwitterionic surfactant with a cationic surfactant. The structure of the thesis is described below.

Chapter 1 **(Introduction)**: This chapter discusses the type and characteristics of surfactants and gives an overview of foam morphology, foamability, foam stability, foam formation process, film elasticity, Marangoni effect, intermolecular and surface forces, interfacial rheology, foam decay, specific ion effect, and the mixed surfactant systems. The objectives of the research are also outlined in this chapter.

Chapter 2 **(Materials and Methods)**: In this chapter, the materials used in the experimental studies and their sources are given. Detailed information on the sample preparation methods, equipment used, and the experimental procedures is provided.

Chapter 3 **(Foaming in Aqueous Solutions of Zwitterionic Surfactant: Effects of Oil and Salts)**: In this chapter, a study on the foams generated from the aqueous solutions of a zwitterionic surfactant (i.e., DDAPS) in the presence of NaCl, $CaCl_2$, and $AlCl_3$ is reported. The effect of oil (i.e., n-hexane) on foam stability is also presented. The

adsorption of DDAPS at the air–water and oil–water interfaces in the presence of the salts is studied by surface and interfacial tension measurements. The Blender Test is used to investigate the foamability and foam stability. The size distribution of the hexane droplets in the aqueous phase is measured by using dynamic light scattering. The electrical properties of the oil–water interface are also measured and explained. The entering, bridging, and spreading coefficients are calculated, and these are used to explain the stability of foams in the presence of oil.

Chapter 4 **(Foaming in Aqueous Solutions of Zwitterionic Surfactant in Presence of Monovalent Salts: The Specific Ion Effect)**: In this chapter, the stability of foams prepared from the aqueous solutions of DDAPS in the presence of three 1:1 salts having the same anion (i.e., NaCl, CsCl, and LiCl) is reported. The adsorption of DDAPS at the air–water and hexane–water interfaces in the presence of these monovalent salts is studied by surface and interfacial tension measurements. The efficiency of these salts in decreasing the surface tension and foam stability is explained. The zeta potential at the hexane–water interface in the presence of DDAPS and these salts is measured and explained. The interaction between the surfactant and salts is analyzed.

Chapter 5 **(Foaming in Aqueous Solutions of a Mixture of Zwitterionic and Cationic Surfactants in the Presence of an Electrolyte)**: In this chapter, the synergism in the mixture of a zwitterionic (i.e., DDAPS) and a cationic (i.e., CTAB) surfactant is reported. These studies are carried out at different ratios of the surfactants and in the presence of NaCl. The interaction between the adsorbed surfactant molecules at the air–water interface influences the monolayer properties. Adsorption at the air–water interface is studied by measuring the surface tension. The synergism between DDAPS and CTAB is studied by measuring the surface tension at various compositions of the surfactants and

the salt. The foamability and foam stability are studied by employing the Blender Test. The zeta potential at the air–water interface in the mixed surfactant systems is also measured and explained.

Chapter 6 **(Summary and Scope for Future Work)**: This chapter presents the summary of the work reported in this thesis, and provides new ideas for future research.

References

[1] Kaptay, G. The chemical (not mechanical) paradigm of thermodynamics of colloid and interface science. *Adv. Colloid Interface Sci.* **2018,** 256, 163–192.

[2] Bradley, L. C.; Chen, W.-H.; Stebe, K. J.; Lee, D. Janus and patchy colloids at fluid interfaces. *Curr. Opin. Colloid Interface Sci.* **2017,** 30, 25–33.

[3] Barnes, G.; Gentle, I., *Interfacial Science: An Introduction*; Oxford University Press: Oxford, 2011.

[4] Adamson, A. W.; Gast, A. P., *Physical Chemistry of Surfaces*; John Wiley & Sons, Inc.: New York, 1967.

[5] Rosen, M. J., *Surfactants and Interfacial Phenomena*; John Wiley & Sons: New York, 2004.

[6] Mozetič, M.; Vesel, A.; Primc, G.; Eisenmenger-Sittner, C.; Bauer, J.; Eder, A.; Schmid, G. H. S.; Ruzic, D. N.; Ahmed, Z.; Barker, D.; Douglass, K. O.; Eckel, S.; Fedchak, J. A.; Hendricks, J.; Klimov, N.; Ricker, J.; Scherschligt, J.; Stone, J.; Strouse, G.; Capan, I.; Buljan, M.; Milošević, S.; Teichert, C.; Cohen, S. R.; Silva, A. G.; Lehocky, M.; Humpoliček, P.; Rodriguez, C.; Hernandez-Montelongo, J.; Mercier, D.; Manso-Silván, M.; Ceccone, G.; Galtayries, A.; Stana-Kleinschek, K.; Petrov, I.; Greene, J. E.; Avila, J.; Chen, C. Y.; Caja-Munoz, B.; Yi, H.; Boury, A.; Lorcy, S.; Asensio, M. C.; Bredin, J.; Gans, T.; O'Connell, D.; Brendin, J.; Reniers, F.; Vincze, A.; Anderle, M.; Montelius, L. Recent developments in surface science and engineering, thin films, nanoscience, biomaterials, plasma science, and vacuum technology. *Thin Solid Films* **2018,** 660, 120–160.

[7] Berg, J. C., *An Introduction to Interfaces & Colloids: The Bridge to Nanoscience*; World Scientific: Singapore, 2010.

[8] Zangwill, A., *Physics at Surfaces*; Cambridge University Press: Cambridge, 1988.

[9] Baletto, F.; Ferrando, R. Structural properties of nanoclusters: Energetic, thermodynamic, and kinetic effects. *Rev. Mod. Phys.* **2005,** 77, 371.

[10] Attwood, D., *Surfactant Systems: Their Chemistry, Pharmacy and Biology*; Chapman and Hall: London, 2012.

[11] De, S.; Malik, S.; Ghosh, A.; Saha, R.; Saha, B. A review on natural surfactants. *RSC Adv.* **2015,** 5, 65757–65767.

[12] Kanicky, J. R.; Lopez-Montilla, J.-C.; Pandey, S.; Shah, D. O., *Handbook of Applied Surface and Colloid Chemistry*; John Wiley & Sons Ltd.: West Sussex, 2002.

[13] Bhardwaj, A.; Hartland, S. Applications of surfactants in petroleum industry. *J. Dispersion Sci. Technol.* **1993,** 14, 87–116.

[14] Watcharasing, S.; Kongkowit, W.; Chavadej, S. Motor oil removal from water by continuous froth flotation using extended surfactant: Effects of air bubble parameters and surfactant concentration. *Sep. Purif. Technol.* **2009,** 70, 179–189.

[15] Kandadai, M. A.; Mohan, P.; Lin, G.; Butterfield, A.; Skliar, M.; Magda, J. J. Comparison of surfactants used to prepare aqueous perfluoropentane emulsions for pharmaceutical applications. *Langmuir* **2010,** 26, 4655–4660.

[16] Kowalczuk, P. B. Determination of critical coalescence concentration and bubble size for surfactants used as flotation frothers. *Ind. Eng. Chem. Res.* **2013,** 52, 11752–11757.

[17] Clara, M.; Scharf, S.; Scheffknecht, C.; Gans, O. Occurrence of selected surfactants in untreated and treated sewage. *Water Res.* **2007,** 41, 4339–4348.

[18] Zana, R.; Xia, J., *Gemini Surfactants: Synthesis, Interfacial and Solution-Phase Behavior, and Applications*; Marcel Dekker, Inc.: New York, 2003.

[19] Kralova, I.; Sjöblom, J. Surfactants used in food industry: A review. *J. Dispersion Sci. Technol.* **2009,** 30, 1363–1383.

[20] Aloui, F.; Kchaou, S.; Sayadi, S. Physicochemical treatments of anionic surfactants wastewater: Effect on aerobic biodegradability. *J. Hazard. Mater.* **2009,** 164, 353–359.

[21] Landfester, K.; Bechthold, N.; Tiarks, F.; Antonietti, M. Miniemulsion polymerization with cationic and nonionic surfactants: A very efficient use of surfactants for heterophase polymerization. *Macromol.* **1999,** 32, 2679–2683.

[22] Lawrence, M. J. Surfactant systems: Their use in drug delivery. *Chem. Soc. Rev.* **1994,** 23, 417–424.

[23] Shimizu, M.; Fujii, S.; Tanaka, T.; Kataura, H. Effects of surfactants on the electronic transport properties of thin-film transistors of single-wall carbon nanotubes. *J. Phys. Chem. C* **2013,** 117, 11744–11749.

[24] Dai, Q.; Berman, D.; Virwani, K.; Frommer, J.; Jubert, P.-O.; Lam, M.; Topuria, T.; Imaino, W.; Nelson, A. Self-assembled ferrimagnet–polymer composites for magnetic recording media. *Nano Lett.* **2010,** 10, 3216–3221.

[25] Matsuhisa, N.; Kaltenbrunner, M.; Yokota, T.; Jinno, H.; Kuribara, K.; Sekitani, T.;

Someya, T. Printable elastic conductors with a high conductivity for electronic textile applications. *Nat. Commun.* **2015,** 6, 7461–7472.

[26] Lim, S.; Park, S. H.; An, T. K.; Lee, H. S.; Kim, S. H. Electrohydrodynamic printing of poly(3,4-ethylenedioxythiophene):poly(4-styrenesulfonate) electrodes with ratio-optimized surfactant. *RSC Adv.* **2016,** 6, 2004–2010.

[27] Mulligan, C.; Yong, R.; Gibbs, B. Surfactant-enhanced remediation of contaminated soil: A review. *Eng. Geol.* **2001,** 60, 371–380.

[28] Park, J. W.; Takahata, Y.; Kajiuchi, T.; Akehata, T. Effects of nonionic surfactant on enzymatic hydrolysis of used newspaper. *Biotechnol. Bioeng.* **1992,** 39, 117–120.

[29] Tanford, C., *The Hydrophobic Effect: Formation of Micelles and Biological Membranes*; John Wiley & Sons: New York, 1980.

[30] Scriven, L. Equilibrium bicontinuous structure. *Nature* **1976,** 263, 123–125.

[31] Schramm, L. L.; Stasiuk, E. N.; Marangoni, D. G. Surfactants and their applications. *Annu. Rep. Prog. Chem., Sect. C: Phys. Chem.* **2003,** 99, 3–48.

[32] Porter, M. R., *Handbook of Surfactants*; Chapman and Hall: London, 1994.

[33] Bhakta, A.; Ruckenstein, E. Decay of standing foams: Drainage, coalescence and collapse. *Adv. Colloid Interface Sci.* **1997,** 70, 1–124.

[34] Wilson, A. J., *Foams: Physics, Chemistry and Structure*; Springer: London, 1989.

[35] Moody, C. A.; Field, J. A. Perfluorinated surfactants and the environmental implications of their use in fire-fighting foams. *Environ. Sci. Tech.* **2000,** 34, 3864–3870.

[36] Vinogradov, A. V.; Kuprin, D.; Abduragimov, I.; Kuprin, G.; Serebriyakov, E.; Vinogradov, V. V. Silica foams for fire prevention and firefighting. *Appl. Mater. Interfaces* **2016,** 8, 294–301.

[37] Yang, J.; Jovancicevic, V.; Ramachandran, S. Foam for gas well deliquification. *Colloids and Surf. A* **2007,** 309, 177–181.

[38] Golemanov, K.; Denkov, N.; Tcholakova, S.; Vethamuthu, M.; Lips, A. Surfactant mixtures for control of bubble surface mobility in foam studies. *Langmuir* **2008,** 24, 9956–9961.

[39] Simjoo, M.; Dong, Y.; Andrianov, A.; Talanana, M.; Zitha, P. CT scan study of immiscible foam flow in porous media for enhancing oil recovery. *Ind. Eng. Chem. Res.* **2013,** 52, 6221–6233.

[40] Deliyanni, E. A.; Kyzas, G. Z.; Matis, K. A. Various flotation techniques for metal ions removal. *J. Mol. Liq.* **2017,** 225, 260–264.

[41] Nguyen, A.; Schulze, H. J., *Colloidal Science of Flotation*; Marcel Dekker: New York, 2004.

[42] Cantat, I.; Cohen-Addad, S.; Elias, F.; Graner, F.; Höhler, R.; Pitois, O.; Rouyer, F.; Saint-Jalmes, A., *Foams: Structure and Dynamics*; Oxford University Press: Oxford, 2013.

[43] Hill, C.; Eastoe, J. Foams: From nature to industry. *Adv. Colloid Interface Sci.* **2017,** 247, 496–513.

[44] Weaire, D. L.; Hutzler, S., *The Physics of Foams*; Oxford University Press: Dublin, 2000.

[45] Montanaro, L.; Jorand, Y.; Fantozzi, G.; Negro, A. Ceramic foams by powder processing. *J. Eur. Ceram. Soc.* **1998,** 18, 1339–1350.

[46] Bienvenu, Y. Application and future of solid foams. *Comptes Rendus Physique* **2014,** 15, 719–730.

[47] Ross, S.; Nishioka, G., *Foams*; John Wiley & Sons: New York, 1980.

[48] Deshpande, N.; Barigou, M. The flow of gas–liquid foams in vertical pipes. *Chem. Eng. Sci.* **2000,** 55, 4297–4309.

[49] Cohen-Addad, S.; Höhler, R. Rheology of foams and highly concentrated emulsions. *Curr. Opin. Colloid Interface Sci.* **2014,** 19, 536–548.

[50] Pugh, R. Experimental techniques for studying the structure of foams and froths. *Adv. Colloid Interface Sci.* **2005,** 114, 239–251.

[51] Langevin, D. Aqueous foams: A field of investigation at the frontier between chemistry and physics. *ChemPhysChem* **2008,** 9, 510–522.

[52] Stone, H.; Koehler, S.; Hilgenfeldt, S.; Durand, M. Perspectives on foam drainage and the influence of interfacial rheology. *J. Phys.: Condens. Matter* **2002,** 15, 283–290.

[53] Durian, D. J. Foam mechanics at the bubble scale. *Phys. Rev. Lett.* **1995,** 75, 4780–4783.

[54] Weaire, D. The rheology of foam. *Curr. Opin. Colloid Interface Sci.* **2008,** 13, 171–176.

[55] Koehler, S. A.; Hilgenfeldt, S.; Stone, H. A. Liquid flow through aqueous foams:

The node-dominated foam drainage equation. *Phys. Rev. Lett.* **1999,** 82, 4232–4235.

[56] Narsimhan, G.; Ruckenstein, E. Effect of bubble size distribution on the enrichment and collapse in foams. *Langmuir* **1986,** 2, 494–508.

[57] Koczo, K.; Racz, G. Flow in a Plateau border. *Colloids Surf.* **1987,** 22, 95–96.

[58] Butt, H. J.; Graf, K.; Kappl, M., *Physics and Chemistry of Interfaces*; Wiley-VCH: Weinheim, 2004.

[59] Rio, E.; Drenckhan, W.; Salonen, A.; Langevin, D. Unusually stable liquid foams. *Adv. Colloid Interface Sci.* **2014,** 205, 74–86.

[60] Gonzenbach, U. T.; Studart, A. R.; Tervoort, E.; Gauckler, L. J. Stabilization of foams with inorganic colloidal particles. *Langmuir* **2006,** 22, 10983–10988.

[61] Chang, C.-H.; Franses, E. I. Adsorption dynamics of surfactants at the air/water interface: A critical review of mathematical models, data, and mechanisms. *Colloids and Surf. A* **1995,** 100, 1–45.

[62] Coke, M.; Wilde, P. J.; Russell, E. J.; Clark, D. C. The influence of surface composition and molecular diffusion on the stability of foams formed from protein/surfactant mixtures. *J. Colloid Interface Sci.* **1990,** 138, 489–504.

[63] Wang, J.; Nguyen, A. V.; Farrokhpay, S. A critical review of the growth, drainage and collapse of foams. *Adv. Colloid Interface Sci.* **2016,** 228, 55–70.

[64] Georgieva, D.; Cagna, A.; Langevin, D. Link between surface elasticity and foam stability. *Soft Matter* **2009,** 5, 2063–2071.

[65] Wang, L.; Yoon, R.-H. Effects of surface forces and film elasticity on foam stability. *Int. J. Miner. Process.* **2008,** 85, 101–110.

[66] Grassia, P.; Ubal, S.; Giavedoni, M. D.; Vitasari, D.; Martin, P. J. Surfactant flow between a Plateau border and a film during foam fractionation. *Chem. Eng. Sci.* **2016,** 143, 139–165.

[67] Vitasari, D.; Grassia, P.; Martin, P. Surfactant transport onto a foam lamella. *Chem. Eng. Sci.* **2013,** 102, 405–423.

[68] Myers, T. Application of non-Newtonian models to thin film flow. *Phys. Rev. E,* **2005,** 72, 66302–66312.

[69] Marangoni, C.; Stefanelli, P.; Liceo, R. Monografia sulle bolle liquide. *Il Nuovo Cimento* **1872,** 7, 301–356.

[70] Slattery, J.C., *Interfacial Transport Phenomena*; Springer: Boston, 2007.

[71] Molder, E.; Tenno, T.; Nigu, P. The influence of surfactants on oxygen mass-transfer through the air−water surface. *Crit. Rev. Anal. Chem.* **1998,** 28, 75–80.

[72] Goodridge, F.; Bricknell, D. Interfacial resistance in the carbon dioxide−water system. *Trans. Inst. Chem. Eng* **1962,** 54–60.

[73] Harvey, E.; Smith, W. The absorption of carbon dioxide by a quiescent liquid. *Chem. Eng. Sci.* **1959,** 10, 274–280.

[74] Princen, H.; Mason, S. The permeability of soap films to gases. *J. Colloid Sci.* **1965,** 20, 353–375.

[75] Princen, H.; Overbeek, J. Th. G.; Mason, S. The permeability of soap films to gases: II. A simple mechanism of monolayer permeability. *J. Colloid Interface Sci.* **1967,** 24, 125–130.

[76] Fameau, A.-L.; Carl, A.; Saint-Jalmes, A.; Von Klitzing, R. Responsive aqueous foams. *ChemPhysChem* **2015,** 16, 66–75.

[77] Hilgenfeldt, S.; Koehler, S. A.; Stone, H. A. Dynamics of coarsening foams: Accelerated and self-limiting drainage. *Phys. Rev. Lett.* **2001,** 86, 4704–4707.

[78] Bos, M. A.; van Vliet, T. Interfacial rheological properties of adsorbed protein layers and surfactants: A review. *Adv. Colloid Interface Sci.* **2001,** 91, 437–471.

[79] Derjaguin, B. Experimental investigations on solvation of surfaces with application to the development of a mathematical theory of the stability of lyophobic colloids. *Bull. Acad. Sci. URSS Phys. Ser.* **1937,** 5, 1153–1164.

[80] Derjaguin, B. On the repulsive forces between charged colloid particles and on the theory of slow coagulation and stability of lyophobe sols. *Trans. Faraday Soc.* **1940,** 35, 203–215.

[81] Mysels, K. J.; Shinoda, K.; Frankel, S., *Soap Films: Studies of their Thinning*; Pergamon press: London, 1959.

[82] Bergeron, V. Forces and structure in thin liquid soap films. *J. Phys.: Condens. Matter* **1999,** 11, R215–R238.

[83] Stubenrauch, C.; Von Klitzing, R. Disjoining pressure in thin liquid foam and emulsion films−new concepts and perspectives. *J. Phys.: Condens. Matter* **2003,** 15, R1197–R1232.

[84] Churaev, N. V. Derjaguin's disjoining pressure in the colloid science and surface phenomena. *Adv. Colloid Interface Sci.* **2003,** 104, XV–XX.

[85] Derjaguin, B.; Churaev, N. On the question of determining the concept of disjoining pressure and its role in the equilibrium and flow of thin films. *J. Colloid Interface Sci.* **1978,** 66, 389–398.

[86] Israelachvili, J. N., *Intermolecular and Surface Forces*; Academic Press: London, 2011.

[87] Hunter, R. J., *Foundations of Colloid Science*; Oxford University Press: Oxford, 2001.

[88] Hamaker, H. The London–van der Waals attraction between spherical particles. *Physica* **1937,** 4, 1058–1072.

[89] Lyklema, J., *Fundamentals of Interface and Colloid Science: Soft Colloids*; Academic Press: San Diego, 2005.

[90] Scheludko, A.; Exerowa, D. Über den elektrostatischen und van der Waalsschen zusätzlichen Druck in wässerigen Schaumfilmen. *Kolloid-Zeitschrift* **1960,** 168, 24–28.

[91] Ivanov, I., *Thin liquid films*; Marcel Dekker: New York, 1988.

[92] Möbius, D.; Miller, R., *Proteins at Liquid Interfaces*; Elsevier: Amsterdam, 1998.

[93] Sheludko, A. Thin liquid films. *Adv. Colloid Interface Sci.* **1967,** 1, 391–464.

[94] Joye, J. L.; Hirasaki, G. J.; Miller, C. A. Dimple formation and behavior during axisymmetrical foam film drainage. *Langmuir* **1992,** 8, 3083–3092.

[95] Narsimhan, G.; Ruckenstein, E. Hydrodynamics, enrichment, and collapse in foams. *Langmuir* **1986,** 2, 230–238.

[96] Nikolov, A.; Wasan, D.; Denkov, N.; Kralchevsky, P.; Ivanov, I. Drainage of foam films in the presence of nonionic micelles. *Progr. Colloid Polym. Sci.* **1990,** 82, 87–98.

[97] Ghosh, P.; Juvekar, V. Analysis of the drop rest phenomenon. *Chem. Eng. Res. Des.* **2002,** 80, 715–728.

[98] Kunz, W., *Specific Ion Effects*; World Scientific: Singapore, 2010.

[99] Kritzer, P. Corrosion in high-temperature and supercritical water and aqueous solutions: A review. *J. Supercrit. Fluids* **2004,** 29, 1–29.

[100] Tucceri, R. A review about the surface resistance technique in electrochemistry. *Surf. Sci. Rep.* **2004,** 56, 85–157.

[101] Tavares, F.; Bratko, D.; Prausnitz, J. The role of salt–macroion van der Waals

interactions in the colloid–colloid potential of mean force. *Curr. Opin. Colloid Interface Sci.* **2004,** 9, 81–86.

[102] Gradzielski, M. Investigations of the dynamics of morphological transitions in amphiphilic systems. *Curr. Opin. Colloid Interface Sci.* **2004,** 9, 256–263.

[103] Bharat, T. V.; Das, P.; Buragadda, V. Specific ion effects on surrogate compatibility indices of bentonite for hydraulic barrier applications. *Int. J. Geotech. Eng.* **2019,** 13, 360–368.

[104] Finlayson-Pitts, B. The tropospheric chemistry of sea salt: A molecular-level view of the chemistry of NaCl and NaBr. *Chem. Rev.* **2003,** 103, 4801–4822.

[105] Finlayson-Pitts, B. J.; Hemminger, J. C. Physical chemistry of airborne sea salt particles and their components. *J. Phys. Chem. A* **2000,** 104, 11463–11477.

[106] Hu, J.; Shi, Q.; Davidovits, P.; Worsnop, D.; Zahniser, M.; Kolb, C. Reactive uptake of Cl_2 (g) and Br_2 (g) by aqueous surfaces as a function of Br-and I-ion concentration: The effect of chemical reaction at the interface. *J. Phys. Chem.* **1995,** 99, 8768–8776.

[107] Knipping, E.; Lakin, M.; Foster, K.; Jungwirth, P.; Tobias, D.; Gerber, R.; Dabdub, D.; Finlayson-Pitts, B. Experiments and simulations of ion-enhanced interfacial chemistry on aqueous NaCl aerosols. *Science* **2000,** 288, 301–306.

[108] Laskin, A.; Gaspar, D. J.; Wang, W.; Hunt, S. W.; Cowin, J. P.; Colson, S. D.; Finlayson-Pitts, B. J. Reactions at interfaces as a source of sulfate formation in sea salt particles. *Science* **2003,** 301, 340–344.

[109] Oum, K.; Lakin, M.; Finlayson-Pitts, B. Bromine activation in the troposphere by the dark reaction of O_3 with seawater ice. *Geophys. Res. Lett.* **1998,** 25, 3923–3926.

[110] Spicer, C. W.; Plastridge, R. A.; Foster, K. L.; Finlayson-Pitts, B. J.; Bottenheim, J. W.; Grannas, A. M.; Shepson, P. B. Molecular halogens before and during ozone depletion events in the Arctic at polar sunrise: Concentrations and sources. *Atmos. Environ.* **2002,** 36, 2721–2731.

[111] Hofmeister, F. About the water withdrawing effect of the salts. *Arch. Exp. Path. Pharm.* **1888,** 25, 1–30.

[112] Hofmeister, F. Investigations about the swelling process. *Arch. Exp. Path. Pharm.* **1890,** 27, 395–413.

[113] Hofmeister, F. The contribution of dissolved components to swelling processes.

Arch. Exp. Path. Pharm. **1891,** 28, 210–238.

[114] Hofmeister, F. About regularities in the protein precipitating effects of salts and the relation of these effects with the physiological behavior of salts. *Arch. Exp. Path. Pharm.* **1887,** 24, 247–260.

[115] Schwierz, N.; Horinek, D.; Netz, R. R. Reversed anionic Hofmeister series: The interplay of surface charge and surface polarity. *Langmuir* **2010,** 26, 7370–7379.

[116] Boström, M.; Tavares, F. W.; Finet, S.; Skouri-Panet, F.; Tardieu, A.; Ninham, B. Why forces between proteins follow different Hofmeister series for pH above and below pI. *Biophys. Chem.* **2005,** 117, 217–224.

[117] Boström, M.; Kunz, W.; Ninham, B. W. Hofmeister effects in surface tension of aqueous electrolyte solution. *Langmuir* **2005,** 21, 2619–2623.

[118] Jones, G.; Dole, M. The viscosity of aqueous solutions of strong electrolytes with special reference to barium chloride. *J. Am. Chem. Soc.* **1929,** 51, 2950–2964.

[119] Jones, G.; Ray, W. A. The surface tension of solutions. *J. Am. Chem. Soc.* **1935,** 57, 957–958.

[120] Jones, G.; Ray, W. A. The surface tension of solutions of electrolytes as a function of the concentration. I. A differential method for measuring relative surface tension. *J. Am. Chem. Soc.* **1937,** 59, 187–198.

[121] Jones, G.; Ray, W. A. The surface tension of solutions of electrolytes as a function of the concentration. III. Sodium chloride. *J. Am. Chem. Soc.* **1941,** 63, 3262–3263.

[122] Jones, G.; Ray, W. A. The surface tension of solutions of electrolytes as a function of the concentration II. *J. Am. Chem. Soc.* **1941,** 63, 288–294.

[123] Langmuir, I. The constitution and fundamental properties of solids and liquids. II. Liquids. *J. Am. Chem. Soc.* **1917,** 39, 1848–1906.

[124] Onsager, L.; Samaras, N. N. The surface tension of Debye–Hückel electrolytes. *J. Chem. Phys.* **1934,** 2, 528–536.

[125] Wagner, C. The surface tension of dilute solutions of electrolytes. *Phys. Z.* **1924,** 25, 474–477.

[126] Bhuiyan, L.; Bratko, D.; Outhwaite, C. Electrolyte surface tension in the modified Poisson–Boltzmann approximation. *J. Phys. Chem.* **1991,** 95, 336–340.

[127] Boström, M.; Williams, D. R. M.; Ninham, B. W. Surface tension of electrolytes: Specific ion effects explained by dispersion forces. *Langmuir* **2001,** 17,

4475–4478.

[128] Dole, M. A theory of surface tension of aqueous solutions. *J. Am. Chem. Soc.* **1938,** 60, 904–911.

[129] Dole, M.; Swartout, J. A. A twin-ring surface tensiometer. I. The apparent surface tension of potassium chloride solutions. *J. Am. Chem. Soc.* **1940,** 62, 3039–3045.

[130] Dos Santos, A. P.; Levin, Y. Ion specificity and the theory of stability of colloidal suspensions. *Phys. Rev. Lett.* **2011,** 106, 167801–167804.

[131] Ennis, J.; Kjellander, R.; Mitchell, D. J. Dressed ion theory for bulk symmetric electrolytes in the restricted primitive model. *J. Chem. Phys.* **1995,** 102, 975–991.

[132] Jarvis, N. L.; Scheiman, M. A. Surface potentials of aqueous electrolyte solutions. *J. Phys. Chem.* **1968,** 72, 74–78.

[133] Jungwirth, P.; Tobias, D. J. Molecular structure of salt solutions: A new view of the interface with implications for heterogeneous atmospheric chemistry. *J. Phys. Chem. B* **2001,** 105, 10468–10472.

[134] Karakashev, S.; Tsekov, R.; Manev, E. Adsorption of alkali dodecyl sulfates on air/water surface. *Langmuir* **2001,** 17, 5403–5405.

[135] Kjellander, R. Modified Debye–Hückel approximation with effective charges: An application of dressed ion theory for electrolyte solutions. *J. Phys. Chem.* **1995,** 99, 10392–10407.

[136] Markin, V. S.; Volkov, A. G. Quantitative theory of surface tension and surface potential of aqueous solutions of electrolytes. *J. Phys. Chem. B* **2002,** 106, 11810–11817.

[137] Markovich, T.; Andelman, D.; Podgornik, R. Surface tension of electrolyte solutions: A self-consistent theory. *Europhys. Lett.* **2014,** 106, 16002–16007.

[138] Randles, J. Ionic hydration and the surface potential of aqueous electrolytes. *Discuss. Faraday Soc.* **1957,** 24, 194–199.

[139] Sakai, M. Physico-chemical properties of small bubbles in liquids. *Progr. Colloid Polym. Sci.* **1988,** 77, 136–142.

[140] Slavchov, R. I.; Novev, J. K. Surface tension of concentrated electrolyte solutions. *J. Colloid Interface Sci.* **2012,** 387, 234–243.

[141] Weissenborn, P. K.; Pugh, R. J. Surface tension of aqueous solutions of electrolytes: Relationship with ion hydration, oxygen solubility, and bubble coalescence. *J.*

Colloid Interface Sci. **1996,** 184, 550–563.

[142] Kunz, W.; Nostro, P. L.; Ninham, B. W. The present state of affairs with Hofmeister effects. *Curr. Opin. Colloid Interface Sci.* **2004,** 9, 1–18.

[143] Cox, W.; Wolfenden, J. The viscosity of strong electrolytes measured by a differential method. *Proc. R. Soc. Lond. A* **1934,** 145, 475–488.

[144] Frank, H. S.; Evans, M. W. Free volume and entropy in condensed systems III. Entropy in binary liquid mixtures; partial molal entropy in dilute solutions; structure and thermodynamics in aqueous electrolytes. *J. Chem. Phys.* **1945,** 13, 507–532.

[145] Powale, R. S.; Bhagwat, S. S. Influence of electrolytes on foaming of sodium lauryl sulfate. *J. Dispersion Sci. Technol.* **2006,** 27, 1181–1186.

[146] Para, G.; Jarek, E.; Warszynski, P. The surface tension of aqueous solutions of cetyltrimethylammonium cationic surfactants in presence of bromide and chloride counterions. *Colloids and Surf. A* **2005,** 261, 65–73.

[147] Para, G.; Jarek, E.; Warszynski, P. The Hofmeister series effect in adsorption of cationic surfactants-theoretical description and experimental results. *Adv. Colloid Interface Sci.* **2006,** 122, 39–55.

[148] Warszyński, P.; Lunkenheimer, K.; Czichocki, G. Effect of counterions on the adsorption of ionic surfactants at fluid−fluid interfaces. *Langmuir* **2002,** 18, 2506–2514.

[149] Christian, S. D.; Scamehorn, J. F., *Solubilization in Surfactant Aggregates*; Marcel Dekker: New York, 1995.

[150] Holland, P. M.; Rubingh, D. N., *Mixed Surfactant Systems*; American Chemical Society: Washington, 1992.

[151] Rosen, M. J.; Hua, X. Y. Surface concentrations and molecular interactions in binary mixtures of surfactants. *J. Colloid Interface Sci.* **1982,** 86, 164–172.

[152] Zhou, Q.; Rosen, M. J. Molecular interactions of surfactants in mixed monolayers at the air/aqueous solution interface and in mixed micelles in aqueous media: The regular solution approach. *Langmuir* **2003,** 19, 4555–4562.

[153] Rosen, M. J.; Zhou, Q. Surfactant−surfactant interactions in mixed monolayer and mixed micelle formation. *Langmuir* **2001,** 17, 3532–3537.

[154] Bhat, M.; Gaikar, V. Characterization of interaction between butyl benzene

sulfonates and cetyl trimethylammonium bromide in mixed aggregate systems. *Langmuir* **1999,** 15, 4740–4751.

CHAPTER 2

MATERIALS AND EXPERIMENTAL METHODS

2.1 Materials

The zwitterionic surfactant, N-Dodecyl-N,N-dimethyl-3-ammonio-1-propanesulfonate (DDAPS) ($C_{19}H_{41}NO_3S$) (97% assay) and the cationic surfactant, cetyltrimethylammonium bromide (CTAB) [$CH_3(CH_2)_{15}N(Br)(CH_3)_3$] (99% assay) were purchased from Sigma Aldrich (Bangalore, India). Sodium chloride (99% assay), calcium chloride (98% assay), and aluminum chloride (98% assay) were procured from Merck (Mumbai, India). Lithium chloride (> 98% assay) and cesium chloride (> 98% assay) were purchased from Spectrochem (Mumbai, India). *n*-hexane (> 98% assay) was used as the oil phase. It was purchased from Merck (Mumbai, India). These chemicals were used as received. Experiments were performed using water purified from an ultrapure laboratory water purification system [make: Millipore (Molsheim Cedex, France), model: Elix–3 Milli–Q]. The conductivity and surface tension of this water were 1×10^{-5} S m^{-1} and 72.5 mN m^{-1}, respectively.

2.2 Surface and interfacial tension measurement

Aqueous solutions of DDAPS and CTAB were prepared at different concentrations varying between 0.1 to 2.8 mol m^{-3} and 0.1 to 1.0 mol m^{-3}, respectively. The surface tension of these solutions and the same for the mixed surfactant systems were measured in the presence and in the absence of the salts. A digital tensiometer [make: Kyowa Interface Science (Saitama, Japan), model: DY–300] was used to carry out the measurements. This tensiometer had provisions for a Wilhelmy plate and a du Noüy ring (made of an alloy of platinum and iridium) to measure the surface and interfacial tension. The procedure described in the ASTM (American Society for Testing and Materials) Standard D1331–14 (2014) was followed for measuring these tensions.

The Wilhelmy plate method was used to measure the equilibrium surface tension at the air–water interface. Before each measurement, the Wilhelmy plate and the sample vessels were cleaned. The plate was cleaned by burning it in the blue flame of a Bunsen burner until it became red hot. The material adhering to the plate from the previous experiment was completely removed by burning. Also, the contact angle reduced to zero so that the liquid wetted the plate completely. The plate was dipped inside the surfactant solution to an appropriate depth. The air–water interface was allowed to stand for 1 h to attain equilibrium surfactant adsorption. After that, the plate was slowly pulled out (~0.5 mm s^{-1}) through the interface. The surface tension measured by this method was easily reproducible.

The force (F) exerted by the vertically suspended plate on the air–water interface at the point of detachment is correlated with the surface tension (γ) by the following equation:

$$\gamma = \frac{F}{L_w \cos\theta} \tag{2.1}$$

The Wilhelmy plate method does not have any correction factor since the weight of the film hanging from the plate is insignificant.

The du Noüy ring method may be used to measure the surface and interfacial tension. The procedure adopted for measuring the interfacial tension employing the du Noüy ring was similar to that described in the previous paragraph. The ring was made of an alloy of platinum and iridium. In du Noüy ring method, the maximum force required to detach from the surface (or interface) is measured. The force of detachment (F_d) is equal to the product of the surface (or interfacial) tension and the two circumferences

(i.e., inside and outside) of the ring. Therefore,

$$F_d = 4\pi R_r \gamma \tag{2.2}$$

where R_r is the radius of the ring. It is assumed that the ring is made of a very thin wire, and therefore, its inner and outer radii are equal. The force applied on the ring is continuously measured by the micro-balance as the liquid lamella is withdrawn while the ring moves from the lower liquid phase to the upper phase. The force measured in this way also includes the weight of the liquid raised beneath the ring when the latter is pulled. Therefore, the value of γ obtained from equation (2.2) usually has some error. Harkins and Jordan[1] derived a correction factor (f) experimentally. Incorporating the correction factor in equation (2.2), the corrected surface tension is obtained from the following equation:

$$\gamma = \left(\frac{F}{4\pi R_r}\right) f \tag{2.3}$$

The correction factor depends on the complex shape of the meniscus as the ring detaches, the density of the liquid, the radius of the ring (R_r), and the radius of wire (r_w) with which the ring is made. Huh and Mason[2] have graphically presented the variation of f with R_r^3/V (where V is the volume of the meniscus) and R_r/r_w. The correlation developed by Zuidema and Waters[3] for f is widely used due to its simplicity. Many equipment manufacturers use this correlation. It is given by,

$$f = 0.725 + \left[\frac{0.00363\gamma_{\text{Expt}}}{\pi^2 R_r^2 \Delta\rho} + 0.04534 - 1.679\left(\frac{r_w}{R_r}\right)\right]^{1/2} \tag{2.4}$$

where $\Delta\rho$ is the density difference between the two fluids, γ_{Expt} is the experimentally measured value of surface (or interfacial) tension. It has been found that the

Zuidema–Waters correlation gives accurate results when $\gamma_{Expt} < 35$ mN m^{-1} and $\Delta\rho > 0.1$ kg dm^{-3}. The surface tension measurements were repeated at least five times for each sample, and the mean values are reported. Figure 2.1 shows the principles of the Wilhelmy plate and the du Noüy ring methods. A photograph of the tensiometer used for the above-mentioned experiments is also given.

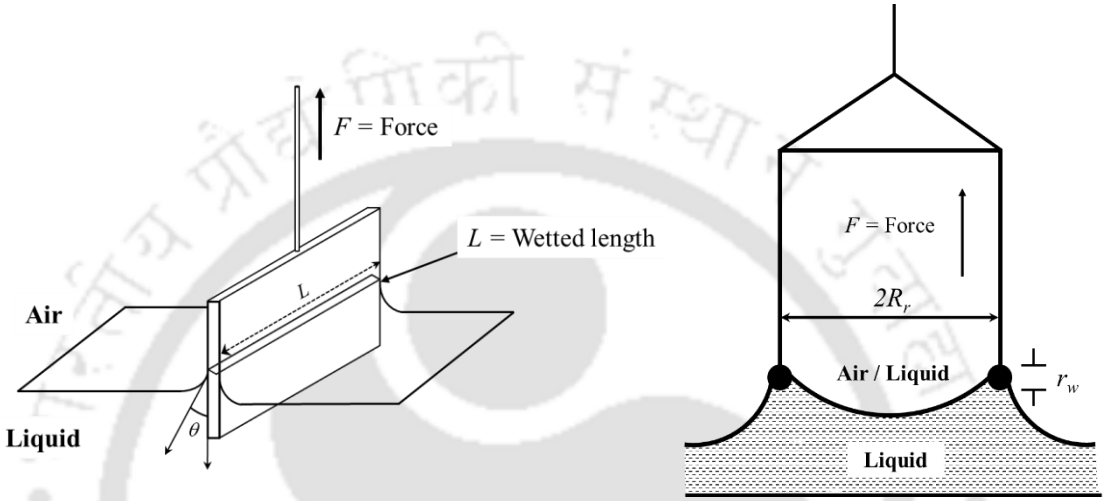

(a) Wilhelmy plate method (b) du Noüy ring method

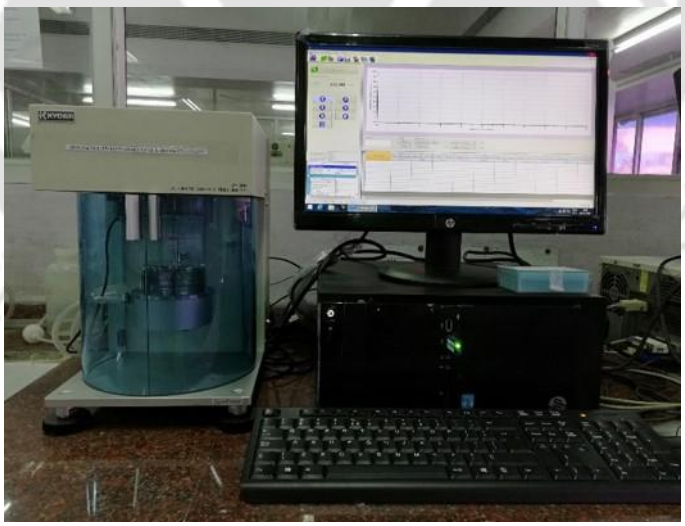

(c)

Figure 2.1. (a) The Wilhelmy plate method, (b) the du Noüy ring method, and (c) the tensiometer used to measure surface and interfacial tension.

2.3 Foamability and foam stability tests

The foam was generated, and its stability was measured by employing the blender test, as described in the ASTM Standard D3519–88 (2007). To produce foam, 200 cm^3 of the aqueous DDAPS solution was placed in the blender [make: Morphy Richards (Mumbai, India), model: Divo essentials] jar and was stirred for 30 s at 15,000 rpm. The foam was very quickly transferred to a measuring cylinder of 1000 cm^3 capacity. The initial foam volume was measured, and the subsequent decrease in volume was noted for a period of 60 to 100 min. The change in foam volume with time was recorded with a DSLR camera [make: Nikon (Bangkok, Thailand), model: D5100]. Each experiment was repeated five times, and the mean values are reported.

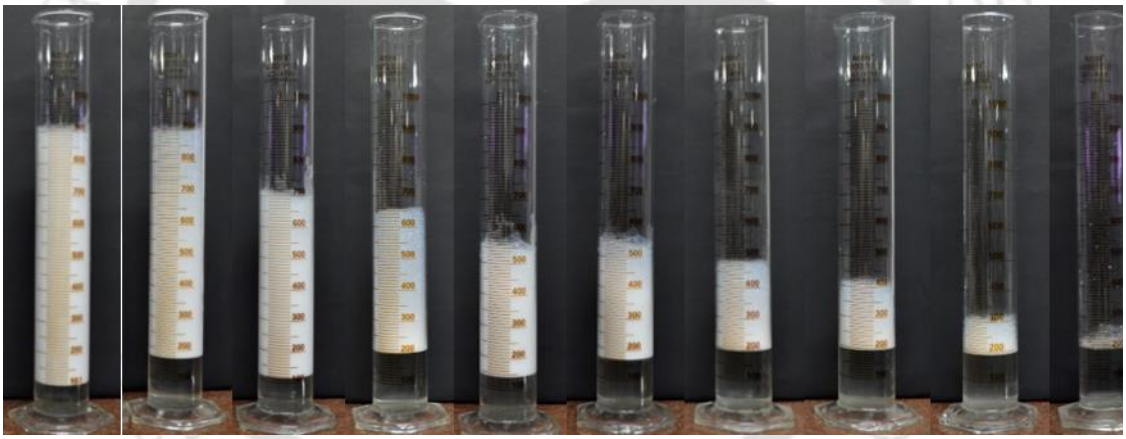

(a) (b) (c) (d) (e) (f) (g) (h) (i) (j)

Figure 2.2. Photographs of a typical foaming experiment. The decrease in foam volume can be observed from (a) to (j) over 100 min, at 10 min interval. Foam volume refers to the volume occupied by the foam and not the liquid surfactant solution.

The structure of the foam bubbles and foam films was observed under a microscope [make: Carl Zeiss (Jena, Germany), model: Axiostar plus]. The microscope

was equipped with a long-distance objective, a camera adapter, and a DSLR camera, as mentioned in the previous paragraph. The foam bubbles were placed on the microscope slide. The foam film was pressed between the microscope slide and a 0.1 mm thick glass slide in such a way that the excess liquid (of the dispersion medium) was drawn out. The samples were observed by transmitted phase-contrast because it effectively employs a contrast-enhancing optical technique to produce clear and sharp high-contrast images. Figure 2.3 depicts the experimental setup for taking the photographs of foams using the microscope.

Figure 2.3. Experimental setup for taking photographs of foams using the microscope.

To analyze the effect of oil on foam, *n*-hexane was solubilized in the aqueous solutions of DDAPS in the presence of salt at various concentrations. A magnetic stirrer

[make: IKA (Staufen, Germany), model: Color Squid (white)] was used to mix 50 cm^3 of *n*-hexane with 200 cm^3 of the aqueous solution. The mixing was carried out for 3 h at 1000 rpm. The excess oil was separated with the help of a separating funnel. The foaming experiments were conducted on these samples, as described in the first paragraph of this section. These samples were also used for measuring the size distribution of the oil droplets.

2.4 Measurements of droplet size distribution and zeta potential

The size distribution of the oil droplets dispersed in the aqueous phase was measured by a particle size analyzer [make: Beckman Coulter (Nyon, Switzerland), model: Delsa Nano C]. About 5 cm^3 of the sample was transferred to a cuvette and was examined by dynamic light scattering (DLS). DLS measures time-dependent fluctuations in the intensity of the scattered light from the dispersed particles moving under Brownian motion to obtain their hydrodynamic size distribution. He–Ne laser of 632.8 nm wavelength was used to irradiate the sample, which produced intensity fluctuations of the scattered light. The scattered light that comes from a collection of scattering elements within a scattering volume depends on the scattering angle and detection apertures. As the particles are in Brownian motion (and move about randomly), the scattered intensity of fluctuations is also random. The fluctuations occur rapidly for smaller and faster-moving particles, and more slowly for the larger particles.

The fluctuations of the scattered light were analyzed using the autocorrelation function. A method of non-negative least squares was used to obtain the overall size distribution. The software associated with the equipment performed all the computations for measuring the droplet size distribution. By observing the motion of the dispersed oil

droplet that diffuses in the aqueous solution, the diffusion coefficient (D) was computed by the Stokes–Einstein equation,

$$D = \frac{k_B T}{3\pi\mu d} \tag{2.5}$$

where d is the hydrodynamic diameter, k_B is the Boltzmann's constant, T is the absolute temperature, and μ is the viscosity. Equation (2.5) indicates that D would be relatively small for the larger droplet, and thus the movement of the droplet would be slower. On the other hand, D would have a larger value for the smaller droplet, and its movement would be faster.

Figure 2.4. The equipment used for measuring the droplet size distribution and zeta potential.

The zeta potential is the electric potential of a charged droplet at the plane of shear. This plane is located close to the boundary of the diffuse electrostatic double layer.[4] The zeta potential at the *n*-hexane–water interface was determined by measuring the electrophoretic mobility of the *n*-hexane droplets in water. This potential was used as a measure of the surface charge of the *n*-hexane droplets. The same equipment that was

used for the DLS was used for measuring the zeta potential. About 1 cm^3 of the *n*-hexane-in-water emulsion was injected to the flow cell. The zeta potential of the hexane–water interface was calculated by using the Smoluchowski equation, given by,

$$\zeta = \left(\frac{\mu}{\varepsilon \varepsilon_0} \right) U \tag{2.6}$$

For measuring the zeta potential at the air–water interface, the following procedure was followed. Water was aerated by sparging air millibubbles through it by using an air-diffuser. The surfactant solutions were prepared by using this water. After that, this solution was sonicated in an ultrasonic bath [make: Telsonic Ultrasonics (Bronschhofen, Switzerland), model: TPC 15 H] for 900 s. Micronanobubbles (MNBs) of air were generated in the solution which were dispersed in water. A small amount of the prepared dispersion (~1 cm^3) was quickly transferred to the flow cell of the equipment.

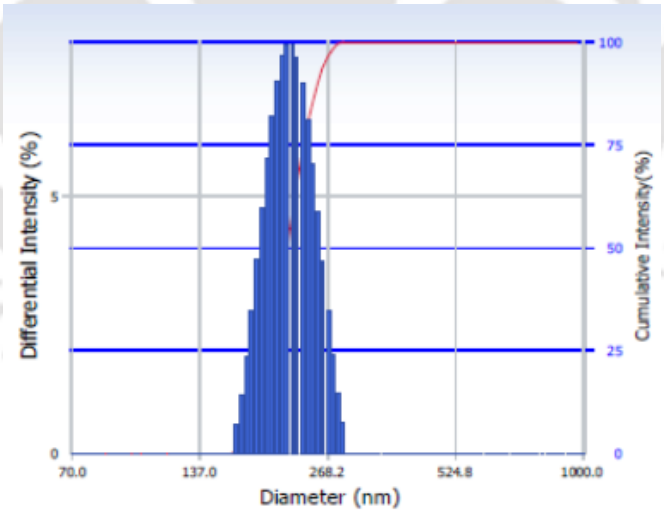

Figure 2.5. Size distribution of MNBs in the aqueous 2.4 mol m^{-3} DDAPS solution (*Z*-average diameter = 220.8 nm and standard deviation = 26.9 nm).

The same equipment, used for the DLS was used for measuring the zeta potential.

The MNBs moved through a narrow capillary in the glass flow cell under an electric field. The electrophoretic mobility of these MNBs was measured by the Doppler frequency shifts of the scattered light. The zeta potential at the surface of the MNBs was calculated by equation (2.6). The size distribution of the MNBs was measured by DLS. The typical size distribution of the MNBs dispersed in the aqueous surfactant solution is shown in Figure 2.5.

2.5 Determination of isoelectric point (IEP)

The IEP of the surfactant was determined by measuring the zeta potential at the air–water interface over a wide range of pH. The pH was adjusted by using HCl and NaOH. The pH at which the zeta potential passed through zero and then reversed its sign was taken as the IEP.

References

[1] Harkins, W. D.; Jordan, H. F. A method for the determination of surface and interfacial tension from the maximum pull on a ring. *J. Am. Chem. Soc.* **1930,** 52, 1751–1772.

[2] Huh, C.; Mason, S. A rigorous theory of ring tensiometry. *Colloid. Polym. Sci.* **1975,** 253, 566–580.

[3] Zuidema, H.; Waters, G. Ring method for the determination of interfacial tension. *Ind. Eng. Chem. Anal. Ed.* **1941,** 13, 312–313.

[4] Adamson, A. W.; Gast, A. P., *Physical Chemistry of Surfaces*; John Wiley & Sons: New York, 1967.

CHAPTER 3

FOAMING IN AQUEOUS SOLUTIONS OF ZWITTERIONIC SURFACTANT: EFFECTS OF OIL AND SALTS

3.1. Introduction

Surfactants adsorb at the fluid–fluid interfaces and alter their characteristic properties. Therefore, they are widely employed in varied industrial applications such as food processing,[1] petroleum recovery,[2] wetting,[3] foaming,[4] and polymerization.[5] During the past few decades, ionic[6–8] and nonionic[9,10] surfactants have been extensively used for research, and in the industries. However, the use of zwitterionic surfactants has increased owing to their wide applicability, particularly in the high-value formulations.[11] The presence of both anionic and cationic moieties in the structure of a zwitterionic surfactant makes it a unique molecule to study at the fluid–fluid interface. The cationic fraction is preferably based on the ammonium group while the anionic fraction may include carboxylic and sulfonic acids, and sulfuric acid esters.[12]

Zwitterionic surfactants have exceptional dermatological properties, and hence they are best suited for use in cosmetics, personal care, and household cleaning products.[13] In addition, they exhibit low toxicity, good solubility in water, and varied isoelectric ranges.[14,15] Also, they are compatible with other surfactants. However, these surfactants are usually more expensive than their anionic and cationic counterparts. Hence, they are mostly used in combination with these surfactants. In spite of their wide applicability and increasing commercial use, the effects of various inorganic salts and oils on the foaming properties of the aqueous solutions of these surfactants have received very little attention.

The structure of a zwitterions surfactant molecule is comprised of positively- and negatively-charged hydrophilic groups, along with a long hydrophobic chain.[16] The structure of N-Dodecyl-N,N-dimethyl-3-ammonio-1-propanesulfonate (DDAPS) is shown in Figure 3.1. This surfactant molecule contains an outer negative sulfonate group

and an inner positive ammonium group.

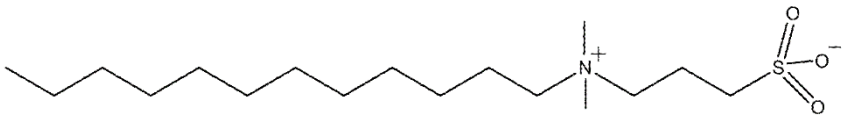

Figure 3.1. Structure of the DDAPS molecule.

Equilibrium adsorption of surfactant molecules from the solution to the interface depends on electrostatic interaction, van der Waals force, hydrophobic interaction, hydrogen bonding, and solvation energy.[17] Thus, the adsorption mechanism depends on surfactant concentration, its type, the structure of the molecule, the solvent, and the interface. The effects of inorganic ions on the adsorption mechanism of cationic, anionic, and nonionic surfactants have been investigated in detail.[18,19] It has been observed that the inorganic ions induce a significant effect on the adsorption of these surfactants. The salt ions decrease the electrostatic repulsion among the surfactant head-groups and hence increase their adsorption at the interface. This is reflected in the increased concentration of surfactant at the fluid–fluid interface and a concomitant reduction in the interfacial tension.[20] Therefore, the ionic strength of the solution plays a pivotal role in the surfactant adsorption. Some of the ionic surfactants precipitate out of the solution at high salt concentrations, especially when the salts of divalent and trivalent ions (e.g., Ca^{2+} and Al^{3+}) are present in the solution.

Foams are extensively used in materials processing, geology, detergency, biology, cosmetics, fire-fighting, foods, and enhanced oil recovery.[21] Personal care and cosmetic products use zwitterionic surfactants in their formulations. Therefore, the investigation of their foaming properties is very important. Foams stabilized by zwitterionic surfactants have hardly been studied in sufficient details. The desirability and amount of foam

generation depend on the requirements of the consumer. Water used in the domestic and industrial applications inherently contains several salts. Therefore, the influence of salts on the formation of foam and its stability has a lot of importance. The valence of the ions can significantly affect the adsorption of surfactant molecules. The oil droplets present in the foam can alter its stability.[22] The properties of zwitterionic surfactants vary with pH. It has been reported that, when the isoelectric point (IEP) of the system is reached, the foam film's stability decreases.[23]

Chorro et al.[24] investigated the micellization and adsorption of an N-dodecyl betaine (NDB) at the solid–liquid interface and the effect of salt on these phenomena. The micelle aggregation number of NDB remained constant with increasing salt concentration. The degree of counterion binding for Na^+, Ca^{2+}, and Cl^- on the micelles was determined. It was found that the adsorption at solid–liquid interface depended on temperature and the concentrations of NDB and the salt. Deng et al.[25] examined the mechanism of performance enhancement of the foams of dodecyl sulfobetaine (DSB) using hyperbranched exopolysaccharide (EPS). The EPS interacted with DSB via the hydrogen bonds and the electrostatic attraction force. The EPS molecules were entrapped inside the DSB foam film, which effectively inhibited the coalescence of the foam bubbles. This increased the water content in the films, which imparted higher stability to the foam.

Kwaambwa et al.[26] studied the interactions of DDAPS with a protein extracted from the *Moringa oleifera* seeds by analyzing the surface tension and ultrasonic velocity. The surface tension was not influenced by the presence of protein because the protein molecules were entirely displaced from the interface when the surfactant concentration reached the critical micelle concentration (CMC). The protein did not interact with the

DDAPS significantly because the zwitterionic surfactant behaved like a nonionic surfactant. Li et al.[27] analyzed the adsorption of carboxybetaine (i.e., CBET−17) and sulfobetaine (i.e., SBET−17) on quartz sand in the presence of NaCl and $CaCl_2$. It was found that the adsorption of sulfobetaine on the surface of quartz decreased with increasing pH, which was attributed to the charges on the surfactant molecule and the quartz surface. Pinazo et al.[28] studied the adsorption of N-dodecyl-N,N dimethyl aminobetaine chlorohydrate (DDAB·HCl) at the air−water interface in the presence and absence of a phosphate buffer. The larger values of the equilibrium adsorption parameters for the buffer solution implied that an amphoteric form of the surfactant was more surface active than the cationic form. The former was formed in the presence of the buffer, and the latter form was present in its absence.

Zhao et al.[16] investigated the properties of three propyl sulfobetaines and two hydroxyl propyl sulfobetaines at both air−water and oil−water interfaces. The CMC was determined from the surface tension measurements. It depended on the molecular structure of the surfactant. The CMC decreased with increasing alkyl chain length and increased upon the addition of the hydroxyl group. The surface tension at the CMC decreased with increasing alkyl chain length and with the addition of the hydroxyl group.

The main objective of this work was to investigate the stability of foams in the presence of a zwitterionic surfactant. We have investigated the adsorption of DDAPS at the air–water interface in the presence of salts containing Na^+, Ca^{2+}, and Al^{3+} ions by surface tension measurements. Foaming and foam stability were studied by employing the Blender Test. The effect of oil (i.e., *n*-hexane) on foam stability was also studied. Dynamic light scattering (DLS) was employed to measure the size distribution of the hexane droplets in the aqueous phase. The electrical potential of the interface was also

measured.

3.2. Results and Discussion

3.2.1. Surface tensions of DDAPS solutions

The surface tensions of the DDAPS solutions with and without NaCl are plotted in Figure 3.2. A decrease in surface tension was observed upon increasing the DDAPS concentration. The surface tension profile in the absence of salt approached a plateau at ~2.4 mol m^{-3} surfactant concentration, which indicated the saturation of the air–water interface with the monolayer of the surfactant molecules. Therefore, the CMC of DDAPS was ~2.4 mol m^{-3}, which is close to the literature value.[14]

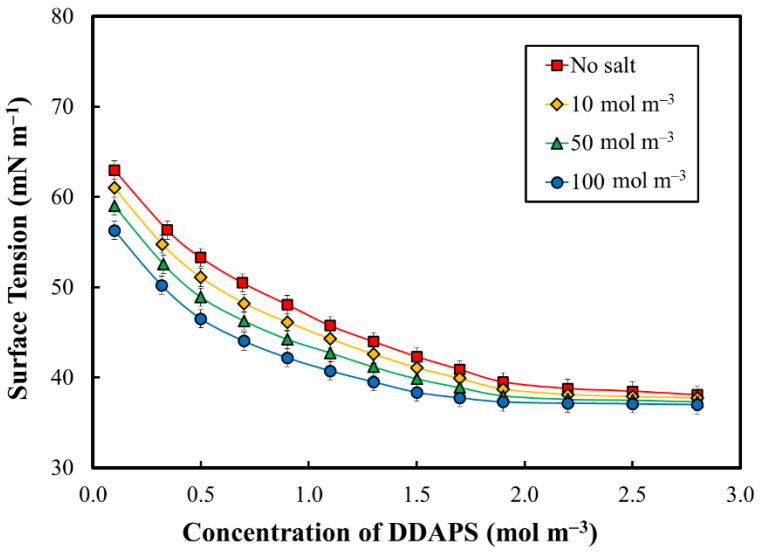

Figure 3.2. Variation of surface tension with DDAPS concentration at various concentrations of NaCl.

The mechanism of adsorption of a zwitterionic surfactant at the air–water interface involves electrostatic interactions among the charged cores of the molecules and the

hydrophobic interaction among the paraffin chains.[29] For these surfactants, the nature of the head-groups has a minor effect on surface activity,[24] but the spacer group has a considerable effect on the surface tension and CMC. The spacer group (i.e., propyl) in the DDAPS molecule is rigid and hydrophobic, which prohibits strong electrostatic attraction between the positively- and negatively-charged cores. This causes a feeble electrostatic attraction between the two head-groups (i.e., quaternary ammonium and sulfonate), which reduces the ability of the surfactant to pack tightly.[16]

Figure 3.2 also depicts the effect of NaCl on surface tension. Addition of 10 mol m^{-3} NaCl reduced the surface tension. However, this reduction was smaller than that observed for an ionic surfactant,[30] but more than that for a non-ionic surfactant.[31] After the addition of more NaCl (i.e., at 50 and 100 mol m^{-3} concentrations), the surface tension reduced further (especially at the low DDAPS concentrations), indicating enhanced adsorption of the surfactant molecules. This indicates that the air–water interface could accommodate more surfactant molecules at these concentrations. The CMCs were approached at 2.1, 2.0, and 1.9 mol m^{-3} concentrations of DDAPS at these concentrations of NaCl, respectively. This rather small reduction in surface tension achieved by the addition of NaCl may be due to the neutral nature of the zwitterionic surfactant molecule, which behaves like a non-ionic surfactant even though it has two ionic groups.[14] The pH of the solution was measured between 3.0 – 4.1.

Salts reduce the electrostatic repulsion between the charged head-groups of the surfactant molecules. This decrease enhances the adsorption of the surfactant molecules at the interface.[32] The repulsive interaction energy between the surfactant head-groups can be expressed by the Debye–Hückel equation.[33]

$$\phi_R = \left(\frac{z_1 z_2 e^2}{4\pi\varepsilon\varepsilon_0 r}\right)\left[\frac{\exp\{-\kappa(r-a)\}}{1+\kappa a}\right] \quad (3.1)$$

where κ, the Debye–Hückel parameter, and is described in Section 1.8.5 of Chapter 1, as Equation (1.7). The lateral repulsive interaction between the counter-ions at the air–water interface can also be expressed by the Debye–Hückel equation [i.e., Equation (3.1)]. As the concentration of the electrolyte is increased, the Debye length is decreased by a large extent and the repulsive interaction energy (i.e., ϕ_R) decreases.[34] Thus, the addition of salt to the surfactant solution reduces the repulsion between the charged head-groups of the surfactant molecule and favors more adsorption of the surfactant molecules at the air–water interface, which causes a significant reduction in surface tension.[35]

The attractive van der Waals interaction energy between the two parallel hydrophobic chains (i.e., the surfactant tails) is given by,[35-37]

$$\phi_A = -\frac{3\pi CL}{8\delta^2 r^5} \quad (3.2)$$

The surface tension of an aqueous surfactant solution is related to the surface potential (ψ_0), the surface excess concentration (Γ), and the surface charge density (σ) as,[38]

$$\gamma = \gamma_0 - \int \Gamma d\varphi - \int \sigma d\psi_0 \quad (3.3)$$

The binding of counterions to the sulfobetaine molecules is different from that observed for the ionic surfactants.[39] A steady decrease in the surface activity of some zwitterionic surfactants with increasing salt concentration has been reported.[40] The hydrophilic cationic and anionic groups of the surfactant molecule electrostatically attract the Cl^- and Na^+, respectively. Consequently, a strong attraction between the hydrophilic groups of the DDAPS molecule and NaCl is expected. Nonetheless, apart from the

electrostatic attraction, repulsion among the charged cores of the surfactant molecule and NaCl does exist. The Na^+ is repelled by the cationic part of the surfactant molecule. Similarly, the Cl^- encounters repulsion by the negative part of DDAPS. Therefore, NaCl has a rather small interaction with the hydrophilic charged centers of DDAPS, and its effect on the surface activity of DDAPS is rather small.[41]

The surface tension profiles for the $CaCl_2$ and $AlCl_3$ systems were similar to those of the NaCl system and are depicted in Figures 3.3 (a) and 3.3 (b), respectively. The quantity of salt required for reducing the surface tension and attaining the CMC was in the sequence: NaCl > $CaCl_2$ > $AlCl_3$. Compared to NaCl, $CaCl_2$ has a greater capability to screen the electrostatic repulsion, causing more surfactant molecules to adsorb at the air–water interface. This effectively decreased the surface tension, and the CMC was attained at a lower concentration. The hydrated radii of the Ca^{2+} and Al^{3+} ions are 0.41 and 0.48 nm, respectively, as compared to 0.36 nm for the Na^+ ion. Therefore, the Ca^{2+} and Al^{3+} ions perturb the interfacial water molecules more than that by Na^+. The Ca^{2+} and Al^{3+} ions have a much stronger effect on the interfacial water network than Na^+, in accordance with their binding affinities to the sulfonate moieties.[42] Thus, the Ca^{2+}, Al^{3+}, and Cl^- ions adjust themselves near the negatively-charged sulfonate and positively-charged quaternary ammonium groups, respectively. Therefore, the addition of these salts effectively screens the charge of the sulfonate and quaternary ammonium groups. This screening is determined by the ionic strength of the surfactant solution. The polarizability of Al^{3+} is greater than that of Ca^{2+} and Na^+. This allows more Al^{3+} ions to readily approach the interface and get adsorbed.[43] Consequently, a lower concentration of $AlCl_3$ was sufficient for reducing the surface tension and the CMC.

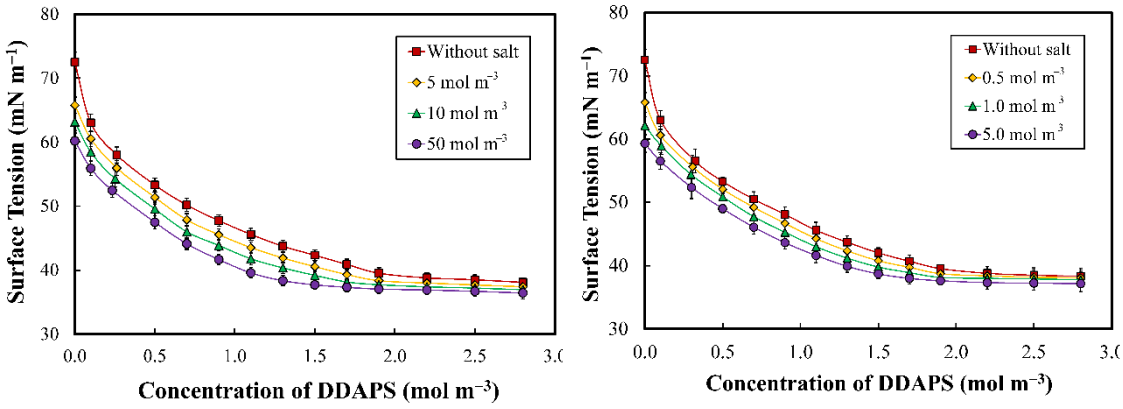

(a) (b)

Figure 3.3. Variation of surface tension with DDAPS concentration at various concentrations of (a) $CaCl_2$ and (b) $AlCl_3$.

3.2.2. Effects of surfactant and salts on foam formation and stability

The effects of NaCl, $CaCl_2$, and $AlCl_3$ on foam formation and stability were studied at different surfactant and salt concentrations. The foams near the bottom of the cylinder were wet with high water content, whereas the upper parts of the foams were dry, having a lower amount of water. Figure 3.4 depicts the variation in foam volume, observed for a period of 1 h, at various DDAPS concentrations in the absence of salt. The initial foam volume increased continuously with increasing surfactant concentration in the range of 0.4 to 2.4 mol m^{-3}. For the systems without salt, the maximum initial foam volume was ~520 cm^3 at 2.4 mol m^{-3} (i.e., at the CMC). This occurred due to the presence of an increased number of surfactant molecules at the air–water interface, as a result of the increased surfactant concentration. This caused an increase in the foam volume as well as the stability of the foam films.[44]

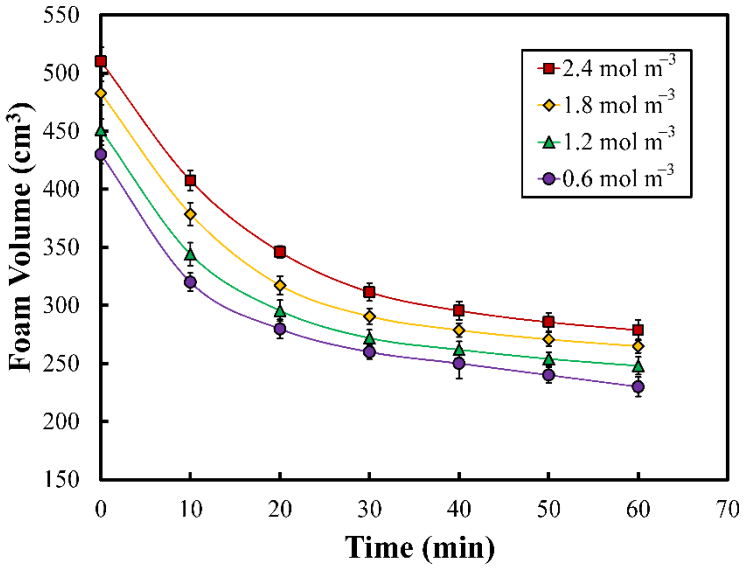

Figure 3.4. Variation of foam volume with time at different concentrations of DDAPS in the absence of salt.

Figure 3.5 depicts the effects of NaCl on foam volume at various concentrations of DDAPS. The foam volume decreased by the addition of salt at a given surfactant concentration. Electrostatic screening between the surfactant molecules is enhanced when the concentration of salt is increased (see Section 3.2.1). Therefore, the increase in NaCl concentration (i.e., from 10 to 100 mol m^{-3}) favors the adsorption of the surfactant molecules at the interface,[45] which is evident from the surface tension profiles shown in Figure 3.2. However, salt also has a strong effect on the disjoining pressure in the foam film. The repulsive pressure between two flat surfaces separated at a distance, δ, is given by Equation (1.9) (Section 1.8.5 of Chapter 1).[35] In the presence of salt, the diffuse layer thickness $\left(\kappa^{-1}\right)$ decreases, and the surface potential $\left(\psi_0\right)$ is also reduced. This reduces the double layer repulsion in the foam film. The initial foam volume decreased upon increasing the salt concentration.[46] This occurred due to the rapid coalescence of the foam bubbles by the rupture of the thin aqueous films.

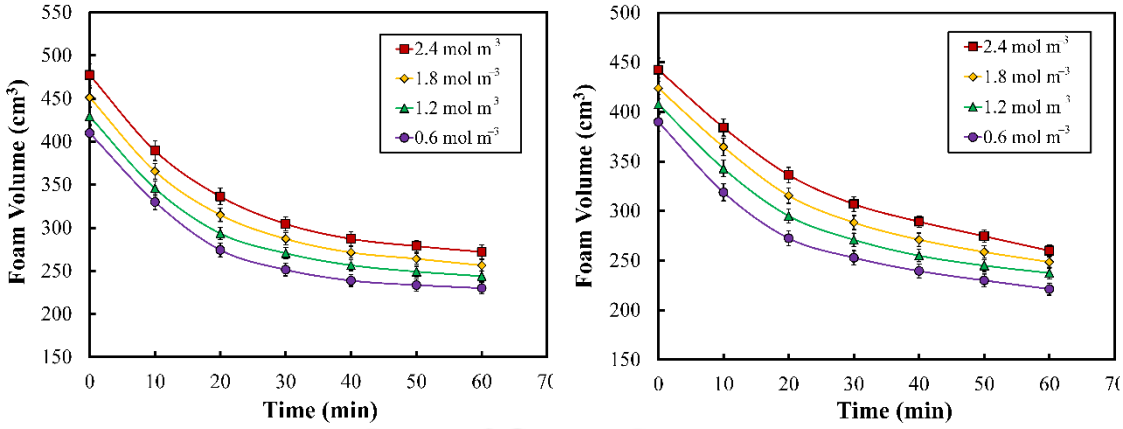

(a) (b)

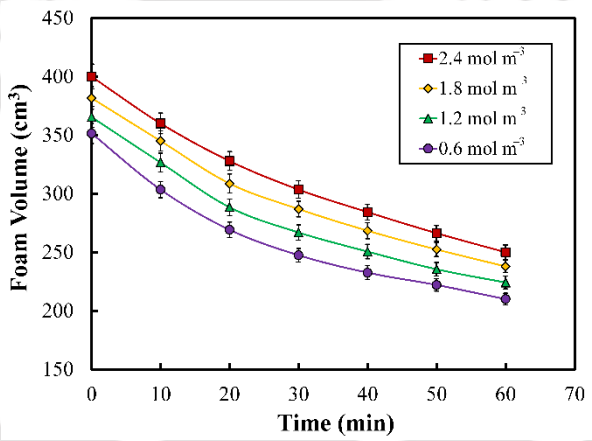

(c)

Figure 3.5. Variation of foam volume with time at different concentrations of DDAPS in the presence of (a) 10, (b) 50, and (c) 100 mol m^{-3} NaCl.

For example, at 2.4 mol m^{-3} surfactant concentration, the initial foam volume was 520 cm^3 in the absence of salt, whereas the same decreased to 480, 440, and 400 cm^3 at 10, 50, and 100 mol m^{-3} NaCl, respectively. The initial foam volume decreased in a similar manner for the other (i.e., 0.6, 1.2, and 1.8 mol m^{-3}) surfactant concentrations. The foam collapse rate was high during the initial period (i.e., 30 min after the formation of foam) in the absence of salt, as well as at a low salt concentration (i.e., 10 mol m^{-3}). The decrease in foam volume at 2.4 mol m^{-3} surfactant concentration during the initial 30

min was 200 and 170 cm^3 in the absence of salt and in the presence of 10 mol m^{-3} NaCl, respectively. However, upon increasing the concentration to 50 and 100 mol m^{-3} NaCl, the foam collapse rate was less, and it did not show any notable variation with the surfactant concentration. For 50 and 100 mol m^{-3} NaCl concentrations, the amounts of foam collapsed (during the same time period) were 130 and 90 cm^3, respectively, at 2.4 mol m^{-3} surfactant concentration. Similar observations were made for 0.6, 1.2, and 1.8 mol m^{-3} surfactant concentrations. However, in the second half of the experiment (i.e., the remaining 30 min), the foam collapse rate was less, and it did not show any notable variation with the surfactant and salt concentrations. A total decrease of 30 cm^3 was observed for 2.4 mol m^{-3} DDAPS in the absence of salt and at 10 mol m^{-3} NaCl concentration. When the NaCl concentration was low, the adsorption of DDAPS molecules was less due to the strong electrostatic repulsion between the similarly charged head-groups of the surfactant molecule. Thus, the EDL repulsion between the foam lamellae was less, causing high rate of foam collapse leading to decrease in the foam volume.

The disjoining pressure isotherms of the foam films vary with the electrolyte concentration.[47,48] When the capillary pressure acting on a foam film is increased, its thickness decreases and the repulsive disjoining pressure increases. The increase in repulsive disjoining pressure causes an unbound rise in the random perturbations leading to a further decrease in the film thickness.[49] This increase in pressure leads to the formation of black spots (~10 nm). These spots eventually cover the entire foam film and give rise to a *common black film* (CBF).[50] CBFs rupture at the lower salt concentrations and their thickness varies between 5 and 20 nm.[51] These factors cause a higher rate of collapse of foams at low salt concentrations (i.e., 10 mol m^{-3}).

At the higher salt concentrations, electrostatic repulsion between the surfactant

molecules is substantially decreased, thus facilitating adsorption of the surfactant molecules at the air–water interfaces in the foam lamellae. The adsorption of surfactant molecules, in the presence of salt, causes the foam lamellae to become rigid, which reduces the film thinning rate.[52] At the higher concentrations of surfactant and salt, the resistance to collapse sharply increases as the surface waves are damped, which causes the foam films to drain below the critical thickness. Instead of rupture, a sudden transition of foam film towards a more stable *Newton black film* (NBF) takes place.[51] NBFs are bilayers of surfactant molecules without a free aqueous core. CBF and NBF represent two different equilibrium states of the black films. The equilibrium of CBFs depends on the stabilizing effect of the EDL. Therefore, their thickness decreases with increasing electrolyte concentration. However, the thickness of the NBFs does not change with the electrolyte concentration. The formation of NBF depends on the capillary pressure, electrolyte and surfactant concentrations, and film radius. This may be responsible for the stable foams at the high salt concentrations. Note that this transition to the stable state instead of collapsing in the presence of salt is contrary to that predicted by the DLVO theory.

A similar variation in initial foam volume was observed for $CaCl_2$ and $AlCl_3$. These results are shown in Figure 3.6 and 3.7, respectively. For $CaCl_2$, the initial foam volumes were 445, 420, and 390 cm^3 in the presence of 5, 10, and 50 mol m^{-3} salt, respectively, at 2.4 mol m^{-3} surfactant concentration. On the other hand, for $AlCl_3$, the initial foam volumes were 430, 400, and 370 cm^3 in the presence of 0.5, 1, and 5 mol m^{-3} salt, respectively, for the same surfactant concentration. A similar decrease in the initial foam volume was observed for 0.6, 1.2, and 1.8 mol m^{-3} DDAPS concentrations, at the salt concentrations mentioned before. The foam collapse rate was high during the initial period (i.e., 30 min after the formation of foam) at low concentrations of $CaCl_2$ and $AlCl_3$.

The decrease in foam volume at 2.4 mol m^{-3} surfactant concentration during this period was 160 and 150 cm^3 in the presence of 5 mol m^{-3} $CaCl_2$ and 0.5 mol m^{-3} $AlCl_3$, respectively. However, at the high salt concentrations (i.e., 10 and 50 mol m^{-3} $CaCl_2$, and 1 and 5 mol m^{-3} $AlCl_3$), the foam collapse rate was less, and it did not vary with the surfactant concentration significantly. For 10 and 50 mol m^{-3} $CaCl_2$, the amounts of foam collapsed (during the same time period) were 130 and 90 cm^3, respectively, at 2.4 mol m^{-3} DDAPS. Similar observations were made for 0.6, 1.2, and 1.8 mol m^{-3} DDAPS.

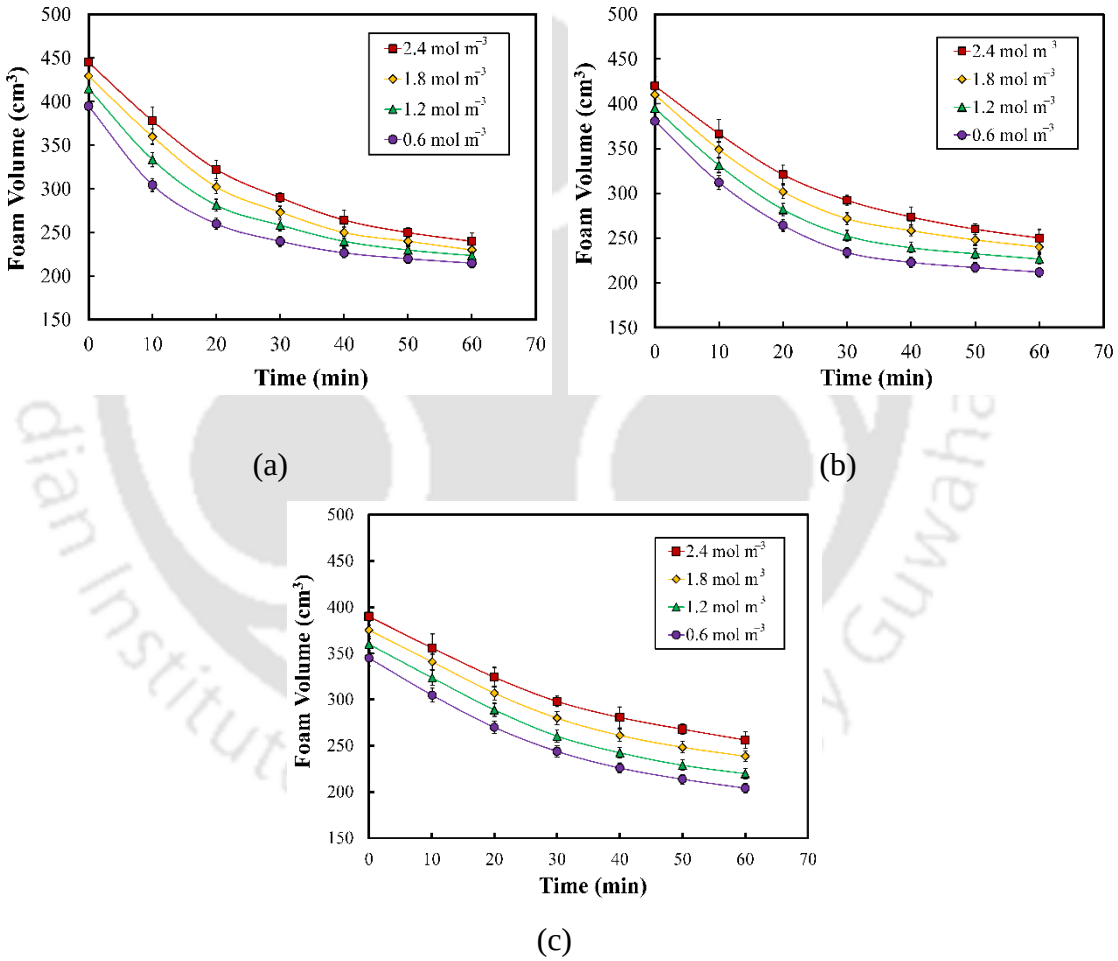

Figure 3.6. Variation of foam volume with time at different concentrations of DDAPS in the presence of (a) 5, (b) 10, and (c) 50 mol m^{-3} $CaCl_2$.

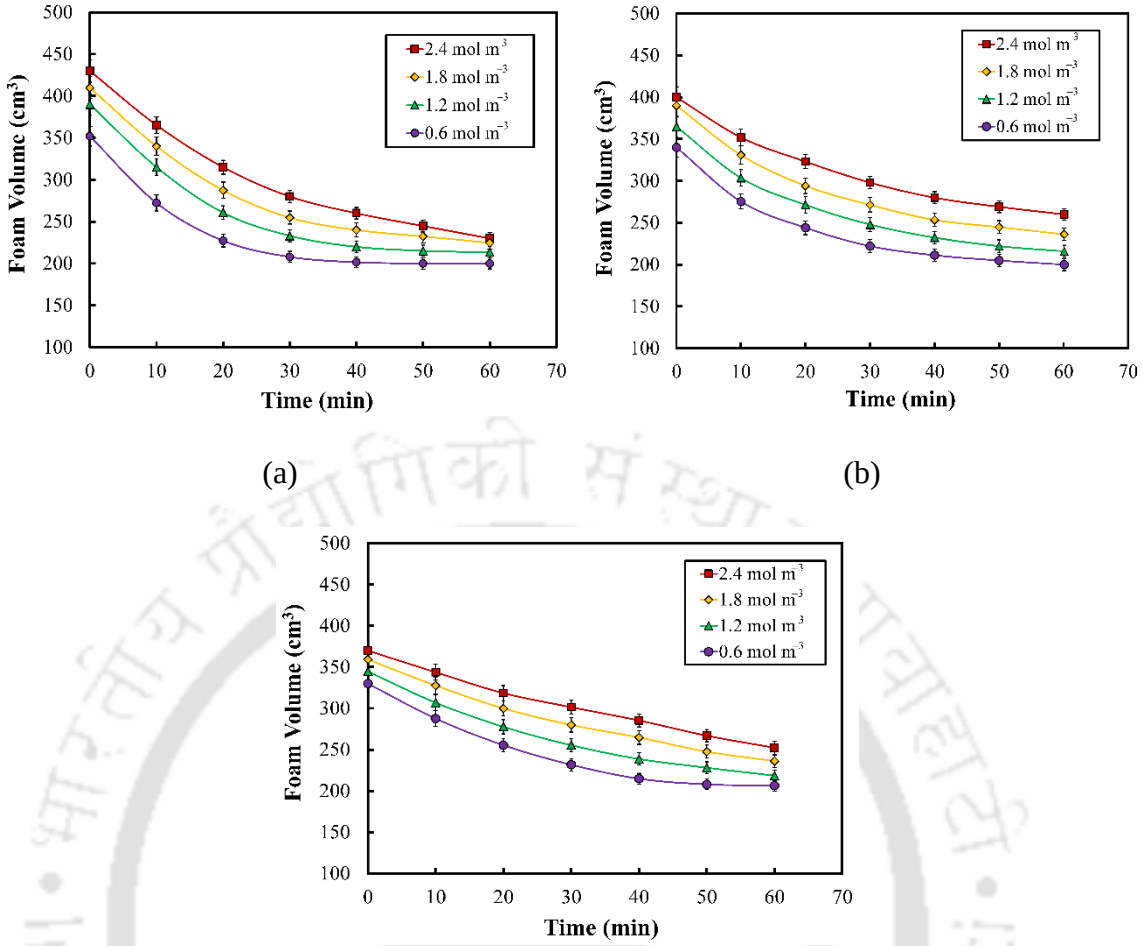

Figure 3.7. Variation of foam volume with time at different concentrations of DDAPS in the presence of (a) 0.5, (b) 1.0, and (c) 5.0 mol m^{-3} $AlCl_3$.

Primary interactions of Ca^{2+} and Al^{3+} with the surfactant head-groups are of electrostatic in nature. With the increase in the concentration of the salts of these ions, the film thickness is reduced, which is due to the screening effect of the EDL.[53] Also, the stronger binding of Ca^{2+} and Al^{3+} with the DDAPS head-groups enhances the adsorption of the surfactant molecules at the interface, as compared to the Na^{+}, and thus increases the foam stability. The adsorbed surfactant molecules possess the ability to heal the weak spots in the foam film generated due to the random perturbations and increase the stability

of the film.[54] These factors, in turn, depend upon the interfacial packing density of the surfactant in addition to the size and configuration of its polar and non-polar groups.[55]

The surface tension was lower in the presence of $CaCl_2$ and $AlCl_3$ due to a greater reduction in the electrostatic repulsion between the surfactant head-groups. The stability of the foam mentioned earlier was also observed upon increasing the concentration of $CaCl_2$ and $AlCl_3$. The interfacial structure dynamics strongly depends on the size of the counterions due to the difference in the hydrated ionic radius of the Na^+ (0.36 nm), Ca^{2+} (0.41 nm), and Al^{3+} (0.48 nm). These factors are likely to be responsible for the DDAPS foams to possess a stronger water-holding ability and slower drainage in the presence of Ca^{2+} and Al^{3+}.

3.2.3. Effect of oil on foam

Foam stability with respect to time was investigated in the presence of oil (i.e., *n*-hexane) and salt. The primary objective of this work was to investigate the impact of oil on foam stability in the presence of salt. Figure 3.8 depicts a typical size distribution of the oil droplets dispersed in the aqueous surfactant solution at various salt concentrations. The droplet size varied with surfactant and salt concentrations. A decrease in droplet diameter was observed upon increasing the salt concentration at a fixed surfactant concentration. This decrease in diameter occurred due to the reduction in the interfacial tension, as a result of the salt addition. In addition, at a particular salt concentration, a decrease in droplet diameter was observed with increasing surfactant concentration for the same reason. The droplet size distributions were bimodal in some cases.

The effect of oil (i.e., *n*-hexane) on foam is shown in Figure 3.9. The initial foam volume considerably decreased in the presence of oil. In most of the samples, foams

rapidly collapsed after their formation. Similar phenomena were observed in the presence of salt. Like the oil-free systems (as discussed in Section 3.2.1), an increase in

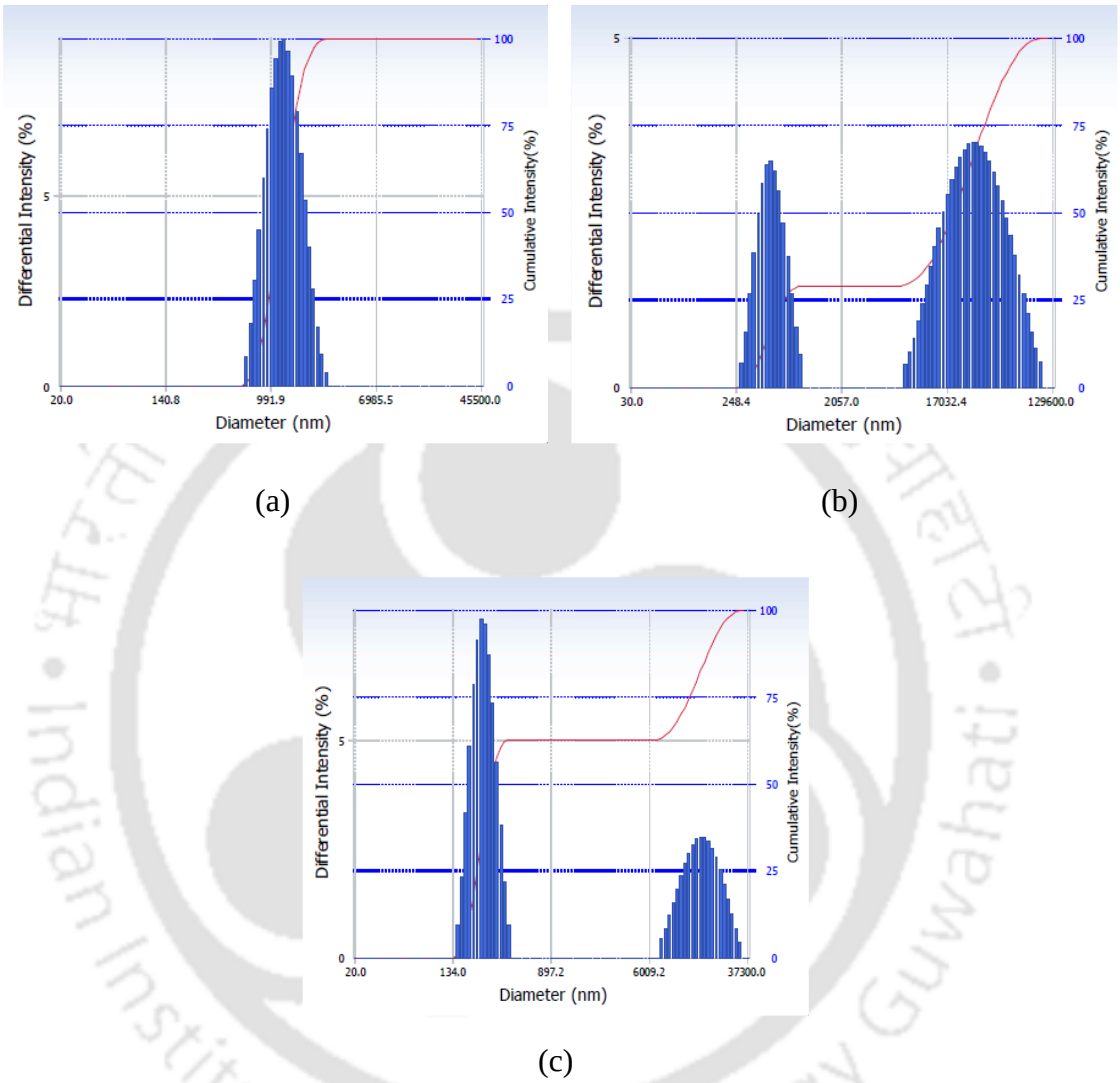

Figure 3.8. Size distributions of oil droplets in 2.4 mol m^{-3} aqueous DDAPS solution in presence of (a) 10 mol m^{-3} NaCl (*Z*-average diameter = 1766.7 nm), (b) 5 mol m^{-3} $CaCl_2$ (Z-average diameter = 1562.5 nm), and (c) 0.5 mol m^{-3} $AlCl_3$ (*Z*-average diameter = 1140.9 nm). The volume fraction of oil in all the samples was 0.2.

initial foam volume was observed upon increasing the DDAPS concentration. It was observed that the initial foam volume decreased upon increasing the NaCl concentration

for a particular DDAPS concentration. The initial foam volumes were 440 and 390 cm^3 at 10 and 50 mol m^{-3} NaCl concentrations, respectively, for 2.4 mol m^{-3} DDAPS. The volume fraction of oil in the dispersion was 0.2. A similar decrease in initial foam volume was observed for 0.6, 1.2, and 1.8 mol m^{-3} DDAPS. The foam collapse rate was high during the initial period (i.e., 30 min after foam formation) at the low salt concentration (i.e., 10 mol m^{-3}). The decrease in foam volume at 2.4 mol m^{-3} DDAPS during the first 30 min was 210 cm^3 in the presence of 10 mol m^{-3} NaCl. However, at the higher NaCl concentration (i.e., 50 mol m^{-3}), the foam collapse rate was slightly less, as compared to that for 10 mol m^{-3} NaCl. For 50 mol m^{-3} NaCl, the amount of foam collapsed (during the same period) was 150 cm^3. Similar observations were made for 0.6, 1.2, and 1.8 mol m^{-3} surfactant concentrations. However, for the second half of the experiment, the foam collapse rate was less, and it did not vary with the surfactant and salt concentrations in the presence of oil significantly.

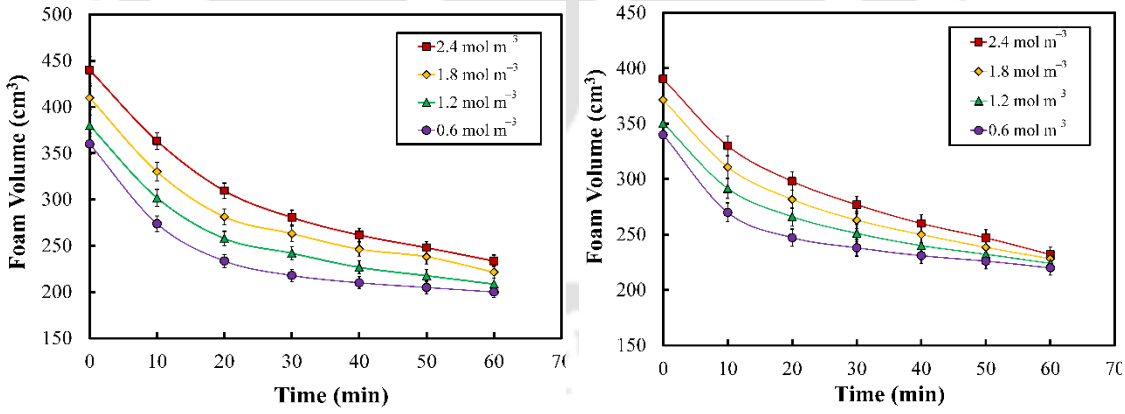

Figure 3.9. Variation of foam volume with time at different concentrations of DDAPS in the presence of *n*-hexane at (a) 10 and (b) 50 mol m^{-3} NaCl.

The stability of foams in the presence of oil depends on the pseudoemulsion film formed between the oil droplet and the gas phase.[56] During the formation of foam, the

oil droplet enters into the air–water interface. The entering point plays a significant part in film stability, and hence on the overall stability of the foam. The oil droplet enters into the foam film in two-steps. In the first step, the oil droplet enters into the lamella as well as the Plateau border of the foam film. In the second step, it spreads spontaneously on the foam lamella creating a weak spot on it and disrupts the foam-stabilizing ability of the surfactant.[57] The oil spread on the foam lamella pushes-off the surfactant molecules ahead of it. The spread of the oil droplet on the foam film leads to a Marangoni effect. The Marangoni flow in the film gives rise to local thinning, and consequently, leads to the rupture of the film.[58] Capillary waves exhibiting large amplitudes and wavelengths are generated due to the spreading of the oil droplet, which may lead to the rupture of the foam film. In addition, the spreading of oil reduces the surface tension and increases the radius of curvature while changing the surface elasticity and surface viscosity, causing the film to lose its stability.[2] A few oil droplets are trapped in the Plateau borders of the foam film, eventually leading to their rupture. It restricts the flow of the aqueous surfactant solution around the Plateau border, which causes the drainage rate to decrease. This may lead to an increased radius of the pseudoemulsion film, and ultimately to the collapse of the complete framework of the foam cell. Hence, the presence of the oil droplet in the foam lamella and Plateau border is important in determining the stability of foams. Figure 3.10 shows a schematic representation of an oil droplet entering, spreading, and rupturing the lamella and Plateau border of a foam film.

Destruction of the foam film by oil can also occur due to the bridging–dewetting.[59] In this mechanism, the penetration of the oil droplet in the foam film creates an oil bridge between the foam lamellae. Since oil is hydrophobic, it induces dewetting of the bridge and causes the foam film to rupture.[58] The analysis of the entering, spreading, and bridging coefficients gives a comprehensive understanding of foam stability. Stability of

foams in the presence of oil can be investigated by using *entering* (*E*), *spreading* (*S*), and *bridging* (*B*) *coefficients*.[60] These coefficients, defined below, depending on surface and interfacial tensions.

$$E = \gamma_{A/W} + \gamma_{O/W} - \gamma_{A/O} \tag{3.4}$$

$$S = \gamma_{A/W} - \gamma_{O/W} - \gamma_{A/O} \tag{3.5}$$

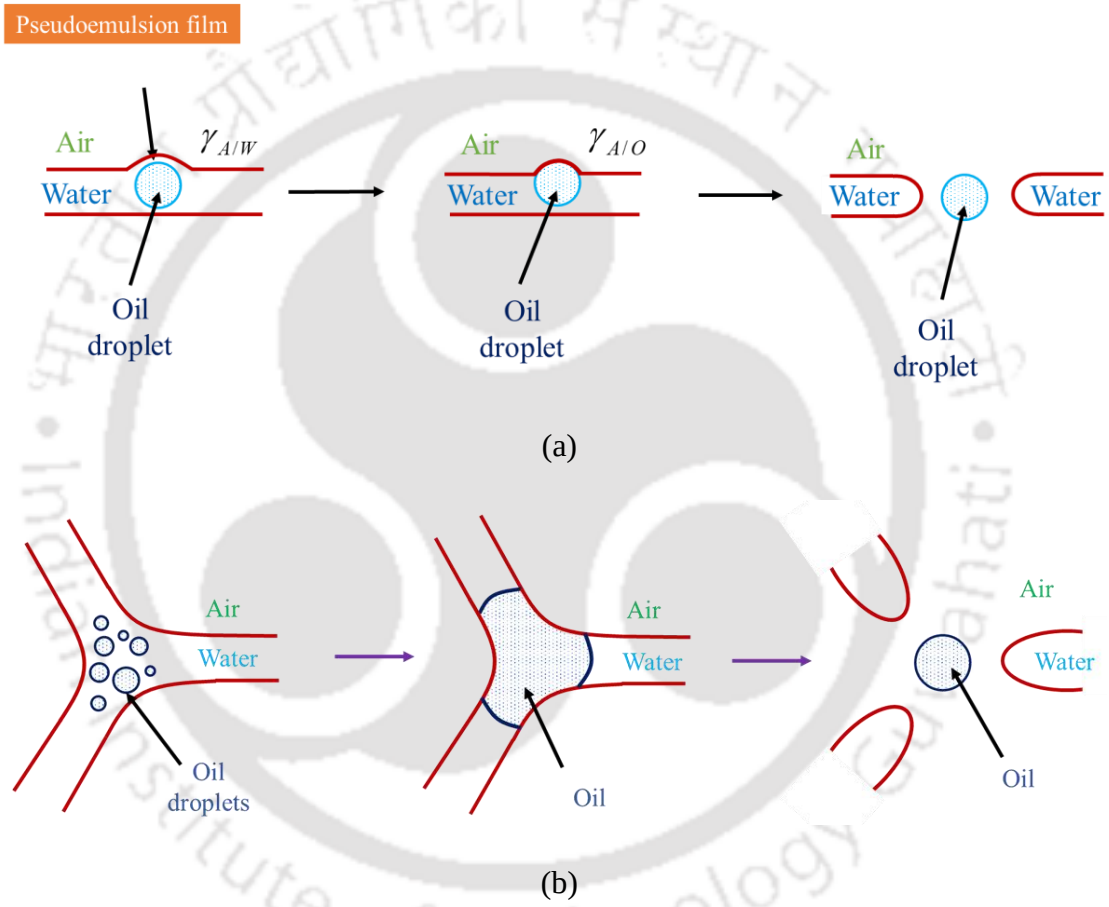

Figure 3.10. Schematic representation of an oil droplet entering, spreading, and rupturing: (a) a foam lamella and (b) the foam film at the Plateau border.

The oil droplet's ability to enter the air–water interface is an essential parameter to disrupt the foam film.[61] A favorable condition for the oil droplet to enter the air–water interface is $E > 0$, while the necessary condition for the oil droplet to exhibit spreading as a duplex

film on each side of the initial film is $S > 0$. Garrett[62] presented a model for foam stability in terms of the *bridging coefficient* (*B*), which is defined as,

$$B = \gamma_{A/W}^2 + \gamma_{O/W}^2 - \gamma_{A/O}^2 \qquad (3.6)$$

For *S* to be negative (i.e., no spreading of the oil droplet), an oil lens forms at the air–water interface. It can rupture the foam film by the bridging mechanism.[62,63] These coefficients help us determine the thermodynamic feasibility of the destruction of the foam film by the oil.[64] However, these coefficients do not predict the rate at which the entering and spreading of oil will occur.[61] Also, they are unable to provide any information about the foamability of the surfactant. However, it is observed that the stability of foam tends to decrease with the increasing values of *E*, *S*, and *B*.

The *entering coefficient* (*E*) reflects the disappearance of two interfaces of tensions, i.e., $\gamma_{A/W}$ and $\gamma_{O/W}$, and the emergence of a new interface of tension, $\gamma_{A/O}$, when the oil droplet enters the air–water interface of a foam film. The new interface of tension, $\gamma_{A/O}$, is formed when the oil droplet ruptures the pseudoemulsion film formed between the oil droplet and the gas phase, and the oil tends to form a lens at air−water interface [Figure 3.10 (a)]. For $E > 0$, and no increase in disjoining pressure (Π), the oil droplet enters the interface spontaneously. A positive value of *E* does not ensure droplet entry.[56,65,66] The necessary conditions for droplet entry are the separation of the oil droplet from the air–water interface and the rupture of the irregular oil–water–air film. Stabilization of the asymmetric film may be achieved by the interplay between the EDL and steric forces. These forces create a barrier (e.g., a critical disjoining pressure) as the droplet enters, and show the presence of maxima (multiple maxima in some cases) in the disjoining pressure isotherm. If the barrier is high, the droplet will not enter, in spite of being energetically favorable $(E > 0)$. In addition, $E < 0$ corresponds to the complete wetting of the oil

droplet by the aqueous phase. This thermodynamically favorable configuration enables the droplet to spontaneously immerse into the foam. It also inhibits the formation of oil bridges between the Plateau borders or foam films. Thus, a negative value of *E* for an oil corresponds to its ability to stay fully immersed inside the aqueous foam film, and hence, such oils are inert to antifoaming activities.[65,67] A positive value of *E* complements the effective ability of the oil to prevent the destruction of foam.

The *spreading coefficient* (*S*) describes the imbalance of interfacial tension between the two fluid phases along a single line of contact. For positive values of *S*, the oil expands as a thin film between air and water, whereas, the negative values indicate the development of oil lenses floating at the air–water interface. The values of *S* for oils are correlated with their efficiency in foam breaking. Positive values of *S* reflect their antifoam activity.[68] The displacement of surfactant film at the surfaces of the lamellae by the oil is possible only if $S > 0$. Reduction in surface elasticity takes place as the spreading oil sweeps the surfactant molecules from the foam films. This may cause the vulnerable spots to thin and rupture, inasmuch as the adsorbed surfactant layer is not dense in such films. The spreading oil thus affects the destabilization of foam films in two ways. Firstly, capillary waves create thin regions on the foam film to make the rupture possible. Secondly, the thin regions carrying sparse surfactant layers are unable to stabilize these films. This may be due to the low surface charge density, and hence small electrostatic repulsion. Apart from this, an asymmetrical surfactant distribution may also lead to the destabilization of the foam film, which may appear after the oil spreads on one of the foam films.

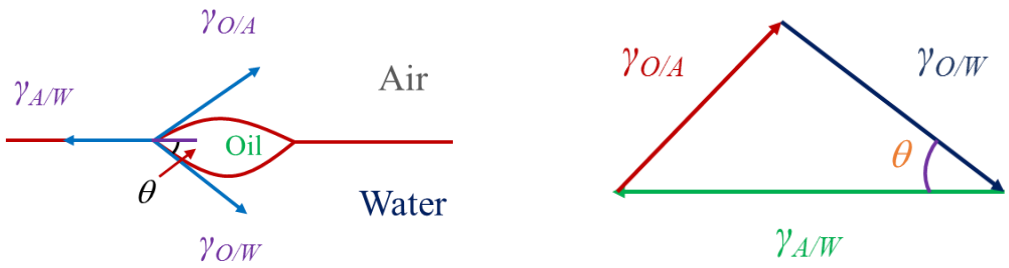

(a) (b)

Figure 3.11. (a) Schematic representation of an oil lens on the air–water interface and (b) Neumann triangle for a three-phase system.

Garrett[62,65] performed a comprehensive study on the oil bridges formed in the foam films. He analyzed the possibility of mechanical equilibrium when the bridge formed by oil is located in a foam film. His analysis also involved the balance between capillary pressure across the interfaces (i.e., air–oil–water) and the Neumann triangle. The angles between oil–water, air–water and air–oil interfaces are governed by the equilibrium of three tensions (i.e. $\gamma_{O/W}$, $\gamma_{A/W}$, and $\gamma_{A/O}$). Neumann triangle is the geometric construction representing the equilibrium of these tensions (see Figure 3.11). If the contact angle is greater than 90°, the capillary pressure across the oil–water interface is much lower than the capillary pressure across the oil–air interface. Thus, it is difficult to obtain a balance between the Neumann triangle and the capillary pressure, as both represent the crucial conditions for mechanical equilibrium in the system. Hence, the oil bridge is considered unstable and causes the foam film to rupture for contact angles greater 90°.[65,67] Thus, a contact angle greater than 90° is equivalent to $B > 0$, and it predicts an unstable bridge (i.e., rupture of the foam film) and subsequent collapse of the foam.[69] For a contact angle smaller than 90°, the bridge is considered as stable, since a perfect balance between the Neumann triangle and capillary pressure is achieved.

Table 3.1 shows the values of *E*, *S*, and *B* for the NaCl system. These values

corroborate our finding that the oil destabilized the foam under the given conditions. Upon increasing the salt concentration, these coefficients decreased, which supports the fact that the rate of foam collapse decreased with increasing NaCl concentration. The positive values of *E* represent a favorable condition for the oil droplets to enter the air–water interface at all concentrations of the surfactant and salt. During this process, several phenomena take place at the microscopic level. It may be possible that the entering oil replaces the symmetrical air–water–air film by an unstable asymmetrical pseudoemulsion film. This may be due to the change in the balance of surface and interfacial tensions, and the disjoining pressure in the film. Additionally, the oil droplets may get strongly compressed in the Plateau border, which may create a strong mechanical shock if the neighboring foam films rupture. This shock also may affect the foam films and Plateau borders located at a distance. An instantaneous discharge of surface energy may also affect the entry of other oil droplets. This may generate additional mechanical stress and thus may lead to the rupture of other films.

Positive values of *S* and *B* were observed at all surfactant and salt concentrations. These values show that *n*-hexane has large spreading and bridging coefficients, and thus, it shows a significant destabilizing effect on the foam. This destabilizing effect of the oil may be due to the lower stability of the asymmetric oil–water–air films.[70,71] With increasing surfactant and salt concentrations, the values of *E*, *S*, and *B* decreased slightly. This is likely due to the formation of a pseudoemulsion film, which tries to provide some stability to the foam film. However, the formation of this film is for a very short duration, and eventually it breaks down due to its asymmetric nature.

Table 3.1. Entering, spreading, and bridging coefficients in the absence of salt, and in the presence of NaCl

Surfactant concentration (mol m^{-3})	Salt concentration (mol m^{-3})	*E* (mN m^{-1})	*S* (mN m^{-1})	*B* (mN^2 m^{-2})
1.6	0	32.8	16.3	1392.9
	10	31.5	15.3	1376.7
	50	30.2	14.9	1350.7
2.0	0	29.6	14.5	1293.9
	10	28.4	13.2	1277.9
	50	27.8	12.8	1260.5
2.4	0	27.6	12.7	1115.0
	10	26.5	12.1	1101.2
	50	25.2	11.7	1076.0

Similar results were obtained for $CaCl_2$ and $AlCl_3$. Tables 3.2 and 3.3 show the values of *E*, *S*, and *B* for these systems. The volume of foam was the least for the $AlCl_3$ system. However, the stability of the foams in the $AlCl_3$ systems was much higher. The effectiveness of the counterions in increasing the foam stability followed the sequence: $Al^{3+} > Ca^{2+} > Na^{+}$. A decrease in the foam volumes was observed in the presence of oil and $AlCl_3$. However, these low-volume foams were quite stable. The entering, spreading, and bridging coefficients were lower for the systems containing a high amount of the salt. Note that low surface and interfacial tensions were observed in these systems (Figure 3.2 and 3.3).

Table 3.2. Entering, spreading, and bridging coefficients in the presence of $CaCl_2$

Surfactant concentration (mol m^{-3})	Salt concentration (mol m^{-3})	*E* (mN m^{-1})	*S* (mN m^{-1})	*B* (mN^2 m^{-2})
1.6	5	32.3	15.5	1389.1
	10	31.7	16.1	1380.8
2.0	5	28.2	15.3	1272.3
	10	26.9	14.0	1255.1
2.4	5	27.5	13.3	1116.2
	10	26.1	11.3	1101.4

Table 3.3. Entering, spreading, and bridging coefficients in the presence of $AlCl_3$

Surfactant concentration (mol m^{-3})	Salt concentration (mol m^{-3})	*E* (mN m^{-1})	*S* (mN m^{-1})	*B* (mN^2 m^{-2})
1.6	0.5	33.2	14.6	1364.2
	1.0	31.3	14.5	1342.3
2.0	0.5	29.5	13.6	1284.9
	1.0	28.0	13.2	1277.1
2.4	0.5	27.1	13.5	1129.2
	1.0	26.4	13.1	1117.8

3.2.4. Effect of salt on zeta potential

Zeta potential is a characteristic electrical property of the interface. It develops as a result of the formation of the EDL near the interface. It is the potential at the surface of shear. Its accurate location is difficult to detect, and it may vary with the surface morphology.

There may be a considerable amount of difference between the zeta potential and the surface potential. The latter is given by the Grahame equation,

$$\psi_0 = \left(\frac{2kT}{ze}\right)\sinh^{-1}\left[\frac{\sigma}{\left(8RT\varepsilon\varepsilon_0 c\right)^{1/2}}\right] \qquad (3.7)$$

The zeta potential is often taken as an approximate measure of the surface potential (i.e., $\zeta \approx \psi_0$). The value of the zeta potential reflects the stability of the colloidal systems that are mainly stabilized by an electrical charge on their surface. A low value of the zeta potential in these colloidal systems reflects poor stability.

The effect of concentrations of surfactant and NaCl on zeta potential is shown in Figure 3.12. The increase in zeta potential with increasing surfactant concentration signifies the importance of surfactant adsorption at the oil–water interface. In the absence of any surfactant and salt, the zeta potential of the oil–water interface was negative. This is due to the adsorption of the hydroxyl ions at the interface. Addition of salt to the aqueous surfactant solution had a pronounced influence on the zeta potential. It enhanced the adsorption of the surfactant molecules inasmuch as the electrostatic repulsion among the head-groups decreased (see Section 3.2.1). The surfactant molecules packed more densely at the interface. This was manifested by the decrease in the interfacial tension in the presence of salt (see Section 3.2.3). As a result, the surface charge density increased, which increased the zeta potential (i.e., made ζ more negative). However, at the high salt concentration (i.e., 50 mol m^{-3}), the zeta potential decreased (i.e., ζ was less negative). This trend is predicted by the Grahame equation [i.e., Equation (3.7)]. Binding of counterions may also play a significant effect on the zeta potential.[74,75]

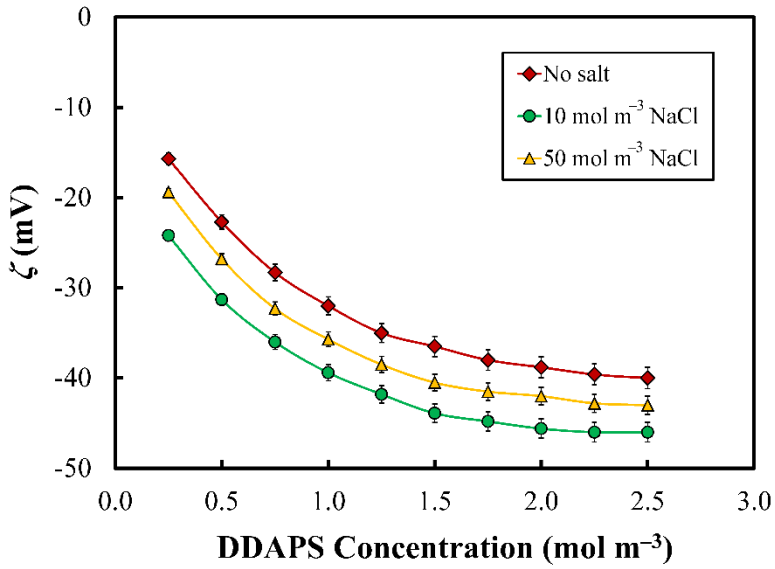

Figure 3.12. Variation of the zeta potential at the hexane–water interface with the concentration of DDAPS at different concentrations of NaCl.

Similar results were obtained for the $CaCl_2$ and $AlCl_3$ systems [See Appendix Figure A2 & A3]. The zeta potential decreased (i.e., ζ became less negative) with increasing charge density at the oil–water interface. The pH of the aqueous medium also plays a substantial effect on the zeta potential. The pH of the surfactant solution containing NaCl and $CaCl_2$ varied in the range of 6.3 ± 0.5. However, the pH was considerably reduced in the presence of $AlCl_3$ (i.e., 4.0 ± 0.5). Hydrated aluminum ions (i.e., $[Al(H_2O)_6]^{+3}$) are formed when aluminum chloride is dissolved in water.[76] Electrons associated with the water molecules are firmly dragged towards aluminum, thus making the hexaaquaaluminum ion acidic. This enables the hydrogens to be more positive, and they attack the solvent water molecules, which act as a base. Thus, deprotonation of the hexaaqua ion takes place, which makes the solution acidic by forming the hydroxonium ion. Low pH usually gives positive zeta potential for interfaces covered with a zwitterionic surfactant.[77] Figure 3.13 depicts that ζ became less negative

with the reduction in pH, and ultimately became positive after crossing the IEP. Our results corroborate those reported in the literature.[78] The effectiveness of salts in decreasing the zeta potential (i.e., making ζ less negative) was in the sequence: $AlCl_3$ > $CaCl_2$ > NaCl (See Appendix A2 and A3).

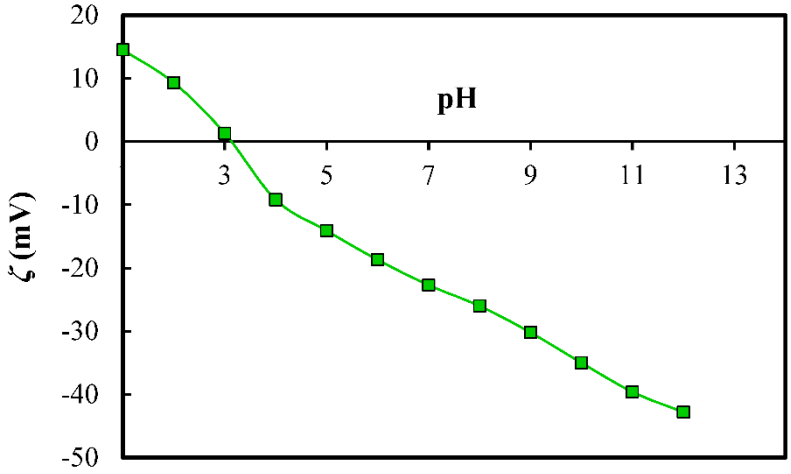

Figure 3.13. Variation of zeta potential at the air–water interface with pH.

3.3. Conclusions

In this chapter, a study on the stability of foams generated from the aqueous solutions of a zwitterionic surfactant (i.e., DDAPS), in the presence of NaCl, $CaCl_2$, and $AlCl_3$ is reported. Our work highlights the mechanism involved in foam stability. The surface tension decreased upon increasing the DDAPS concentration, indicating an increase in the surfactant concentration at the air–water interface. Addition of salt reduced the surface tension of the DDAPS solution, signifying an enhanced adsorption of the DDAPS molecules at the air–water interface. This was accompanied by a reduction in CMC. The quantity of salt necessary for reducing the surface tension and CMC was in the sequence: NaCl > $CaCl_2$ > $AlCl_3$. The initial foam volume increased with increasing DDAPS concentration and decreased in the presence of salt. The number of DDAPS molecules at

the air–water interface increased upon increasing the surfactant concentration, thus causing an increase in the foam volume. The electrostatic repulsion plays an important role in these phenomena. $AlCl_3$ was more effective than $CaCl_2$, and the latter was more effective than NaCl in reducing the foam volume. The foam collapse rate was higher during the initial period after foam formation in the absence of salt and at low salt concentration. In the second half of the experiment, the foam collapse rate was less, and it did not vary significantly with the surfactant and salt concentrations.

The effect of oil on the foam was investigated by solubilizing *n*-hexane in aqueous DDAPS solutions. The diameter of the *n*-hexane droplets decreased upon increasing DDAPS and salt concentrations. This reduction was associated with the reduction in interfacial tension by the addition of salt. In the presence of oil, the initial foam volume decreased with increasing surfactant and salt concentrations. The foam collapse rate was high during the initial period at the low salt concentration (for all salts). However, at the high salt concentrations, the foam collapse rate was less. The entering, spreading, and bridging coefficients were positive. These coefficients decreased with increasing salt concentration. Positive values of the spreading and bridging coefficients show that *n*-hexane had a destabilizing effect on foam. Low stability of the irregular oil–water–air films may impart a destabilizing effect on the foams. The effectiveness of the counterions in increasing the foam stability followed the sequence: $Al^{3+} > Ca^{2+} > Na^{+}$. The zeta potential at the oil–water interface increased (i.e., ζ became more negative) with the increasing concentration of DDAPS up to the CMC. Addition of a small quantity of salt increased the zeta potential. However, the zeta potential decreased at high salt concentration. The effectiveness of salts in reducing the zeta potential was in the sequence: $AlCl_3 > CaCl_2 > NaCl$.

References

[1] Kralova, I.; Sjöblom, J. Surfactants used in food industry: A review. *J. Dispersion Sci. Technol.* **2009,** 30, 1363–1383.

[2] Schramm, L. L., *Surfactants: Fundamentals and Applications in the Petroleum Industry*; Cambridge University Press: Washington DC, 2000.

[3] Rosen, M. J.; Song, L. D. Superspreading, skein wetting, and dynamic surface tension. *Langmuir* **1996,** 12, 4945–4949.

[4] Williams, J. M. High internal phase water-in-oil emulsions: influence of surfactants and cosurfactants on emulsion stability and foam quality. *Langmuir* **1991,** 7, 1370–1377.

[5] Karsa, D. R., *Industrial Applications of Surfactants IV*; Elsevier: Cambridge, 1999.

[6] Dey, J.; Shrivastava, S. Physicochemical characterization and self-assembly studies on cationic surfactants bearing mPEG tail. *Langmuir* **2012,** 28, 17247–17255.

[7] Zhao, J.; Christian, S. D.; Fung, B. M. Mixtures of monomeric and dimeric cationic surfactants. *J. Phys. Chem. B* **1998,** 102, 7613–7618.

[8] Li, M.; Powell, M. J.; Razunguzwa, T. T.; O'Doherty, G. A. A general approach to anionic acid-labile surfactants with tunable properties. *J. Org. Chem.* **2010,** 75, 6149–6153.

[9] Colin, A.; Giermanska-Kahn, J.; Langevin, D.; Desbat, B. Foaming properties of modified ethoxylated nonionic surfactants. *Langmuir* **1997,** 13, 2953–2959.

[10] Elola, M. D.; Rodriguez, J. Structure and dynamics of nonionic surfactants adsorbed at vacuum/ionic liquid interfaces. *Langmuir* **2013,** 29, 13379–13387.

[11] Kamenka, N.; Chevalier, Y.; Zana, R. Aqueous solutions of zwitterionic surfactants with varying carbon number of the intercharge group. 1. Micelle aggregation numbers. *Langmuir* **1995,** 11, 3351–3355.

[12] Rosen, M. J., *Surfactants and Interfacial Phenomena*; John Wiley & Sons: New York, 2004.

[13] Yang, J. Viscoelastic wormlike micelles and their applications. *Curr. Opin. Colloid Interface Sci.* **2002,** 7, 276–281.

[14] McLachlan, A. A.; Marangoni, D. G. Interactions between zwitterionic and conventional anionic and cationic surfactants. *J. Colloid Interface Sci.* **2006,** 295, 243–248.

[15] Tsubone, K.; Uchida, N.; Mimura, K. New amphoteric surfactants containing a phosphoric acid group: II. Binary system of amphoteric/anionic surfactant of sodium 2-(N-2-hydroxytetradecyl-N-methylamino) ethyl hydrogen phosphate. *J. Am. Oil Chem. Soc.* **1990,** 67, 455–458.

[16] Zhao, J.; Dai, C.; Ding, Q.; Du, M.; Feng, H.; Wei, Z.; Chen, A.; Zhao, M. The structure effect on the surface and interfacial properties of zwitterionic sulfobetaine surfactants for enhanced oil recovery. *RSC Adv.* **2015,** 5, 13993–14001.

[17] Zhang, R.; Somasundaran, P. Advances in adsorption of surfactants and their mixtures at solid/solution interfaces. *Adv. Colloid Interface Sci.* **2006,** 123, 213–229.

[18] Sainath, K.; Ghosh, P. Stabilization of silicone oil-in-water emulsions by ionic surfactant and electrolytes: The role of adsorption and electric charge at the interface. *Ind. Eng. Chem. Res.* **2013,** 52, 15808–15816.

[19] Kumar, M. K.; Mitra, T.; Ghosh, P. Adsorption of ionic surfactants at liquid–liquid interfaces in the presence of salt: Application in binary coalescence of drops. *Ind. Eng. Chem. Res.* **2006,** 45, 7135–7143.

[20] Lu, J. R.; Marrocco, A.; Su, T. J.; Thomas, R. K.; Penfold, J. Adsorption of dodecyl sulfate surfactants with monovalent metal counterions at the air–water interface studied by neutron reflection and surface tension. *J. Colloid Interface Sci.* **1993,** 158, 303–316.

[21] Langevin, D. Aqueous foams: A field of investigation at the frontier between chemistry and physics. *Chem. Phys. Chem.* **2008,** 9, 510–522.

[22] Lobo, L.; Nikolov, A.; Wasan, D. Foam stability in the presence of oil: On the importance of the second virial coefficient. *J. Dispersion Sci. Technol.* **1989,** 10, 143–161.

[23] Kristen-Hochrein, N.; Laschewsky, A.; Miller, R.; von Klitzing, R. Stability of foam films of oppositely charged polyelectrolyte/surfactant mixtures: Effect of isoelectric point. *J. Phys. Chem. B* **2011,** 115, 14475–14483.

[24] Chorro, M.; Kamenka, N.; Faucompre, B.; Partyka, S.; Lindheimer, M.; Zana, R. Micellization and adsorption of a zwitterionic surfactant: N-dodecyl betaine-effect of salt. *Colloids and Surf. A* **1996,** 110, 249–261.

[25] Deng, Q.; Li, H.; Li, C.; Lv, W.; Li, Y. Enhancement of foamability and foam stability induced by interactions between a hyperbranched exopolysaccharide and a

zwitterionic surfactant dodecyl sulfobetaine. *RSC Adv.* **2015,** 5, 61868–61875.

[26] Kwaambwa, H. M.; Nermark, F. M. Interactions in aqueous solution of a zwitterionic surfactant with a water treatment protein from Moringa *oleifera* seeds studied by surface tension and ultrasonic velocity measurements. *Green Sustain. Chem.* **2013,** 3, 135–140.

[27] Lima, E. R. A.; Melo B. M.; Baptista, L. T.; Paredes, L. L. Specific ion effects on the interfacial tension of water/hydrocarbon systems. *Braz. J. Chem. Eng.* **2013,** 30, 55–62.

[27] Li, N.; Zhang, G.; Ge, J.; Luchao, J.; Jianqiang, Z.; Baodong, D.; Pei, H. Adsorption behavior of betaine-type surfactant on quartz sand. *Energy Fuels* **2011,** 25, 4430–4437.

[28] Pinazo, A.; Chang, C.-H.; Franses, E. Dynamic surface tension behavior of aqueous solutions of N-dodecyl-N, N dimethyl aminobetaine chlorohydrate. *Colloid. Polym. Sci.* **1994,** 272, 447–455.

[29] Zajac, J.; Chorro, C.; Lindheimer, M.; Partyka, S. Thermodynamics of micellization and adsorption of zwitterionic surfactants in aqueous media. *Langmuir* **1997,** 13, 1486–1495.

[30] Tajima, K. Radiotracer studies on adsorption of surface active substance at aqueous surface. III. The effects of salt on the adsorption of sodium dodecylsulfate. *Bull. Chem. Soc. Jpn.* **1971,** 44, 1767–1771.

[31] Srinivas, A.; Ghosh, P. Coalescence of bubbles in aqueous alcohol solutions. *Ind. Eng. Chem. Res.* **2012,** 51, 795–806.

[32] Warszyński, P.; Lunkenheimer, K.; Czichocki, G. Effect of counterions on the adsorption of ionic surfactants at fluid-fluid interfaces. *Langmuir* **2002,** 18, 2506–2514.

[33] Israelachvili, J. N., *Intermolecular and Surface Forces;* Academic Press: London, 2011.

[34] Ruckenstein, E. The origin of thermodynamic stability of microemulsions. *Chem. Phys. Lett.* **1978,** 57, 517–521.

[35] Somasundaran, P., *Encyclopedia of Surface and Colloid Science*; CRC press: New York, 2006.

[36] Liu, L.; Zhang, Q.; Pan, Q.; Zhang, J.; Li, C.; Pei, M. Interaction between anionic

and zwitterionic surfactants: Sodium dodecyl sulfate and N-alkyl-N, N-dimethylsulfobetain, N-lauroylsarcosine. *J. Dispersion Sci. Technol.* **2007,** 28, 1329–1333.

[37] Wang, L.-C.; Wang, H.-Y.; Zhu, Y.-W.; Song, X.-W.; Liu, S.-J.; Liu, X.; Jiang, S.-X. Studies of interfacial activities of four kinds of surfactants at oil/water interface. *J. Dispersion Sci. Technol.* **2012,** 33, 374–379.

[38] You, J.; Kim, J.; Park, T.; Kim, B.; Kim, E. Highly fluorescent conjugated polyelectrolyte nanostructures: Synthesis, self-assembly, and Al^{3+} ion sensing. *Adv. Funct. Mater.* **2012,** 22, 1417–1424.

[39] Israelachvili, J. N.; Adams, G. E. Measurement of forces between two mica surfaces in aqueous electrolyte solutions in the range 0–100 nm. *J. Chem. Soc. Faraday Trans.* **1978,** 74, 975–1001.

[40] Xu, J.; Wang, A. Electrokinetic and colloidal properties of homogenized and unhomogenized palygorskite in the presence of electrolytes. *J. Chem. Eng. Data* **2012,** 57, 1586–1593.

[41] Dukhin, S. S.; Kretzschmar, G.; Miller, R., *Dynamics of Adsorption at Liquid Interfaces: Theory, Experiment, Application*; Elsevier: Amsterdam, 1995.

[42] Marinova, K. G.; Basheva, E. S.; Nenova, B.; Temelska, M.; Mirarefi, A. Y.; Campbell, B.; Ivanov, I. B. Physico-chemical factors controlling the foamability and foam stability of milk proteins: Sodium caseinate and whey protein concentrates. *Food Hydrocolloids* **2009,** 23, 1864–1876.

[43] Behera, M. R.; Varade, S. R.; Ghosh, P.; Paul, P.; Negi, A. S. Foaming in micellar Solutions: Effects of surfactant, salt, and oil concentrations. *Ind. Eng. Chem. Res.* **2014,** 53, 18497–18507.

[44] Exerowa, D.; Kolarov, T.; Khristov, K. Direct measurement of disjoining pressure in black foam films. I. Films from an ionic surfactant. *Colloids Surf.* **1987,** 22, 161–169.

[45] Kolarov, T.; Cohen, R.; Exerowa, D. Direct measurement of disjoining pressure in black foam films II. Films from nonionic surfactants. *Colloids Surf.* **1989,** 42, 49–57.

[46] Bhakta, A.; Ruckenstein, E. Modeling of the generation and collapse of aqueous foams. *Langmuir* **1996,** 12, 3089–3099.

[47] Hartland, S., *Surface and Interfacial Tension: Measurement, Theory, and*

Applications; Vol. 119, CRC Press: New York, 2004.

[48] Ruckenstein, E.; Bhakta, A. Effect of surfactant and salt concentrations on the drainage and collapse of foams involving ionic surfactants. *Langmuir* **1996,** 12, 4134–4144.

[49] Rao, A.; Wasan, D.; Manev, E. Foam stability-effect of surfactant composition on the drainage of microscopic aqueous films. *Chem. Eng. Commun.* **1982,** 15, 63–81.

[50] Sedev, R.; Exerowa, D. DLVO and non-DLVO surface forces in foam films from amphiphilic block copolymers. *Adv. Colloid Interface Sci.* **1999,** 83, 111–136.

[51] Adamson, A. W.; Gast, A. P., *Physical Chemistry of Surfaces*; John Wiley & Sons: New York, 1967.

[52] Prud'homme, R., *Foams: Theory, Measurements, and Applications*; Marcel Dekker: New York, 2017.

[53] Exerowa, D.; Kruglyakov, P. M., *Foam and Foam Films: Theory, Experiment, Application*; Elsevier: Amsterdam, 1997.

[54] Schramm, L. L., *Emulsions, Foams, and Suspensions: Fundamentals and Applications*; John Wiley & Sons: New York, 2006.

[55] Basheva, E. S.; Ganchev, D.; Denkov, N. D.; Kasuga, K.; Satoh, N.; Tsujii, K. Role of betaine as foam booster in the presence of silicone oil drops. *Langmuir* **2000,** 16, 1000–1013.

[56] Garrett, P.; Davis, J.; Rendall, H. An experimental study of the antifoam behaviour of mixtures of a hydrocarbon oil and hydrophobic particles. *Colloids and Surf. A* **1994,** 85, 159–197.

[57] Lee, J.; Nikolov, A.; Wasan, D. Stability of aqueous foams in the presence of oil: On the importance of dispersed vs solubilized oil. *Ind. Eng. Chem. Res.* **2012,** 52, 66–72.

[58] Wang, C.; Fang, H.; Gong, Q.; Xu, Z.; Liu, Z.; Zhang, L.; Zhang, L.; Zhao, S. Roles of catanionic surfactant mixtures on the stability of foams in the presence of oil. *Energy Fuels* **2016,** 30, 6355–6364.

[59] Garrett, P. R. Preliminary considerations concerning the stability of a liquid heterogeneity in a plane-parallel liquid film. *J. Colloid Interface Sci.* **1980,** 76, 587–590.

[60] Osei-Bonsu, K.; Shokri, N.; Grassia, P. Foam stability in the presence and absence of hydrocarbons: From bubble-to bulk-scale. *Colloids and Surf. A* **2015,** 481, 514–526.

[61] Schramm, L. L.; Novosad, J. J. The destabilization of foams for improved oil recovery by crude oils: Effect of the nature of the oil. *J. Pet. Sci. Eng.* **1992,** 7, 77–90.

[62] Garrett, P., *Defoaming: Theory and Industrial Applications*; Marcel Dekker: New York, 1992.

[63] Birdi, K., *Handbook of Surface and Colloid Chemistry*; CRC Press: Boca Raton, 2002.

[64] Aveyard, R.; Binks, B. P.; Fletcher, P. D. I.; Peck, T.-G.; Garrett, P. R. Entry and spreading of alkane drops at the air/surfactant solution interface in relation to foam and soap film stability. *J. Chem. Soc., Faraday Trans.* **1993,** 89, 4313–4321.

[65] Ross, S. The inhibition of foaming. II. A mechanism for the rupture of liquid films by anti-foaming agents. *J. Phys. Chem.* **1950,** 54, 429–436.

[66] Denkov, N. D. Mechanisms of foam destruction by oil-based antifoams. *Langmuir* **2004,** 20, 9463–9505.

[67] Aronson, A.; Bergeron, V.; Fagan, M. E.; Radke, C. The influence of disjoining pressure on foam stability and flow in porous media. *Colloids and Surf. A* **1994,** 83, 109–120.

[68] Bergeron, V.; Hanssen, J. E.; Shoghl, F. Thin-film forces in hydrocarbon foam films and their application to gas-blocking foams in enhanced oil recovery. *Colloids and Surf. A* **1997,** 123, 609–622.

[69] Berg, J. C., *An Introduction to Interfaces & Colloids: The Bridge to Nanoscience*; World Scientific: Singapore, 2010.

[70] Hiemenz, P. C.; Rajagopalan, R., *Principles of Colloid and Surface Chemistry*; Marcel Dekker: New York, 1997.

[71] Bommaganti, P.; Kumar, M. V.; Ghosh, P. Effects of binding of counterions on adsorption and coalescence. *Chem. Eng. Res. Des.* **2009,** 87, 728–738.

[72] Kralchevsky, P.; Danov, K.; Broze, G.; Mehreteab, A. Thermodynamics of ionic surfactant adsorption with account for the counterion binding: Effect of salts of various valency. *Langmuir* **1999,** 15, 2351–2365.

[73] Cotton, A. F.; Wilkinson, G.; Bochmann, M.; Murillo, C. A., *Advanced Inorganic Chemistry*; Wiley: New York, 1999.

[74] Kim, J.-Y.; Song, M.-G.; Kim, J.-D. Zeta potential of nanobubbles generated by ultrasonication in aqueous alkyl polyglycoside solutions. *J. Colloid Interface Sci.* **2000,** 223, 285–291.

[75] Kim, J.-S.; Park, J.-S.; Lim, J.-C. Measurement of isoelectric point of betaine zwitterionic surfactant by QCM (quartz crystal microbalance). *Korean Chem. Eng. Res.* **2009,** 47, 31–37.

CHAPTER 4

FOAMING IN AQUEOUS SOLUTIONS OF ZWITTERIONIC SURFACTANT IN PRESENCE OF MONOVALENT SALTS: THE SPECIFIC ION EFFECT

4.1. Introduction

The specific ion effect is important for various colloidal dispersions and complex fluids. The varied affinity of the ions towards the interface is the basis of ion specificity. Many interfacial phenomena in the colloidal systems are influenced by the specific ion effect.[1-3] They are prevalent in most of the chemical and biological interactions. They influence numerous processes in aqueous systems such as swelling of tissues, viscosity of solutions, precipitation of proteins, ion exchange, enzymatic activities, and coalescence of bubbles. As the charged surfaces are ubiquitous, the specific ion effect regulates the overall charge of the interfacial region and influences the interfacial forces. The specific ion effect can significantly change the sign of the potential at the interface and assign a unique value to it. This is significant in tailoring the stability of colloidal systems, and critical to the interactions in various physico-chemical[4-6] and biological processes as well.[7] The specific ion effect is related to the Hofmeister series to some extent and has been described in Section 1.10 (Chapter 1).

Since the specific ion effect governs many interfacial phenomena, it has been the subject of hot debate over the last couple of decades.[2,8-13] Aroti et al.[14,15] have studied the specific ion effect in the presence of sodium salts of different monovalent anions on the Langmuir monolayers of zwitterionic phospholipids (with phosphatidylcholine as the head-group) and lamellar lipid systems. They found that a significant interaction existed among the anions and the zwitterionic phospholipids. Rendall and Tiddy[16] used NMR quadrupole splitting for investigating the binding of ions on the surface of the micelles of dodecyl/tetradecyl dimethyl amine oxide (a zwitterionic surfactant). The positive value of quadrupole splitting indicated that the sodium ions were present in the head-group layer. This result demonstrated a significant presence of ions between the head-groups, which did not perturb the bound water.

Hardly any research work has been performed concerning the specific ion effect on the foams stabilized by zwitterionic surfactants. Accordingly, the primary objective of this work was to examine the stability of foams prepared from the aqueous solutions of a zwitterionic surfactant (i.e., DDAPS) in the presence of three 1:1 salts having the same anion (i.e., LiCl, NaCl, and CsCl). The adsorption of DDAPS at the air–water and *n*-hexane–water interfaces was investigated by the surface and interfacial tension measurements, respectively. Studies on foam stability and foamability were carried out by employing the Blender test. The zeta potential of the *n*-hexane–water interface was also measured.

4.2 Results and Discussion

4.2.1 Adsorption of DDAPS in the presence of salts

The surface and interfacial tension profiles are shown in Figures 4.1 and 4.2, respectively. (note that the *x*-axis represents $\ln c$). The concentrations of the salts (i.e., NaCl, LiCl, and CsCl) were 10, 50, and 100 mol m^{-3}. Surface tension depends on the number of surfactant molecules adsorbed on the fluid–fluid interface. While increasing the DDAPS concentration, a decrease in surface tension was observed, which signifies increasing adsorption of the surfactant molecules at the air–water interface.[17] The surface tension profile approached the plateau region at ~2.4 mol m^{-3} surfactant concentration in the absence of salt. At this concentration, the air–water interface was saturated with the surfactant molecules, which led to the formation of a monolayer. Thus, the CMC of DDAPS was ~2.4 mol m^{-3}, which is close to its literature value.[18]

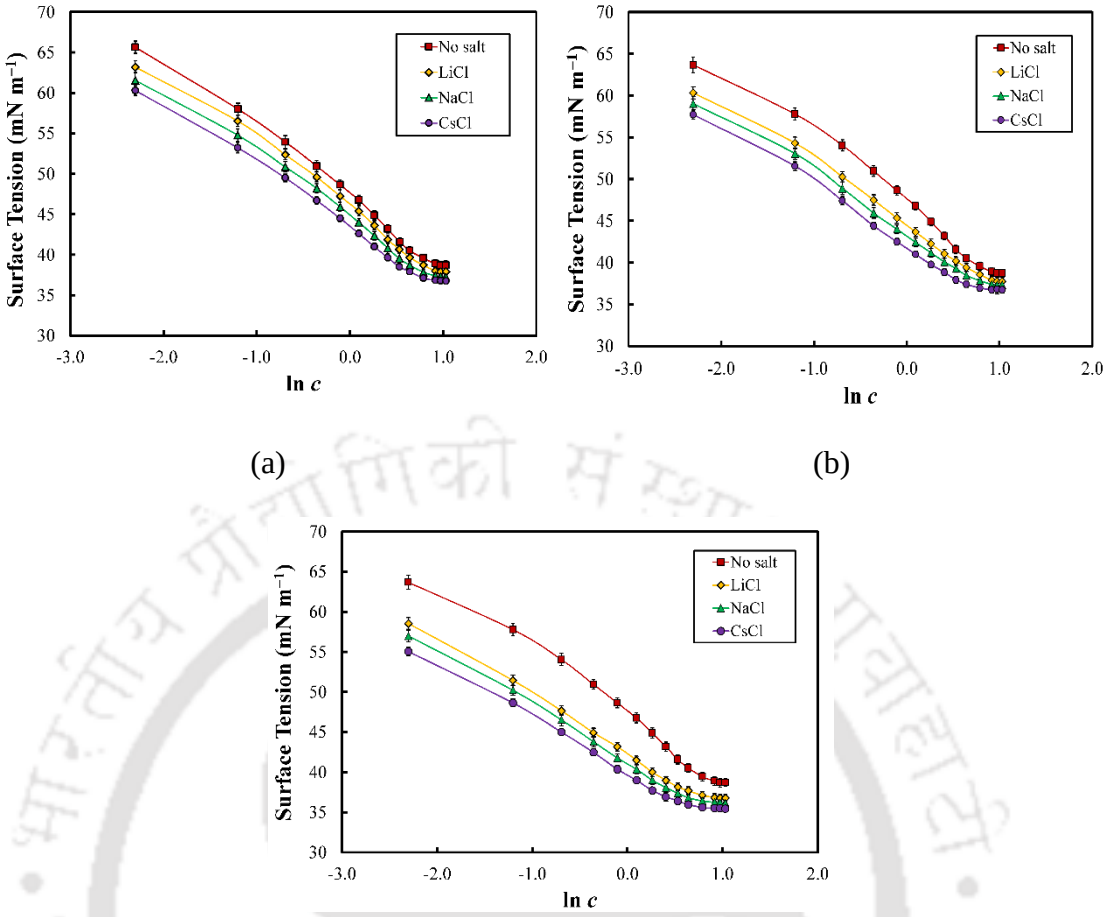

Figure 4.1. Variation of surface tension with the concentration of DDAPS (expressed as $\ln c$) at (a) 10, (b) 50, and (c) 100 mol m^{-3} NaCl, CsCl, and LiCl.

Similar to surface tension, tension at the hexane–water interface also decreased in the presence of DDAPS. The interfacial tension between *n*-hexane and water was ~50 mN m^{-1} in the absence of surfactant, which agrees well with the value reported in the literature.[19] Upon addition of DDAPS, a gradual decrease in interfacial tension was observed, which is shown in Figure 4.2. The interfacial energy between oil and water is lowered as the surfactant adsorption increases. This is clearly reflected in Figure 4.2. The minima of the interfacial tension profiles were attained earlier than the same for surface tension inasmuch as the hydrophobic phases were different. Oil being more

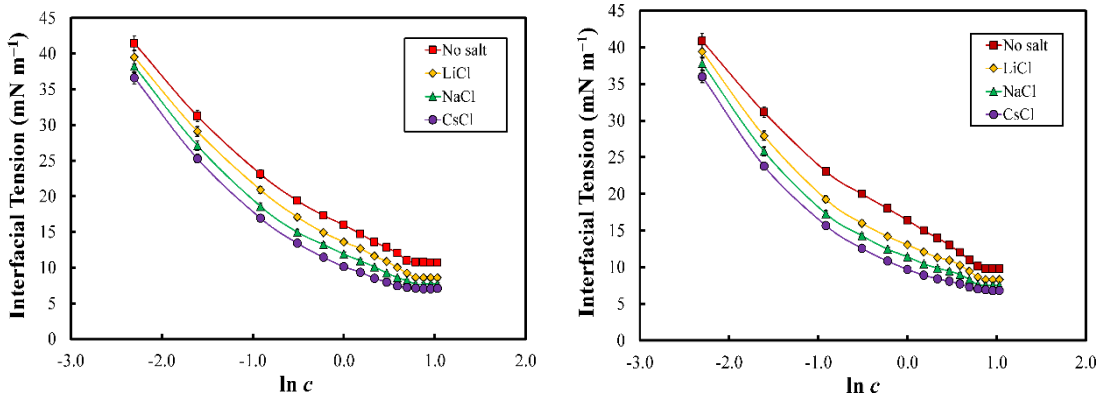

(a) (b)

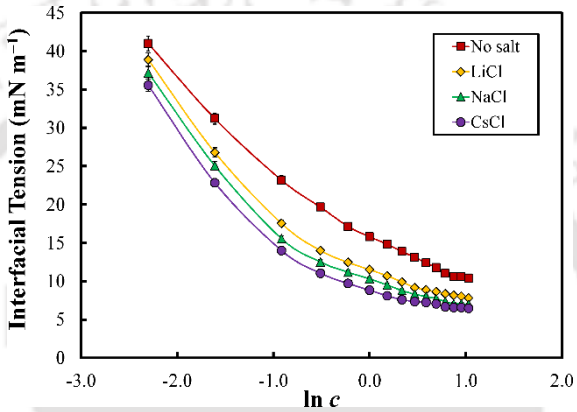

(c)

Figure 4.2. Variation of interfacial tension with the concentration of DDAPS (expressed as $\ln c$) at (a) 10, (b) 50, and (c) 100 mol m^{-3} NaCl, CsCl, and LiCl.

hydrophobic, the surfactant tails encountered more favorable accommodation in it. Therefore, the surfactant adsorption was enhanced at the oil–water interface.

The Gibbs adsorption equation was employed to calculate the surface excess concentration at the CMC for each system. For DDAPS, it is given by,[17,20]

$$\Gamma = -\frac{1}{RT}\frac{d\gamma}{d\ln c} \tag{4.1}$$

A fourth-order least-squares polynomial was fitted to the γ versus $\ln c$ profiles, and the values of $d\gamma/d\ln c$ were computed from this polynomial. Next, Γ was computed from Equation (4.1). The minimum area occupied by a surfactant molecule at the air–

water interface is given by,[17,20]

$$A_m = \frac{1}{\Gamma N_A} \tag{4.2}$$

The values of Γ and A_m at the air–water and *n*-hexane–water interfaces are given in Table 4.1. As expected, the surface excess concentration varied with the concentration of surfactant. The specific ion effect was manifested in the surface excess concentrations, which followed the order: CsCl > NaCl > LiCl. The minimum area occupied by a surfactant molecule followed the reverse order: LiCl > NaCl > CsCl.

Table 4.1. Surface excess concentration of the surfactant and the minimum area occupied by a surfactant molecule at the air–water and *n*-hexane–water interfaces.

Salt Concentration	$\Gamma \times 10^6$ (mol m^{-2})	A_m (nm^2)
	Air–water Interface	
No salt	1.91	0.869
10 mol m^{-3} CsCl	2.35	0.706
10 mol m^{-3} NaCl	2.21	0.751
10 mol m^{-3} LiCl	2.05	0.809
50 mol m^{-3} CsCl	2.88	0.576
50 mol m^{-3} NaCl	2.63	0.633
50 mol m^{-3} LiCl	2.54	0.653
100 mol m^{-3} CsCl	3.34	0.497
100 mol m^{-3} NaCl	3.19	0.520
100 mol m^{-3} LiCl	3.07	0.540

	n-hexane–water Interface	
No salt	1.73	0.959
10 mol m^{-3} CsCl	1.98	0.838
10 mol m^{-3} NaCl	1.91	0.869
10 mol m^{-3} LiCl	1.85	0.897
50 mol m^{-3} CsCl	2.24	0.741
50 mol m^{-3} NaCl	2.11	0.786
50 mol m^{-3} LiCl	2.06	0.805
100 mol m^{-3} CsCl	2.62	0.633
100 mol m^{-3} NaCl	2.46	0.674
100 mol m^{-3} LiCl	2.30	0.721

Adsorption of zwitterionic surfactant at the fluid–fluid interface is governed by electrostatic interactions among the charged centers of the molecules and the hydrophobic interaction.[21] The spacer group (i.e., propyl) of this surfactant plays a more important role in the surface activity as compared to the head-groups (i.e., quaternary ammonium and sulfonate). The spacer group is rigid and hydrophobic, which disallows a strong electrostatic attraction among the negative and positive centers. However, it allows a weak electrostatic attraction between them, which lowers their ability to pack more tightly.[22] Also, it significantly affects the surface tension and the CMC.[23] A remarkable reduction in surface tension was observed for the aqueous DDAPS solution upon addition of 10 mol m^{-3} salt. However, the net decrease in surface tension was rather small as compared to the same for the ionic surfactants,[24] but higher than that for the non-ionic surfactants.[25] Upon addition of salt, a significant reduction in surface tension was

observed at the low concentrations of DDAPS. This signifies that more DDAPS molecules could be accommodated at the air–water interface in the presence of salt at the lower surfactant concentrations. Upon increasing the salt concentration from 10 to 50 mol m^{-3}, and further up to 100 mol m^{-3}, more decrease in the surface tension was observed, indicating enhanced adsorption of the DDAPS molecules. The reduction in surface tension was small at the low salt concentrations. This may be due to the fact that the zwitterionic surfactant molecule behaves like a non-ionic surfactant (due to its core structure) even though it carries two ionic groups.[18]

At the air–water interface, the surfactant head-groups of similar charge repel, whereas, the hydrophobic tails attract each other.[26,27] The repulsive interaction energy between the surfactant head-groups and the attractive van der Waals interaction energy between the two parallel hydrophobic chains can be expressed similarly as described in Section 3.1 (Chapter 3). Unlike the ionic surfactants, the mechanism of binding of counterions to the head-groups of the zwitterionic surfactants is significantly different.[28] Upon increasing the salt concentration, a steady decrease in surface activity has been noticed for a few zwitterionic surfactants.[29] The positive (i.e., Na^+, Cs^+, and Li^+) and the negative (i.e., Cl^-) ions present in the aqueous solution encounter electrostatic attraction with the sulfonate and quaternary ammonium groups of the zwitterionic surfactant molecule, respectively. Therefore, an effective attraction between the head-groups of the DDAPS molecule and the monovalent salt is expected. These salts, therefore, strongly affect the surface activity of the surfactant. However, in addition to the electrostatic attraction, the charged centers of the surfactant molecule and the salt ions experience repulsion between them. For example, the cations (i.e., Na^+, Cs^+, and Li^+) and the anion (i.e., Cl^-) experience repulsion with the ammonium and the sulfonate groups of the surfactant, respectively. Therefore, the monovalent salts have an overall small interaction

with the hydrophilic charged centers of DDAPS, and their effect on the surface activity of DDAPS is rather small.

An increase in surface tension of water with increasing salt concentration (in the absence of surfactant) has been reported for almost all inorganic salts.[30-32] This increase has been attributed to the negative adsorption of the salt ions on the air–water interface.[33] However, the nature of ions plays a significant part in the increase in surface tension. Several theories have been proposed to describe the effect of salt on surface tension and the effect of the ions on it. Jungwirth and Tobias[34] considered the size and polarizability of the ions for explaining the specific ion effect. They hypothesized that the dipole on the anion and an incomplete solvation shell are the main driving forces behind this effect. According to Manciu,[35] the specific ion effect on surface tension and surface potential are based on the volume exclusion effects. They explained the specific ion effect for cations at large electrolyte concentrations in terms of the hydration number of the ions. The distorted water structure may have a significant impact on the specific ion effect. Water possesses a unique ability to form an extensive network of hydrogen bonds, which makes it a well-structured liquid. Analysis of the Hofmeister series has given rise to numerous theories, which consider the effect of salts to modify the dynamic and structural properties of water. Several researchers have suggested that the ions alter the hydrogen bonding network of water, and the capability of the ions in this regard is quite varied.[36,37] The change in the water structure is due to the hydrophobic interaction between the salt ions and the water molecules. The ordered water molecules present at the surface have lower entropy than the water molecules present in the bulk. In an aqueous solution containing surfactant and salt, the interaction between the hydrophilic head-groups and the salt ions can increase or decrease corresponding to that in pure water. This variation between the interacting species depends on the nature of the solvated ions. Hydrophobic

interactions are solvent-induced. Hence, this has led to the distribution of the ions as *kosmotrophes* (i.e., structure-making) or *chaotropes* (i.e., structure-breaking), based on the ability to enhance or disrupting the structure of water. Collins[38] made an important assumption by considering an ion as a sphere with a point charge. He introduced the *law of matching water affinities* to explain a large number of phenomena associated with the specific ion effect. Small (i.e., hard) ions hold a strongly-bound hydration shell. However, the force between these ions is strong enough to squeeze-out the hydration shell. Big (i.e., soft) ions bear a loosely-bound hydration shell. Small monovalent ions of high charge density strongly bind the water molecules, whereas the large ions of low charge density bind the water molecules weakly as compared to the strength of water–water interactions in the bulk solution. The electrostatic interaction is weak enough, but it is sufficiently strong to remove the hydration shell. The presence of hard and soft ions leads to a mismatch, and thus both ions remain detached by a hydration layer. This simple concept has been shown to possess an amazingly predictive power.[38]

According to Figure 4.1, the ability of the salts in reducing the surface tension was in the order: LiCl < NaCl < CsCl. Therefore, among these three salts, CsCl was more efficient in decreasing the surface tension as compared to NaCl and LiCl. Since the anion (i.e., Cl^-) was the same for all salts, a cation effect has been observed. This phenomenon may be depicted by considering the molecular arrangement of the ions at the air–water interface, as illustrated in Figure 4.3. The alkali metals, Li, Na, and Cs, lie in the s-block of the periodic table. Their bare ionic radii are 0.068, 0.095, and 0.169 nm, respectively. However, the hydrated radii of these metal ions are 0.38, 0.36, and 0.33 nm, respectively.[39] Thus, during the adsorption of a surfactant molecule, only a few Li^+ accumulate around it at the interface due to its larger size. This causes less adsorption of the DDAPS molecules at the interface, and hence a lower reduction in surface (or

interfacial) tension. However, when the cesium ions approach the interface, their number around a surfactant molecule at the interface is more due to their smaller size. Hence, Cs^+ reduces the repulsion between the surfactant molecules and enhances their adsorption at the interface. Therefore, the surfactant concentration at the interface was more in the presence of Cs^+. This phenomenon caused a significant decrease in surface tension for CsCl as compared to NaCl and LiCl.

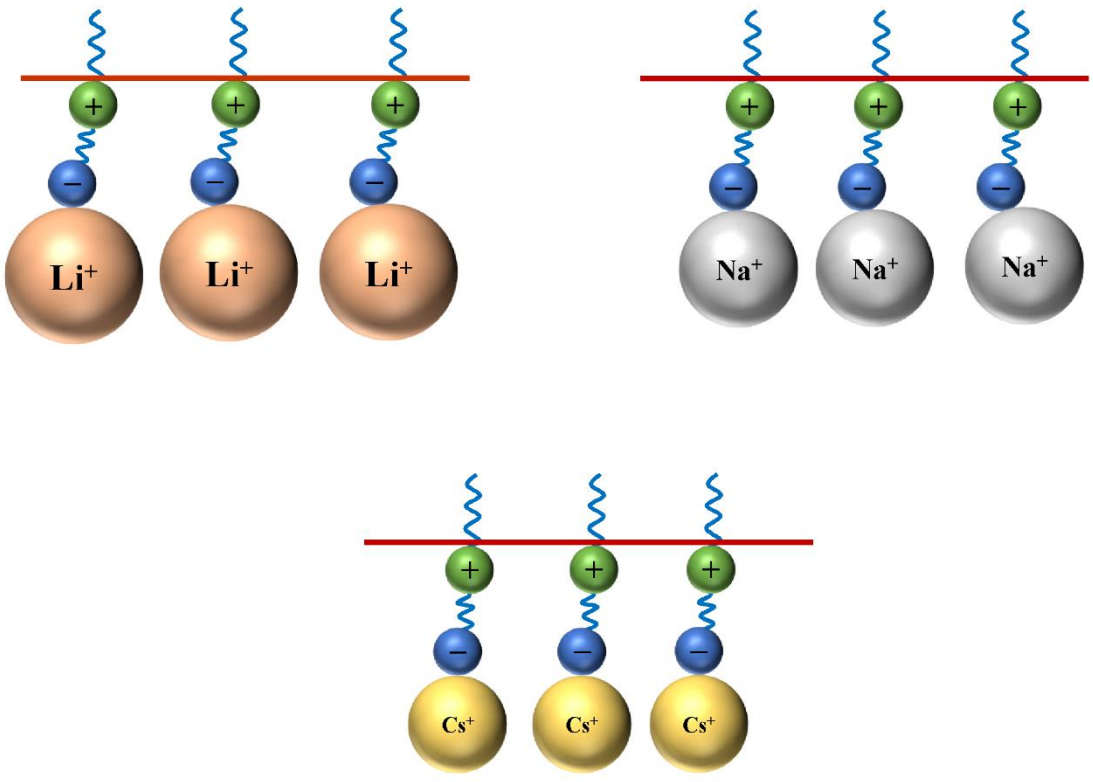

Figure 4.3. Effect of Li^+, Na^+, and Cs^+ on the molecular orientation of DDAPS at the air–water interface.

4.2.2 Specific ion effect on foams

The effects of NaCl, CsCl, and LiCl on foam formation and stability were studied at different ionic strengths. Figure 4.4 depicts the variation of foam volume with time at various DDAPS concentrations in the absence of salt. Figure 4.5 shows the pictorial view

of the decrease in foam volume with time for 2 mol m^{-3} DDAPS in the presence of 50 mol m^{-3} LiCl for a period of 1 h. For the no salt system, the initial foam volume increased continuously with increasing surfactant concentration. Figure 4.4 shows that at 0.6 mol m^{-3} DDAPS, ~430 cm^3 foam was generated. On the other hand, for 2.4 mol m^{-3} DDAPS (i.e., at the CMC), the foam volume was ~520 cm^3. This enhancement in foam volume occurred due to the increase in the number of DDAPS molecules at the air–water interface as the surfactant concentration increased. This increased the stability of the foam films, which increased the foam volume.[40,41]

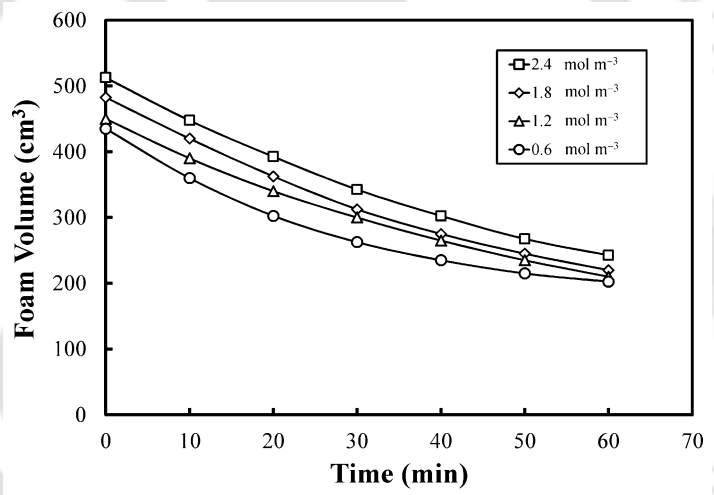

Figure 4.4. Variation of foam volume with time at various concentrations of DDAPS in the absence of any salt.

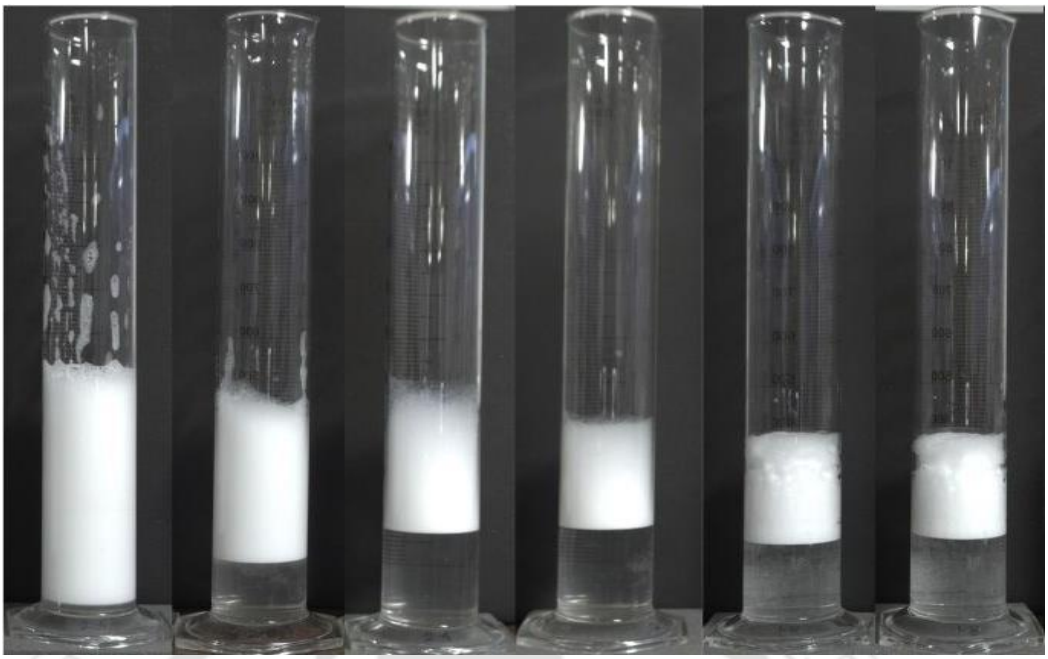

(a) (b) (c) (d) (e) (f)

Figure 4.5. Photographs of foams prepared from 2 mol m^{-3} DDAPS and 50 mol m^{-3} LiCl. A decrease in foam volume can be observed from (a) to (f) over 60 min, at 10 min time interval.

The mechanism of foam formation is important for analyzing the specific ion effect on foamability and foam stability. Foam formation is a complex process, which involves several important phenomena occurring simultaneously. Foams are generated as a result of fusing air into the surfactant solution. The process involves the transportation and distribution of surfactant molecules from the bulk surfactant solution to the air–water interface. Figure 4.6 depicts the adsorption of surfactant molecules along the Plateau border after foam formation. Plateau borders form the junction of the lamellae (i.e., thin liquid films separating the foam bubbles) at a single point in the foam film. The orientation of the surfactant molecules in a foam film is regulated by their surface activity, bulk concentration, and the interactions at the interface. The surface tension (γ) of the aqueous surfactant solution is an essential parameter in the formation of foam. The Gibbs

free energy change (dG) for expanding the surface area (dA) during foam formation is given by, $dG = \gamma dA$. It is often found that for a liquid of high surface tension, the formation of foam does not take place (e.g., pure water does not foam). Foam formation occurs when the surface tension of the aqueous phase is low. Thus, to form foam, a surfactant is added to the liquid, which lowers the surface tension. However, low surface tension may not always ensure the formation of a high volume of foam. Some surfactants (e.g., certain non-ionics) lower the surface tension, yet their solutions do not foam significantly.

For a surfactant solution that generates a significant amount of foam, the surfactant concentration plays a pivotal role in determining the initial foam volume. Dynamic adsorption of surfactant molecules from the bulk surfactant solution to the air–water interface is the most fundamental process during foam formation. It is described by the Ward–Tordai equation given in Section 1.6 (Chapter 1). The foam collapse rate increased with increasing surfactant concentration. This might occur due to the decrease in the Gibbs elasticity of the foam film with increasing surfactant concentration. The Gibbs elasticity (E_G) is defined by Equation (1.4) (Section 1.8.1 of Chapter 1). Using Langmuir and Gibbs adsorption equations, the Gibbs elasticity is given by[42]

$$E_G = \frac{4RT\Gamma_\infty^2 K_L^2 c_s}{h\left(1+K_L c_s\right)^2 + 2\Gamma_\infty K_L} \tag{4.3}$$

A film exhibiting higher elasticity has more stability.[43] The elasticity decreases with increasing surfactant concentration (c_s),[44] which leads to the rapid collapse of the foam.

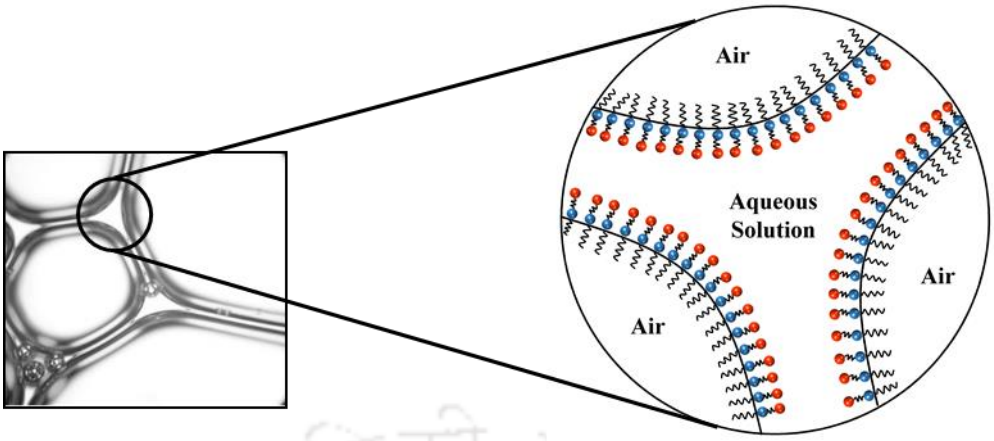

Figure 4.6. Schematic diagram of the adsorption of surfactant molecules at the Plateau border during foam formation.

Figure 4.7 shows the initial foam volume in the presence of LiCl, NaCl, and CsCl. The initial foam volume decreased with increasing salt concentration at all concentrations of DDAPS. For example, at 2.4 mol m^{-3} DDAPS, the initial foam volume was 510 cm^3 in the absence of salt, whereas the same decreased to 480, 440, and 400 cm^3 at 10, 50, and 100 mol m^{-3} NaCl, respectively. This decrease in initial foam volume possibly occurs due to the rapid coalescence of the bubbles by the rupture of the thin aqueous films. The initial foam volume decreased similarly for the other surfactant concentrations (i.e., 0.6, 1.2, and 1.8 mol m^{-3}). The initial foam volumes generated for LiCl and CsCl were similar to NaCl for all concentrations of DDAPS. The minimum and maximum deviation in the initial foam volume among these salts was in the range of ±5 and ±15 cm^3, respectively.

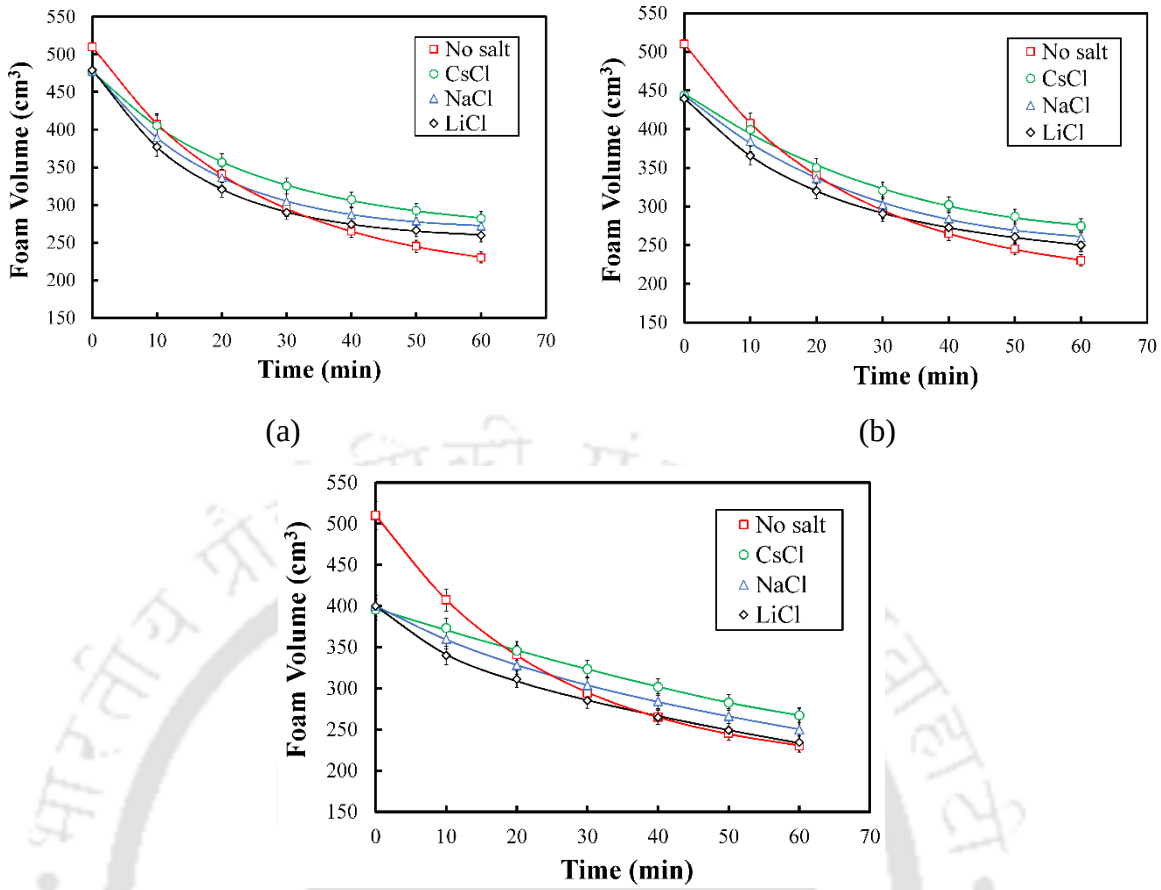

Figure 4.7. A comparative study of the lifetime of foams at 2.4 mol m^{-3} DDAPS at (a) 10, (b) 50, and (c) 100 mol m^{-3} CsCl, NaCl, and LiCl. The solid lines indicate the bi-exponential fits.

Foams can be short-lived (i.e., transient foams) or have a long lifetime (i.e., tenacious foams). Figure 4.7 depicts a comparative study of the lifetime of foams at 2.4 mol m^{-3} DDAPS in the presence of 10, 50, and 100 mol m^{-3} CsCl, NaCl, and LiCl. A comparison with Figure 4.4 (i.e., the no salt system) reflects that the initial foam volume decreased upon increasing the salt concentration.[45] However, the foam stability without salt was lower than that in the presence of the salts. Addition of salt to the surfactant solution decreased the surface tension (Figure 4.1). The increase in salt concentration (i.e., from 10 to 100 mol m^{-3}) enhanced the adsorption of DDAPS molecules and formed

a densely packed layer of these molecules at the air–water interface,[41] which is obvious from the surface tension profiles shown in Figure 4.1. However, salt also has a strong effect on the disjoining pressure in the foam film. The repulsive disjoining pressure due to EDL between two flat foam film separated at a distance is given in Equation (1.9) (Section 1.8.5, Chapter 1). In the presence of salt, the diffuse layer thickness and the surface potential decreased. This reduced the EDL repulsion in the foam film. Increased adsorption of the surfactant molecules at the air–water interface may increase in the density of surfactant molecules in the foam film. This increase in density cause the surfactant molecules to move from the surfactant-rich region to the surfactant-lean region of the film. If the Marangoni flow is significant, it will result in a more stable foam.[46,47] At the lower surfactant concentrations, the Marangoni flow was not significant due to the small surface tension gradient and low diffusion rate of the surfactant molecules.

A bi-exponential decay model, viz., $V = V_1 \exp(-k_1 t) + V_2 \exp(-k_2 t)$ was fitted to the foam volume profiles to characterize the evolution of foam with time. The values of V_1, V_2, k_1, and k_2 are given in Table 4.2. The model fitted the data well. As shown in Figure 4.7 (a), the foam collapse rate was high during the initial period (i.e., 30 min after the formation of foam) in the absence of salt and at a low salt concentration (i.e., 10 mol m^{-3}). In the absence of salt and the presence of 10 mol m^{-3} LiCl, the reduction in foam volume at 2.4 mol m^{-3} DDAPS during the initial 30 min was 210 and 190 cm^3, respectively. For the same salt concentration, the reduction in foam volume was 170 and 150 cm^3 for NaCl and CsCl, respectively. The values of k_1 generally followed the order: LiCl > NaCl > CsCl, at a given salt concentration. The foam collapse rate followed the same trend. However, upon increasing the LiCl concentration to 50 and 100 mol m^{-3}, the foam collapse rate was less, and it did not show any noticeable variation with the

surfactant concentration, as shown in Figure 4.7 (b) and 4.7 (c), respectively. For 50 and 100 mol m^{-3} LiCl, the amounts of foam collapsed (during the same period) were 150 and 120 cm^3, respectively at 2.4 mol m^{-3} DDAPS. For the same concentrations of NaCl and CsCl, the foam collapse rate was also less. The amounts of foam collapsed (during the same period) were 140 and 100 cm^3 for NaCl, and 130 and 90 cm^3 for CsCl, respectively. The values of k_1 and the foam collapse rate followed the same order as mentioned earlier.

Similar observations were made for 0.6, 1.2, and 1.8 mol m^{-3} DDAPS and are shown in Appendix A. Thus, it is apparent that CsCl was able to generate more stable foams in the initial 30 min, as compared to NaCl and LiCl. However, no specific trend was observed for V_1, V_2, and k_2. For the second half of the experiment (i.e., the remaining 30 min) the foam collapse rate was less, and it did not show any notable variation with the surfactant and salt concentrations. The foam volume decreased by 35 cm^3 for 2.4 mol m^{-3} DDAPS in the absence of salt, while the same was 30 cm^3 in the presence of 10 mol m^{-3} NaCl at the same surfactant concentration. Similar observations were made for LiCl and CsCl at the same salt concentration (i.e., 10 mol m^{-3}). Upon increasing the salt concentrations to 50 and 100 mol m^{-3}, no significant variation in the foam collapse rate was observed. The foam collapse rate for the remaining 30 min varied within ±30 cm^3 at these salt concentrations. Thus, the overall stability of foam increased in the order: LiCl > NaCl > CsCl.

Table 4.2. Parameters of the decay model, $V = V_1 \exp(-k_1 t) + V_2 \exp(-k_2 t)$.

System	Salt	V_1 (cm^3)	k_1	V_2 (cm^3)	k_2	R^2
0.6 mol m^{-3} DDAPS and 10 mol m^{-3} salt	CsCl	289.56	0.0306	119.52	–0.0078	0.9988
	NaCl	225.37	0.0507	185.45	–0.0028	0.9980
	LiCl	192.24	0.0725	215.56	–0.0002	0.9998
0.6 mol m^{-3} DDAPS and 50 mol m^{-3} salt	CsCl	207.74	0.0383	183.18	–0.0020	0.9997
	NaCl	176.29	0.0536	214.07	–0.0001	0.9996
	LiCl	137.08	0.0847	250.31	0.0030	0.9994
0.6 mol m^{-3} DDAPS and 100 mol m^{-3} salt	CsCl	193.17	0.0254	161.52	–0.0021	0.9992
	NaCl	103.92	0.0516	247.88	0.0030	0.9992
	LiCl	96.97	0.0810	258.50	0.0042	0.9990
1.2 mol m^{-3} DDAPS and 10 mol m^{-3} salt	CsCl	175.37	0.0548	259.74	0.0006	0.9997
	NaCl	196.25	0.0584	233.49	0.0013	0.9995
	LiCl	193.22	0.0738	238.43	0.0024	0.9997
1.2 mol m^{-3} DDAPS and 50 mol m^{-3} salt	CsCl	266.44	0.0248	138.51	–0.0055	0.9995
	NaCl	190.74	0.0449	217.51	–0.0005	0.9993
	LiCl	261.34	0.0384	146.23	0.0004	0.9992
1.2 mol m^{-3} DDAPS and 100 mol m^{-3} salt	CsCl	220.37	0.0192	147.69	–0.0024	0.9966
	NaCl	151.95	0.0310	214.39	0.0010	0.9981
	LiCl	186.83	0.0355	179.65	0.0019	0.9995
1.8 mol m^{-3} DDAPS and 10 mol m^{-3} salt	CsCl	298.66	0.0281	151.50	–0.0062	0.9989
	NaCl	199.53	0.0567	251.97	0.0001	0.9998
	LiCl	208.31	0.0582	241.16	0.0002	0.9997

1.8 mol m^{-3} DDAPS and 50 mol m^{-3} salt	CsCl	182.61	0.0319	242.34	0.0004	0.9999
	NaCl	216.98	0.0362	207.77	–0.0013	0.9990
	LiCl	167.68	0.0575	257.03	0.0016	0.9999
1.8 mol m^{-3} DDAPS and 100 mol m^{-3} salt	CsCl	362.67	0.0104	21.61	–0.0168	0.9980
	NaCl	207.28	0.0206	174.79	–0.0033	0.9997
	LiCl	96.10	0.0464	285.45	0.0042	0.9993
2.4 mol m^{-3} DDAPS and 10 mol m^{-3} salt	CsCl	196.88	0.0443	280.08	0.0006	0.9998
	NaCl	231.25	0.0499	246.28	–0.0009	0.9995
	LiCl	223.91	0.0611	255.41	0.0001	0.9999
2.4 mol m^{-3} DDAPS and 50 mol m^{-3} salt	CsCl	343.81	0.0194	101.96	–0.0083	0.9974
	NaCl	292.96	0.0269	150.38	–0.0050	0.9991
	LiCl	165.53	0.0537	274.03	0.0019	0.9996
2.4 mol m^{-3} DDAPS and 100 mol m^{-3} salt	CsCl	397.12	0.0068	341.25	–0.1696	0.9993
	NaCl	56.01	0.0513	344.16	0.0054	0.9998
	LiCl	55.02	0.1108	344.79	0.0065	0.9994

The differences in the foam stabilities for the monovalent salts at 10, 50, and 100 mol m^{-3} may be explained by the variation in the water drainage rate from the foam lamellae. The drainage rate is largely influenced by the fluidity of the film. Upon increasing the concentration of salt, an increase in the density of the surfactant molecules occurred in the foam films (Figure 4.4). Increased surfactant adsorption made the foam film more rigid, and hence the flow of water out of the foam film was reduced. A lower drainage rate increased the stability of the foams. The foam stability was higher for CsCl

as compared to NaCl and LiCl. In the case of CsCl, the smaller size of Cs^+ caused more DDAPS molecules to adsorb at the air–water interface. This increased adsorption resulted in a more rigid film, which reduced the flow of water and provided more stability. On the other hand, the larger size of Na^+ and Li^+ allowed a lesser number of surfactant molecules to adsorb on the air–water interface, which has been discussed in the Section 4.2.1 (Chapter 4). This led to the formation of a flexible foam film. The drainage of water from these films was faster, leading to the rupture of the film and destabilization of foam.

4.2.3 Study of specific ion effect on zeta potential

The effect of concentrations of the surfactant and the salts (i.e., CsCl, NaCl, and LiCl) on zeta potential is shown in Figure 4.8. In the absence of any surfactant or salt, the zeta potential at the oil–water interface was –25 mV. This was due to the preferential adsorption of the hydroxyl ions at the interface.[48,49] The zeta potential was negative for the DDAPS systems. Upon increasing the DDAPS concentration, the negative charge of the interface increased, which was reflected in the magnitude of the zeta potential. Addition of salt to the DDAPS solution significantly affected the zeta potential. It enhanced the adsorption of the surfactant molecules since the electrostatic repulsion among the head-groups decreased, as discussed in Section 4.2.1. It is evident from the Grahame equation [i.e., Equation (3.6) of Chapter 3] that there are two counteracting factors, which decide the zeta potential. The increase in the concentration of the DDAPS molecules at the oil–water interface causes an increase in σ and hence tends to increase the zeta potential. On the other hand, the increase in the concentration of salt increases c , and hence, tends to reduce ζ . At low salt concentrations, the former effect dominates over the latter, and the zeta potential becomes more negative. However, at the high salt concentrations, the latter effect dominates, and the zeta potential becomes less negative.

Binding and orientation of counter-ions may also play an important role in the zeta potential.[50,51]

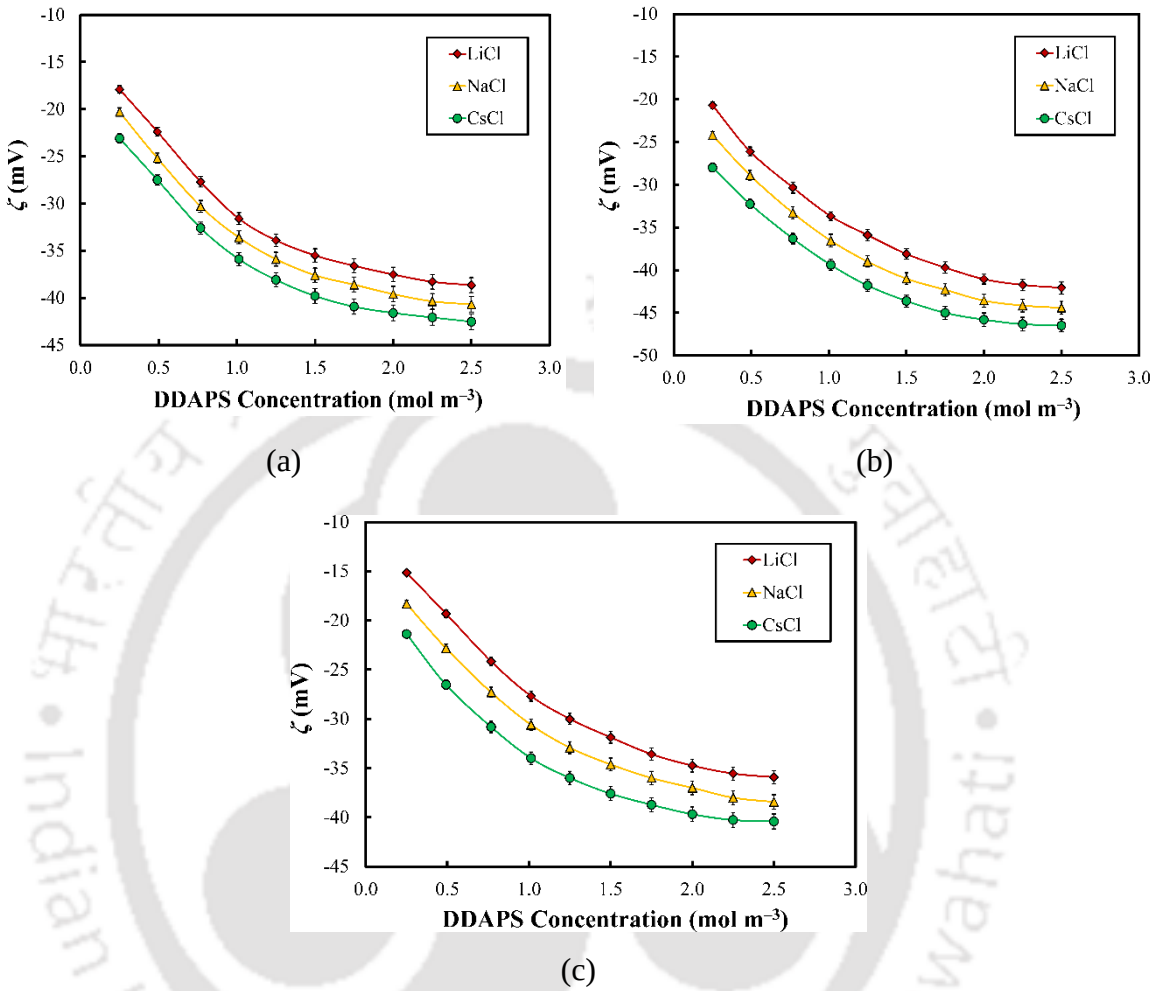

Figure 4.8. Variation of zeta potential at the hexane–water interface with the concentration of DDAPS at (a) 10, (b) 50, and (c) 100 mol m^{-3} salt.

As the zeta potential depends on surfactant adsorption, the efficiency of these 1:1 salts in making the zeta potential more negative followed the order: CsCl > NaCl > LiCl. This substantiates the results shown in Figure 4.2. Since the addition of CsCl led to the highest reduction in the interfacial tension, it also reflects the highest adsorption of the DDAPS molecules at the oil–water interface. This increased the adsorption of the DDAPS molecules, which increased the zeta potential. Therefore, ζ became more negative at 10

and 50 mol m^{-3} CsCl. However, upon increasing the salt concentration to 100 mol m^{-3}, the zeta potential is decreased (i.e., ζ was less negative). This corroborates the findings in the literature and also agrees with the Grahame equation.[52]

4.3. Conclusion

Adsorption of DDAPS at the air–water interface increased with increasing surfactant concentration. This resulted in the reduction in surface and interfacial tension. Addition of salt to the surfactant solution increased the adsorption of the latter. The smaller size of Cs^+ caused more DDAPS molecules to adsorb at the interface, whereas the larger size of Li^+ allowed a lesser number of surfactant molecules to adsorb. The efficiency of the 1:1 salts in decreasing the surface and interfacial tension followed the order: CsCl > NaCl > LiCl. The surface excess concentration increased with the increasing surfactant concentration up to the CMC, for a given salt concentration. At a given salt concentration, the increase in the surface excess concentration followed the order: LiCl < NaCl < CsCl.

The specific ion effect was manifested in the foaming of the aqueous DDAPS solutions. LiCl was more efficient than NaCl, and the latter was more efficient than CsCl in reducing the foam volume. The foam collapse rate was higher during the initial period after foam formation in the absence of salt, and at low salt concentrations. In the second half of the experiments, the foam collapse rate was less, and it did not show any substantial variation with increasing surfactant and salt concentrations. The efficiency of the counterions in decreasing the foam stability followed the order: $Cs^+ > Na^+ > Li^+$. A bi-exponential model was fitted to the foam volume profiles to characterize the evolution of foam with time. The efficiency of the counterions in decreasing the foam stability agreed well with the decay coefficient, k_1. The zeta potential of the oil–water interface became more negative with increasing surfactant concentration. Upon increasing the salt

concentration from 10 to 50 mol m^{-3}, the zeta potential became more negative because more DDAPS molecules adsorbed at the interface. The efficiency of the salts in making the zeta potential more negative followed the order: CsCl > NaCl > LiCl. However, upon increasing the salt concentration to 100 mol m^{-3}, the zeta potential became less negative since the charge density of the counterions increased at the higher salt concentration.

References

[1] Garrett, B. C. Ions at the Air/water interface. *Science* **2004,** 303, 1146−1147.

[2] Knipping, E.; Lakin, M.; Foster, K.; Jungwirth, P.; Tobias, D.; Gerber, R.; Dabdub, D.; Finlayson-Pitts, B. Experiments and simulations of ion-enhanced interfacial chemistry on aqueous NaCl aerosols. *Science* **2000,** 288, 301−306.

[3] Lo Nostro, P.; Peruzzi, N.; Severi, M.; Ninham, B. W.; Baglioni, P. Asymmetric partitioning of anions in lysozyme dispersions. *J. Am. Chem. Soc.* **2010,** 132, 6571−6577.

[4] Brown Jr, G. E.; Henrich, V.; Casey, W.; Clark, D.; Eggleston, C.; Felmy, A.; Felmy, A.; Goodman, D. W.; Gratzel, M.; Maciel, G. Metal oxide surfaces and their interactions with aqueous solutions and microbial organisms. *Chem. Rev.* **1999,** 99, 77−174.

[5] Finlayson-Pitts, B. The tropospheric chemistry of sea salt: A molecular-level view of the chemistry of NaCl and NaBr. *Chem. Rev.* **2003,** 103, 4801−4822.

[6] Kathmann, S. M.; Schenter, G. K.; Garrett, B. C. Ion-induced nucleation: The importance of chemistry. *Phys. Rev. Lett.* **2005,** 94, 116104−116107.

[7] Kunz, W.; Nostro, P. L.; Ninham, B. W. The present state of affairs with Hofmeister effects. *Curr. Opin. Colloid Interface Sci.* **2004,** 9, 1−18.

[8] Collins, K. D. Ion hydration: Implications for cellular function, polyelectrolytes, and protein crystallization. *Biophys. Chem.* **2006,** 119, 271−281.

[9] Hofmeister, F. About the water withdrawing effect of the salts. *Arch. Exp. Path. Pharm.* **1888,** 25, 1−30.

[10] Lo Nostro, P.; Ninham, B. W. Hofmeister phenomena: An update on ion specificity in biology. *Chem. Rev.* **2012,** 112, 2286−2322.

[11] Otten, D. E.; Shaffer, P. R.; Geissler, P. L.; Saykally, R. J. Elucidating the mechanism of selective ion adsorption to the liquid water surface. *Proc. Natl. Acad. Sci.* **2012,** 109, 701−705.

[12] Vlachy, N.; Jagoda-Cwiklik, B.; Vácha, R.; Touraud, D.; Jungwirth, P.; Kunz, W. Hofmeister series and specific interactions of charged headgroups with aqueous ions. *Adv. Colloid Interface Sci.* **2009,** 146, 42−47.

[13] Wang, W.; Park, R. Y.; Travesset, A.; Vaknin, D. Ion-specific induced charges at aqueous soft interfaces. *Phys. Rev. Lett.* **2011,** 106, 56102−56105.

[14] Aroti, A.; Leontidis, E.; Dubois, M.; Zemb, T. Effects of monovalent anions of the hofmeister series on DPPC lipid bilayers Part I: Swelling and in-plane equations of state. *Biophys. J* . **2007,** 93, 1580–1590.

[15] Aroti, A.; Leontidis, E.; Maltseva, E.; Brezesinski, G. Effects of Hofmeister anions on DPPC Langmuir monolayers at the air–water interface. *J. Phys. Chem. B* **2004,** 108, 15238–15245.

[16] Rendall, K.; Tiddy, G. J.; Trevethan, M. A. An investigation of the interactions between electrolytes and a zwitterionic surfactant using 23Na and 2H NMR measurements. *J. Colloid Interface Sci.* **1984,** 98, 565–571.

[17] Rosen, M. J., *Surfactants and Interfacial Phenomena*; John Wiley & Sons: New York, 2004.

[18] McLachlan, A. A.; Marangoni, D. G. Interactions between zwitterionic and conventional anionic and cationic surfactants. *J. Colloid Interface Sci.* **2006,** 295, 243–248.

[19] Zeppieri, S.; Rodríguez, J.; López de Ramos, A. Interfacial tension of alkane + water systems. *J. Chem. Eng. Data* **2001,** 46, 1086–1088.

[20] Ghosh, P., *Colloid and Interface Science*; PHI Learning: New Delhi, 2009.

[21] Zajac, J.; Chorro, C.; Lindheimer, M.; Partyka, S. Thermodynamics of micellization and adsorption of zwitterionic surfactants in aqueous media. *Langmuir* **1997,** 13, 1486–1495.

[22] Zhao, J.; Dai, C.; Ding, Q.; Du, M.; Feng, H.; Wei, Z.; Chen, A.; Zhao, M. The structure effect on the surface and interfacial properties of zwitterionic sulfobetaine surfactants for enhanced oil recovery. *RSC Adv.* **2015,** 5, 13993–14001.

[23] Chorro, M.; Kamenka, N.; Faucompre, B.; Partyka, S.; Lindheimer, M.; Zana, R. Micellization and adsorption of a zwitterionic surfactant: N-dodecyl betaine-effect of salt. *Colloids Surf. A* **1996,** 110, 249–261.

[24] Tajima, K. Radiotracer studies on adsorption of surface active substance at aqueous surface. III. The effects of salt on the adsorption of sodium dodecylsulfate. *Bull. Chem. Soc. Jpn.* **1971,** 44, 1767–1771.

[25] Srinivas, A.; Ghosh, P. Coalescence of bubbles in aqueous alcohol solutions. *Ind. Eng. Chem. Res.* **2012,** 51, 795–806.

[26] Karakashev, S.; Tsekov, R.; Manev, E. Adsorption of alkali dodecyl sulfates on air/water surface. *Langmuir* **2001,** 17, 5403–5405.

[27] Manev, E.; Sazdanova, S.; Tsekov, R.; Karakashev, S.; Nguyen, A. Adsorption of ionic surfactants. *Colloids Surf. A* **2008,** 319, 29–33.

[28] Somasundaran, P., *Encyclopedia of Surface and Colloid Science*; CRC Press: New York, 2006.

[29] Liu, L.; Zhang, Q.; Pan, Q.; Zhang, J.; Li, C.; Pei, M. Interaction between anionic and zwitterionic surfactants: Sodium dodecyl sulfate and N-alkyl-N, N-dimethylsulfobetain, N-lauroylsarcosine. *J. Dispersion Sci. Technol.* **2007,** 28, 1329–1333.

[30] Hey, M. J.; Shield, D. W.; Speight, J. M.; Will, M. C. Surface tensions of aqueous solutions of some 1:1 electrolytes. *J. Chem. Soc. Faraday Trans.* **1981,** 77, 123–128.

[31] Johansson, K.; Eriksson, J. C. γ and dγ/dT measurements on aqueous solutions of 1,1-electrolytes. *J. Colloid Interface Sci.* **1974,** 49, 469–480.

[32] Weissenborn, P. K.; Pugh, R. J. Surface tension of aqueous solutions of electrolytes: Relationship with ion hydration, oxygen solubility, and bubble coalescence. *J. Colloid Interface Sci.* **1996,** 184, 550–563.

[33] Adam, N. K., *Physics and Chemistry of Surfaces*; Oxford University Press: London, 1941.

[34] Jungwirth, P.; Tobias, D. J., Ions at the air/water interface, *J. Phys. Chem. B* **2002,** 25, 6361−6373.

[35] Manciu, M.; Manciu, F. S.; Ruckenstein, E. Ion-specific effects on surface potential and surface tension of water solutions explained via volume exclusion effects. *Colloids Surf. A* **2016,** 494, 156–161.

[36] Cappa, C. D.; Smith, J. D.; Wilson, K. R.; Messer, B. M.; Gilles, M. K.; Cohen, R. C.; Saykally, R. J. Effects of alkali metal halide salts on the hydrogen bond network of liquid water. *J. Phys. Chem. B* **2005,** 109, 7046−7052.

[37] Petersen, P. B.; Saykally, R. J. Evidence for an enhanced hydronium concentration at the liquid water surface. *J. Phys. Chem. B* **2005,** 109, 7976–7980.

[38] Collins, K. D. Ions from the Hofmeister series and osmolytes: Effects on proteins in solution and in the crystallization process. *Methods* **2004,** 34, 300–311.

[39] Israelachvili, J. N., *Intermolecular and Surface Forces*; Academic Press: London,

2011.

[40] Dukhin, S. S.; Kretzschmar, G.; Miller, R., *Dynamics of Adsorption at Liquid Interfaces: Theory, Experiment, Application*; Elsevier: Amsterdam, 1995.

[41] Marinova, K. G.; Basheva, E. S.; Nenova, B.; Temelska, M.; Mirarefi, A. Y.; Campbell, B.; Ivanov, I. B. Physico-chemical factors controlling the foamability and foam stability of milk proteins: Sodium caseinate and whey protein concentrates. *Food Hydrocolloids* **2009,** 23, 1864–1876.

[42] Wang, L.; Yoon, R.-H. Effects of surface forces and film elasticity on foam stability. *Int. J. Miner. Process.* **2008,** 85, 101–110.

[43] Xu, W.; Nikolov, A.; Wasan, D. T.; Gonsalves, A.; Borwankar, R. P. Foam film rheology and thickness stability of foam-based food products. *Colloids Surf. A* **2003,** 214, 13–21.

[44] Rao, A.; Wasan, D.; Manev, E. Foam stability-effect of surfactant composition on the drainage of microscopic aqueous films. *Chem. Eng. Commun.* **1982,** 15, 63–81.

[45] Behera, M. R.; Varade, S. R.; Ghosh, P.; Paul, P.; Negi, A. S. Foaming in micellar Solutions: Effects of surfactant, salt, and oil concentrations. *Ind. Eng. Chem. Res.* **2014,** 53, 18497–18507.

[46] Marangoni, C.; Stefanelli, P.; Liceo, R. Monografia sulle bolle liquide. *Il Nuovo Cimento* **1872,** 7, 301–356.

[47] Varade, S. R.; Ghosh, P. Foaming in aqueous solutions of zwitterionic surfactant: Effects of oil and salts. *J. Dispersion Sci. Technol.* **2017,** 38, 1–15.

[48] Drzymala, J.; Sadowski, Z.; Holysz, L.; Chibowski, E. Ice/water interface: Zeta potential, point of zero charge, and hydrophobicity. *J. Colloid Interface Sci.* **1999,** 220, 229–234.

[49] Takahashi, M. ζ potential of microbubbles in aqueous solutions: Electrical properties of the gas-water interface. *J. Phys. Chem. B* **2005,** 109, 21858–21864.

[50] Bommaganti, P.; Kumar, M. V.; Ghosh, P. Effects of binding of counterions on adsorption and coalescence. *Chem. Eng. Res. Des.* **2009,** 87, 728–738.

[51] Kralchevsky, P.; Danov, K.; Broze, G.; Mehreteab, A. Thermodynamics of ionic surfactant adsorption with account for the counterion binding: Effect of salts of various valency. *Langmuir* **1999,** 15, 2351–2365.

[52] Yang, C.; Dabros, T.; Li, D.; Czarnecki, J.; Masliyah, J. H. Measurement of the zeta

potential of gas bubbles in aqueous solutions by microelectrophoresis method. *J. Colloid Interface Sci.* **2001,** 243, 128–135.

CHAPTER 5

FOAMING IN AQUEOUS SOLUTIONS OF A MIXTURE OF ZWITTERIONIC AND CATIONIC SURFACTANTS IN PRESENCE OF AN ELECTROLYTE

5.1. Introduction

Mixed surfactant systems are widely used in commercial applications such as drug delivery, cosmetics, enhanced oil recovery, detergency, foaming/defoaming, and cleaning.[1–4] Therefore, a surfactant system containing a mixture of surfactants of different type is of prime importance for research. Interaction between two different surfactant head-groups has been extensively studied inasmuch as it plays a significant role in enhancing the interfacial properties, which affect solubilization, suspension, and dispersion in various processes.[5–11] When two surfactants are mixed, a synergistic effect can produce a significant change in the bulk and interfacial properties such as decrease in CMC, increase in surface activity, and formation of mixed micelles.[3] Synergism exhibited by a mixed surfactant system is due to the non-ideal mixing of the surfactants, which causes the CMC to reduce and results in a lower interfacial tension than those produced by the individual surfactants. The physicochemical properties of a binary surfactant system are often more desirable than those of a single surfactant system.[12] Thus, the synergistic behavior in the mixed surfactant systems has aroused a great amount of scientific and industrial interest.

Synergism can be classified into three types. *Type I synergism* is exhibited when the mixed surfactant system attains a lower surface tension at its CMC than that achieved by either of the individual surfactants at their CMCs. *Type II synergism* occurs when a certain interfacial tension can be reached at a total mixed surfactant concentration that is lower than the concentrations required for the individual surfactants. When the CMC of the mixture of two surfactants is smaller than that of the individual surfactants, it is called *Type III synergism*. Rosen[13] has given the criteria for these three types of synergism.

In a mixed-surfactant system, not only the nature of the individual surfactants but

also the interactions between themselves and with the electrolyte present in the system are of great importance in the stability of the foam films. The interaction among the surfactant molecules can be well understood from the comparative study of CMC as a function of surfactant concentration obtained experimentally and theoretically. Inorganic salts influence the adsorption of surfactants and can be used to produce the desired results.[14–16] Salts are often vital in numerous applications involving emulsification and detergency. The addition of an inorganic salt generally decreases the surface tension of the aqueous solution of an ionic surfactant and its CMC. It also reduces the surface tension at the CMC (i.e., γ_{CMC}). The decrease in surface tension upon the addition of salt is attributed to the increased electrostatic screening and decreased repulsion between the surfactant head-groups.[17] The ionic strength of the solution and binding of counterions are important factors in the reduction of γ_{CMC}.[18] In addition, the presence of salt affects the synergism between the ionic and zwitterionic surfactants.[19,20]

Guo et. al.,[21] investigated the mixed surfactant systems of sodium perfluorooctanoate (SPFO) with N-triethoxylated heptanylamide (HEA8-3), with 3-(decyldimethylammonino)-1-propanesulfonate (DEDIAP), and with octyltrimethylammonium bromide (OCTAB) using surface tension and F and H NMR. For the anionic SPFO/cationic OCTAB mixed system, the CMC is reduced tremendously upon mixing and the NMR studies combined with centrifugation results indicate the mixed surfactants coacervate to form large aggregates. In addition to the normal mixed micelles, large aggregates appear at higher surfactant concentrations.

Bauduin et. al.,[22] investitagted the micellar composition of two binary surfactant systems, sodium dodecyl sulfate (SDS)/pentaethylene glycol monodecyl ether ($C_{10}E_5$) and SDS/lauryl amido propyl betaine (LAPB) using pulsed gradient spin echo NMR. Data

collected for different total surfactant concnetrations and compositions of the binary mixtures have shown that SDS and $C_{10}E_5$ moderately interact.

Hines et. al.,[23] used surface tension and NMR to study the surface composition of aqueous solution of mixtures of SDS and *n*-dodecyl-*β*-D-maltoside (C_{12}maltoside) and C_{12}maltoside and n-dodecyl-N,N'-dimethylamino betaine (C_{12}betaine). The interaction parameters values were calculated from the surface tension and CMC using the pseudo-phase separation model. Direct measurements of the surface excess using NMR on isotopic mixtures of the surfactants were found to be consistent with the surface tension measurements using the integrated form of the Gibbs equation.

In this work, we have investigated the synergism in a mixture of a zwitterionic and a cationic surfactant. DDAPS and hexadecyltrimethylammonium bromide (CTAB) have been used as zwitterionic and cationic surfactants, respectively. We have studied the adsorption of these surfactants at various concentration ratios at the air–water interface in the presence of NaCl by surface tension measurements. In this work, foamability and foam stability have been studied by employing the blender test. The zeta potential at the air–water interface in the mixed surfactant systems was also measured.

5.2. Results and Discussion

5.2.1. Adsorption studies on mixed surfactant systems

The adsorption studies were performed on the mixtures of CTAB and DDAPS at various concentration ratios over a wide range. Similar studies were performed on the individual surfactants as well. Figure 5.1 shows the surface tension versus concentration profiles for pure CTAB and DDAPS. The CMCs of CTAB and DDAPS were found to be ~1.0 and ~2.4 mol m^{-3}, respectively. These values agree well with those reported in the literature.[24,25] The surface tension profiles obtained in this way helped us to determine

the interaction parameters for the monolayer and the micelle.

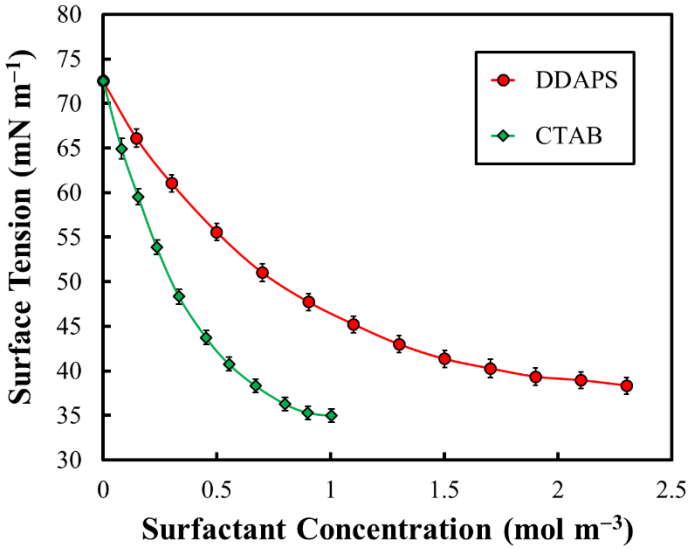

Figure 5.1. Variation of surface tension of aqueous solutions of CTAB and DDAPS at different concentrations.

The surface tension profiles for the single surfactants (i.e., CTAB and DDAPS) decreased significantly upon increasing the surfactant concentration. Near the CMC, surface tension showed very less variation, indicating the saturation of the air–water interface with the surfactant molecules. The surface tension profiles of DDAPS in the presence of NaCl have been reported and discussed in Section 3.2.1 (Chapter 3). The surface tension profiles of CTAB in the presence of NaCl are shown in Figure 5.2. It was observed that the surface tension decreased with increasing NaCl concentration from 10 to 100 mol m^{-3}. The surface tension profiles underwent substantial change upon increasing the NaCl concentration. The surface tension minimum $\left(\text{i.e. } \gamma_{CMC}\right)$ was obtained at a significantly lower surfactant concentration as the NaCl concentration increased. NaCl enhanced the adsorption of the surfactant molecules and hence reduced the surface tension. This enhancement in adsorption was primarily due to the reduction

in electrostatic repulsion among the surfactant head-groups, which favored more surfactant molecules to adsorb at the interface. For DDAPS, the effect of NaCl on adsorption was not that pronounced as compared to CTAB, inasmuch as the DDAPS molecule acts like a nonionic surfactant to some extent.

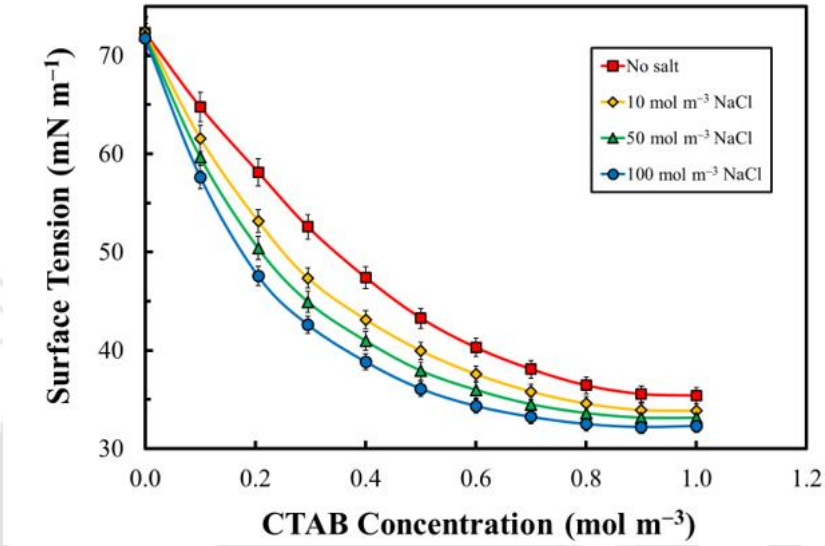

Figure 5.2. Variation of surface tension with CTAB at various concentrations of NaCl.

In this work, the concentration of DDAPS was fixed, while the same of CTAB was varied. The surface tension profiles obtained in this way helped us to determine the interaction parameters for the monolayer and the micelle (i.e., β^{σ} and β^{M}). The DDAPS concentration was fixed at 0.6, 1.2, 1.8, and 2.4 mol m^{-3}. The CTAB concentration was varied from 0.1 to 1.0 mol m^{-3}. The surface tension profiles for the mixed CTAB–DDAPS surfactant systems are shown in Figure 5.3. These profiles indicate that the surface tension decreased considerably upon the addition of CTAB to the DDAPS solution. This occurred due to the increase in the total concentration of surfactant in the aqueous solution. Accordingly, the adsorption of both the surfactants was enhanced, and the formation of mixed micelles took place. Therefore, in the profiles shown in Figure 5.3, the CMC was

attained at a lower concentration of CTAB as the DDAPS concentration was increased.

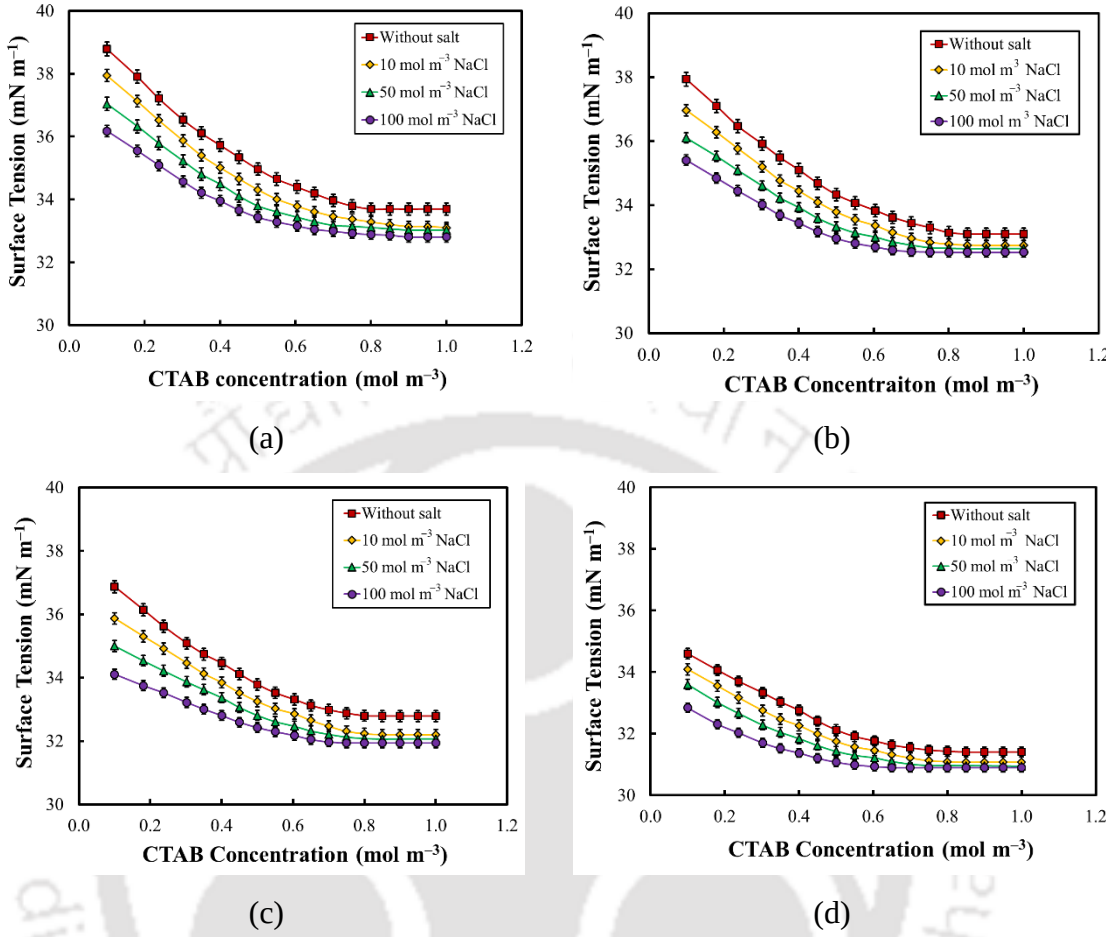

Figure 5.3. Variation of surface tension at different concentrations of CTAB at (a) 0.6, (b) 1.2, (c) 1.8, and (d) 2.4 mol m^{-3} DDAPS.

The CMC decreased by the addition of salt. The γ_{CMC} values were lower than those for the single surfactant systems in the presence of salt. For DDAPS, the γ_{CMC} was 38.4 mN $m^{-1,}$ and the same for CTAB was 34.9 mN m^{-1}. A significant reduction in the γ_{CMC} was observed for the mixed surfactant systems in the absence and presence of salt. This occurred because NaCl enhanced the adsorption of the surfactant molecules at the air–water interface due to the reduced electrostatic repulsion among the surfactant molecules. The CMCs were observed at lower CTAB concentrations as the concentration

of DDAPS was increased, for all salt concentrations. This is expected because the interface was occupied more and more by the DDAPS molecules. The interface was saturated at a lower CTAB concentration, and formation of the mixed micelles occurred subsequently. Thus, increase in the DDAPS concentration played a significant role in reducing the surface tension and shifting the CMC towards a lower CTAB concentration.

The values of the interaction parameters (i.e., β^{σ} and β^{M}) for the CTAB–DDAPS systems in the presence and absence of salt at 1.2 and 1.8 mol m^{-3} DDAPS are presented in Table 5.1. The values shown in columns 7, 9, and 10 indicate that the conditions required for Type I synergism [i.e., Equations (1.17) and (1.18)] were satisfied by these mixed systems. The values of β^{σ} were larger than those of β^{M}, which indicates a more robust interaction in the mixed monolayers than that in the mixed micelles. In the absence of salt, the average values of β^{σ} and β^{M} for the CTAB–DDAPS system were found to be –2.71 and –1.14, respectively. The negative values indicate attractive interaction between the surfactants. This result corroborates the results reported in the literature.[13] The values of these interaction parameters in the presence of 10 mol m^{-3} NaCl were –3.21 and –1.86, respectively. Therefore, the attractive interaction among the surfactant head-groups increased upon the addition of salt. This increase in the value of the interaction parameter may be due to the reduction in electrostatic repulsion between the surfactant head-groups in the presence of NaCl. A similar observation was made for 50 and 100 mol m^{-3} NaCl concentrations. The values of β^{σ} and β^{M} agree well with those reported in the literature for the mixed systems of zwitterionic and cationic surfactants.[13,26] The values of the interaction parameters for the CTAB–DDAPS system in the presence and absence of salt at 0.6 and 2.4 mol m^{-3} DDAPS are presented in Table 5.2.

5.2.2. Study of foams in the mixed surfactant systems

The effects of NaCl on foam formation and foam stability were investigated at the different concentration ratios of the surfactants and different NaCl concentrations, mentioned in Section 5.2.1. Figure 5.4 depicts the variation in foam volume for the individual DDAPS and CTAB systems over a period of 100 min. The initial foam volumes for the 1.0 mol m^{-3} CTAB and 2.4 mol m^{-3} DDAPS systems were 500 and 520 cm^3, respectively. The initial foam volume and foam stability for the DDAPS system in the presence of NaCl have been reported in Section 3.2.2 (Chapter 3). The effect of NaCl on the CTAB system is shown in Figure 5.5.

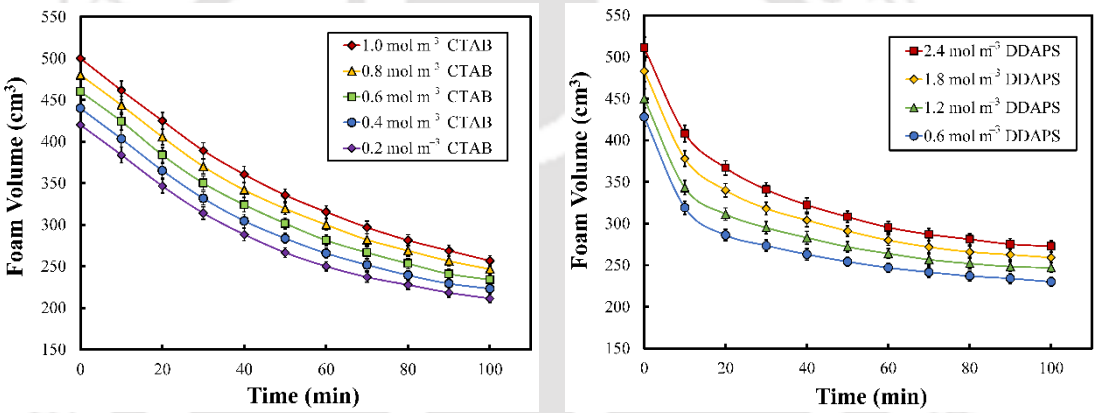

(a) CTAB (b) DDAPS

Figure 5.4. Variation of foam volume with time for the single surfactant systems up to 100 min.

Table 5.1. Interaction parameters for the CTAB–DDAPS binary mixtures.

System	C_1 (mol m^{-3})	C_2 (mol m^{-3})	γ (mN m^{-1})	x_1	x_1^M	β^σ	β^M	$\left(\beta^\sigma - \beta^M\right)$	$\ln\left(\frac{C_1^{0,CMC}C_2^{0,M}}{C_2^{0,CMC}C_1^{0,M}}\right)$
DDAPS (1) + CTAB (2)	1.20	0.50	36.1	0.49	0.42	–1.50	–0.94	–0.56	0.15
DDAPS (1) + CTAB (2) + 10 mol m^{-3} NaCl		0.45	36.4	0.46	0.41	–2.17	–1.54	–0.63	0.54
DDAPS (1) + CTAB (2) + 50 mol m^{-3} NaCl		0.30	36.4	0.44	0.37	–2.51	–1.80	–0.71	0.31
DDAPS (1) + CTAB (2) + 100 mol m^{-3} NaCl		0.35	36.1	0.41	0.35	–3.11	–2.21	–0.90	0.29
DDAPS (1) + CTAB (2)	1.80	0.60	33.6	0.58	0.40	–2.71	–1.14	–1.57	0.85
DDAPS (1) + CTAB (2) + 10 mol m^{-3} NaCl		0.60	33.4	0.56	0.39	–3.21	–1.86	–1.35	0.64
DDAPS (1) + CTAB (2) + 50 mol m^{-3} NaCl		0.60	33.3	0.55	0.35	–4.28	–2.72	–1.56	0.41
DDAPS (1) + CTAB (2) + 100 mol m^{-3} NaCl		0.40	33.5	0.51	0.46	–4.91	–3.65	–1.26	0.75

Table 5.2. Interaction parameters for the CTAB–DDAPS binary mixtures.

System	c_1 (mol m^{-3})	c_2 (mol m^{-3})	γ (mN m^{-1})	x_1	x_1^{M}	β^{σ}	β^{M}	$\left(\beta^{\sigma}-\beta^{M}\right)$	$\ln\left(\frac{c_1^{0,CMC}c_2^{M}}{c_2^{0,CMC}c_1^{M}}\right)$
DDAPS (1) + CTAB (2)	0.6	0.58	39.8	0.58	0.45	–0.98	–0.54	–0.44	0.32
DDAPS (1) + CTAB (2) + 10 mol m^{-3} NaCl		0.44	39.5	0.57	0.43	–1.09	–0.64	–0.45	0.45
DDAPS (1) + CTAB (2) + 50 mol m^{-3} NaCl		0.31	39.4	0.55	0.39	–1.29	–0.80	–0.49	0.30
DDAPS (1) + CTAB (2) + 100 mol m^{-3} NaCl		0.24	39.1	0.53	0.37	–1.41	–1.02	–0.39	0.52
DDAPS (1) + CTAB (2)	2.4	0.41	32.7	0.42	0.38	–5.08	–4.14	–1.84	0.37
DDAPS (1) + CTAB (2) + 10 mol m^{-3} NaCl		0.35	32.4	0.39	0.35	–5.95	–4.56	–0.49	0.42
DDAPS (1) + CTAB (2) + 50 mol m^{-3} NaCl		0.31	32.3	0.36	0.34	–6.78	–5.72	–1.06	0.65
DDAPS (1) + CTAB (2) + 100 mol m^{-3} NaCl		0.28	32.5	0.38	0.31	–7.71	–6.14	–1.57	0.48

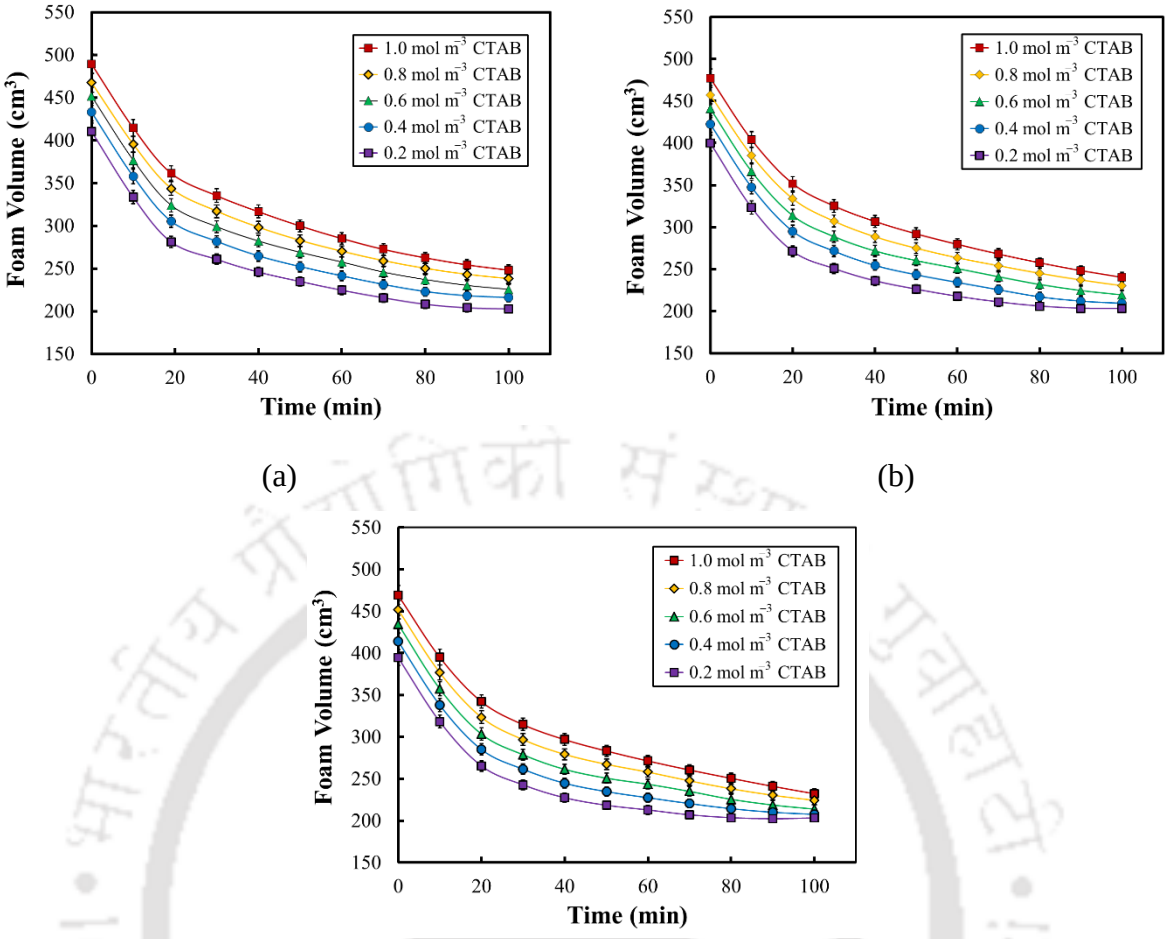

Figure 5.5. Variation of foam volume with time at different concentrations of CTAB in the presence of (a) 10, (b) 50, and (c) 100 mol m^{-3} NaCl.

Foam production from a mechanically-agitated blender appears to be a simple macroscopic process. However, it is a significantly complex process having several microscopic processes occurring simultaneously. Air diffused into the aqueous surfactant solution generates the foam. Foam bubbles formed in the initial stages are very unstable, and many of them completely disappear within a few minutes after formation. It was observed that foam at the bottom of the measuring cylinder was wet with high water content, whereas the upper part of the foam was dry, having much less amount of water. The process of formation, parameters regulating this process, importance of surface tension of the solution in foaming, significance of surfactant concentration in initial foam

volume, and dynamic adsorption of the surfactant molecules at the air–water interface have been discussed in Sections 1.6 (Chapter 1) and 4.2.2 (Chapter 4).

To investigate the foam stability, a standing foam was used to eliminate the complications arising from the foam movement. Figure 5.6 (a) shows the foam in the later stages of evolution. The polyhedral cells of foam with characteristic lamella and Plateau border are easily visible. In Figure 5.6 (b), the orientation of the surfactant molecules in the foam film is illustrated schematically. The evolution of foams causes the lamellae to stretch and dilate, which leads to an increase in the bubble surface area. The disjoining pressure (Π) arises due to surface forces acting in the foam film. The foam film thickness and its rupture depend on the disjoining pressure. The net interaction in the thin foam film can be described by using the DLVO theory. It has been described in Section 1.8.5 (Chapter 1). Figure 5.7 illustrates the evolution of foam prepared with DDAPS and CTAB in the presence of NaCl.

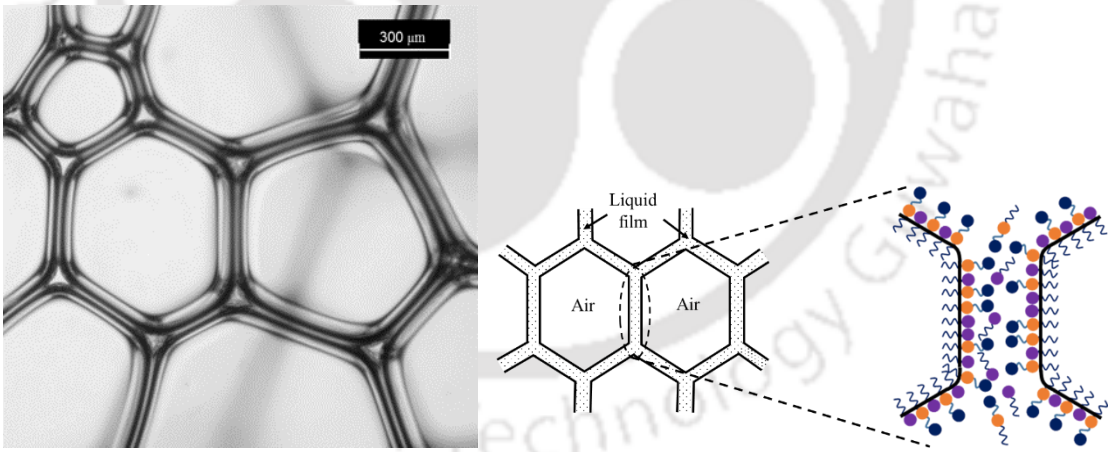

(a) (b)

Figure 5.6. (a) Foam cells depicting the lamellae and the Plateau border and (b) adsorption of the zwitterionic and cationic surfactant molecules at the surfaces of the foam lamella.

Figure 5.8 shows the variation in foam volume, observed for 100 min, at different

ratios of DDAPS and CTAB in the presence and absence of salt. It depicts the effect of NaCl on foam volume at fixed concentrations of DDAPS (i.e., at 1.2 and 2.4 mol m^{-3}) and at different concentrations of CTAB varying between 0.1 and 1.0 mol m^{-3}. The foamability (i.e., the initial volume of foam) of the mixed surfactant system in the presence of salt was measured at different surfactant concentrations. The rapid increase in the foam volume upon increasing the surfactant concentration indicates that foaming was highly influenced by the quantity of surfactant present in the solution. An excellent foamability was accomplished because the surfactant molecules rapidly covered the

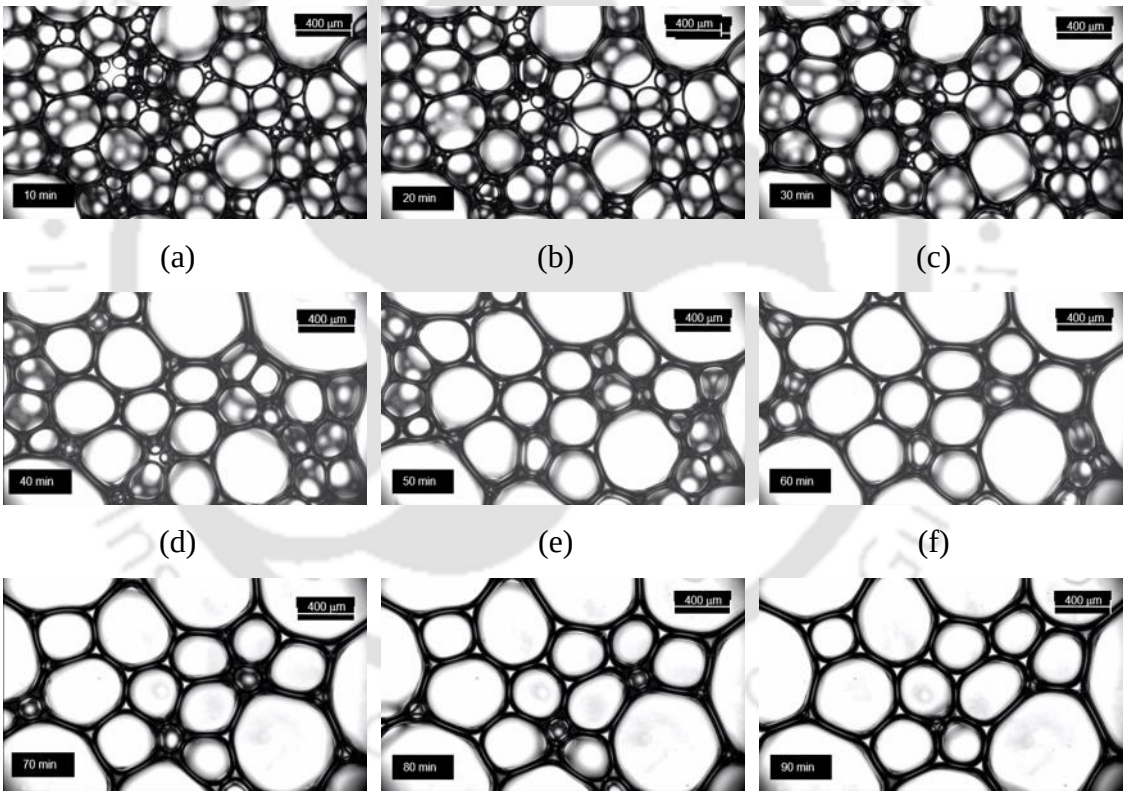

Figure 5.7. Evolution of foam prepared from 1.2 mol m^{-3} DDAPS and 0.8 mol m^{-3} of CTAB in the presence of 10 mol m^{-3} NaCl for 90 min at 10 min intervals.

bubble surfaces and prevented their coalescence. Upon addition of NaCl, the foam

volume decreased. Increase in the concentration of salt enhanced the electrostatic screening among the charged head-groups of the surfactant molecules (see Section 5.2.1). Therefore, this caused more surfactant molecules to adsorb at the air–water interface.[27] This is corroborated by the surface tension profiles (Figure 5.3). Furthermore, addition of NaCl produced a substantial effect on the EDL repulsion in the foam film. The repulsive disjoining pressure between two flat surfaces is given by Equation (1.9) (Section 1.8.5, Chapter 1). In the presence of salt, the surface potential and the diffuse layer thickness are both decreased. Therefore, the EDL repulsion in the foam was reduced. Rapid coalescence of the foam bubbles occurred by the rupture of the thin aqueous films. These caused the reduction in the initial foam volume with increasing salt concentration.[28] In the absence of NaCl, the initial foam volume was ~500 cm^3 with 1.2 mol m^{-3} of DDAPS and 0.2 mol m^{-3} of CTAB. For the same DDAPS concentration with 0.4, 0.6, 0.8, and 1.0 mol m^{-3} CTAB, the initial foam volumes were 520, 540, 550, and 580 cm^3, respectively. Therefore, it is clear that the initial foam volume was enhanced upon increasing the concentration of CTAB. In the presence of 10 mol m^{-3} NaCl, the initial foam volumes were 480, 500, 525, 540, and 560 cm^3 for the above-mentioned concentrations of the two surfactants. The initial foam volume decreased with increasing NaCl concentration (i.e., at 50 and 100 mol m^{-3} NaCl). The synergistic behavior was apparent in foamability. The mixed surfactant systems produced higher initial foam volumes as compared to the individual surfactants. The variation of foam volume with time at 0.6 and 1.8 mol m^{-3} DDAPS in the presence of NaCl at different concentrations of CTAB are given in Figure 5.9.

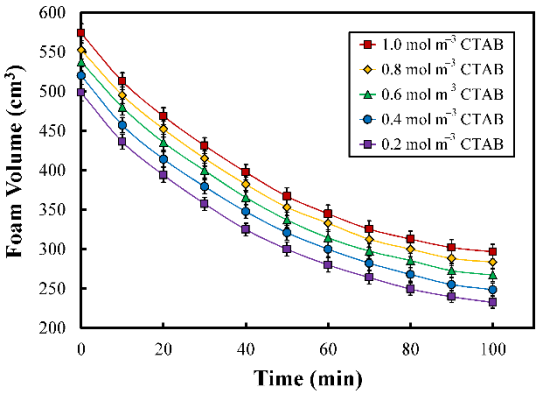

(a) 1.2 mol m^{-3} DDAPS and no salt

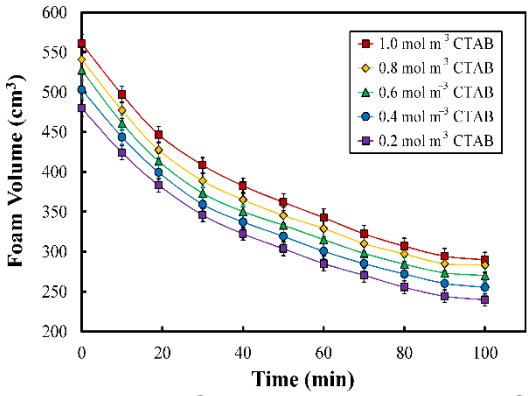

(b) 1.2 mol m^{-3} DDAPS and 10 mol m^{-3} NaCl

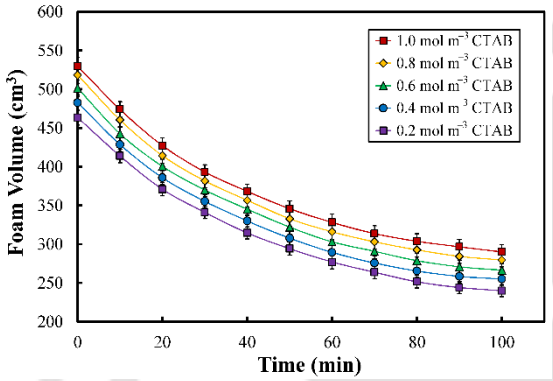

(c) 1.2 mol m^{-3} DDAPS and 50 mol m^{-3} NaCl

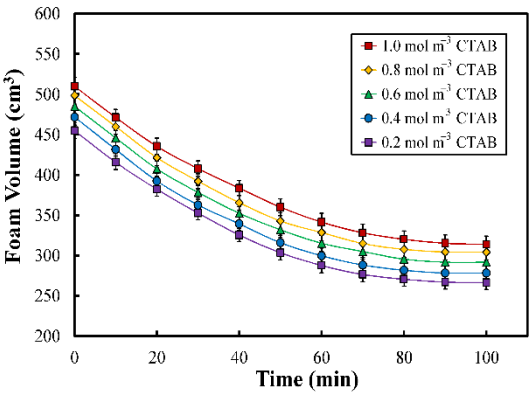

(d) 1.2 mol m^{-3} DDAPS and 100 mol m^{-3} NaCl

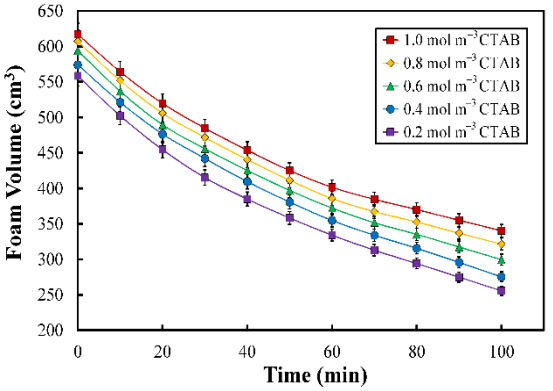

(e) 2.4 mol m^{-3} DDAPS and no salt

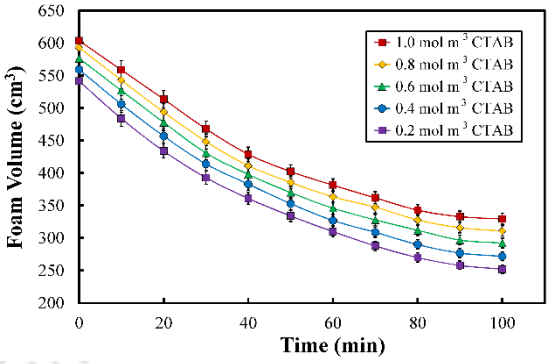

(f) 2.4 mol m^{-3} DDAPS and 10 mol m^{-3} NaCl

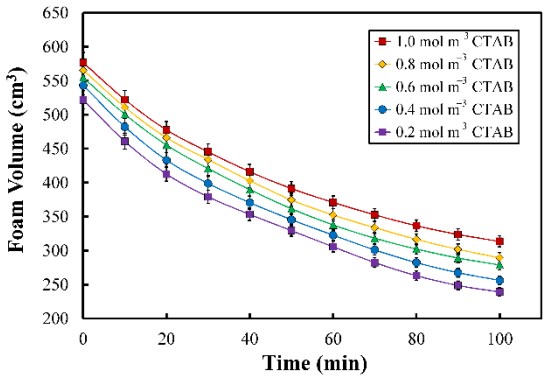

(g) 2.4 mol m^{-3} DDAPS and 50 mol m^{-3} NaCl

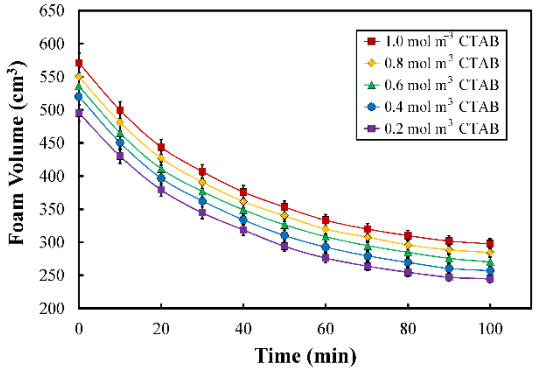

(h) 2.4 mol m^{-3} DDAPS and 100 mol m^{-3} NaCl

Figure 5.8. Effect of NaCl on foam volume at fixed concentrations of DDAPS (i.e., at 1.2 and 2.4 mol m^{-3}) at different concentrations of CTAB.

The foam behavior was noticeably different when the surfactant ratio was varied (i.e., the concentration of DDAPS was kept constant, and the same of CTAB was changed). The foam collapse rate was high during the initial period (i.e., 50 min after the formation of foam) in the absence of salt and at its low concentrations (e.g. 10 mol m^{-3}) for all the foam systems investigated. For 1.2 mol m^{-3} DDAPS and 0.2 mol m^{-3} CTAB, the decrease in the foam volume after the initial period was 200 cm^3 in the absence of NaCl, and 190 cm^3 in the presence of 10 mol m^{-3} NaCl. However, with 50 and 100 mol m^{-3} NaCl, the extent of foam collapse was less (i.e., 170 and 150 cm^3, respectively for the aforementioned system), and it did not show any noticeable variation with surfactant concentration. However, for the second half of the experiment (i.e., the remaining 50 min), the amount of foam collapse was less, and no significant change was observed upon varying the surfactant and salt concentrations. An average decrease of 60 cm^3 in the foam volume was noticed for 1.2 mol m^{-3} DDAPS and 0.2 mol m^{-3} CTAB. When the NaCl concentration was low, the adsorption of surfactant molecules was less due to the strong

electrostatic repulsion between the charged head-groups of the surfactant molecules. Thus, the EDL repulsion between the foam lamellae was less. The disjoining pressure isotherm of the foam films varies with the electrolyte concentration.[29] When the capillary pressure acting on a foam film is increased, its thickness decreases and the repulsive disjoining pressure increases. The increase in the repulsive disjoining pressure causes an unbound rise in the random perturbations, leading to a further decrease in the film thickness.[30] This increase in disjoining pressure leads to the formation of black spots. These black spots eventually cover the entire foam film and give rise to a common black film (CBF).[31] CBFs rupture at the lower salt concentrations and their thickness varies between 5 and 20 nm. These factors cause a higher rate of collapse of foams at low salt concentrations (i.e., 10 mol m^{-3}).

At the higher salt concentration (i.e., 100 mol m^{-3} NaCl), the adsorption of the surfactants was higher because the electrostatic repulsion between the surfactant molecules was reduced. This facilitated more surfactant molecules to adsorb in the foam lamellae in the later stages (i.e., after 50 min) after the formation of foam. The adsorption of surfactant molecules, in the presence of salt, caused the foam lamellae to become rigid, which reduced the film thinning rate.[32] At higher surfactant and salt concentrations, the resistance to collapse sharply increased as the surface waves were damped, which caused the foam films to drain below the critical thickness. Instead of rupture, a sudden transition of the foam film towards a more stable Newton black film (NBF) may take place.[31] NBFs are bilayers of surfactant molecules without a free aqueous core. CBF and NBF are the two different equilibrium states of the black films, and they have been described in Section 1.8.5 (Chapter 1). The equilibrium of CBFs depends on the stabilizing effect of the EDL. Therefore, their thickness decreases with increasing electrolyte concentration. However, the thickness of the NBFs does not change with electrolyte concentration. The

formation of NBF depends on the capillary pressure, electrolyte and surfactant concentrations, and film radius. This may be responsible for the stable foams at the high salt concentrations (i.e., 100 mol m^{-3} NaCl). This transition to the stable state instead of collapsing in the presence of salt is contrary to that predicted by the DLVO theory.

In addition to the effect of salt, the interaction between the head-groups of the surfactant molecules also affects the foam stability. In a foam film, the molecules of CTAB and DDAPS orient, as shown in Figure 5.6 (b). The DDAPS molecule contains both cationic and anionic head-groups (i.e., sulfonate and ammonium, respectively), while CTAB has one cationic group (i.e., ammonium). The monolayer in the foam film formed from these two surfactants consists of both types of the surfactant molecules. As the CTAB and DDAPS molecules orient, the negative head-group of DDAPS (i.e., sulfonate) gets attracted to the positive head-group of CTAB (i.e., ammonium).

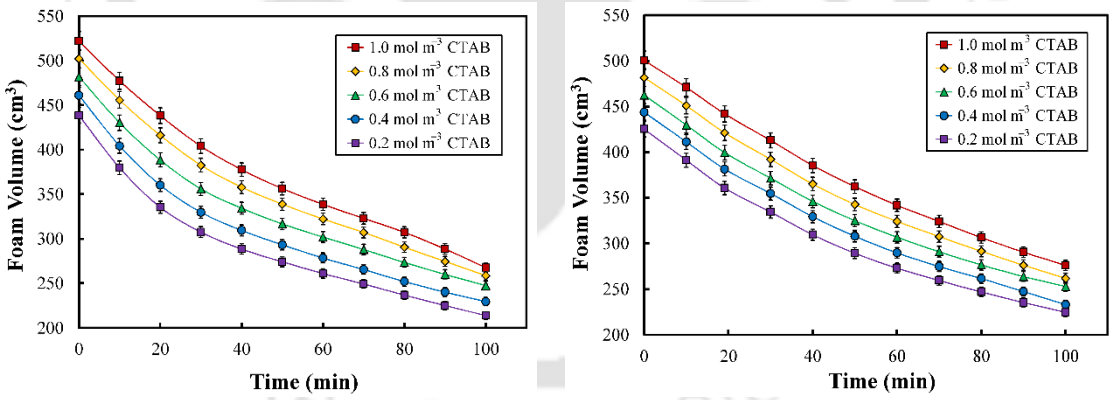

(a) 0.6 mol m^{-3} DDAPS and no salt

(b) 0.6 mol m^{-3} DDAPS and 10 mol m^{-3} NaCl

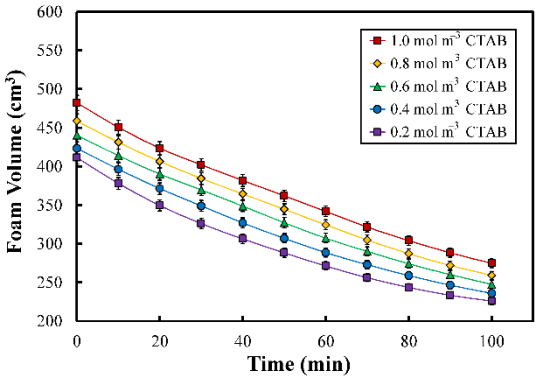

(c) 0.6 mol m^{-3} DDAPS and 50 NaCl

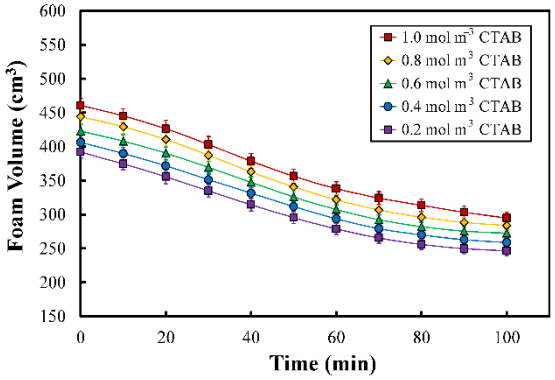

(d) 0.6 mol m^{-3} DDAPS and 100 mol m^{-3} NaCl

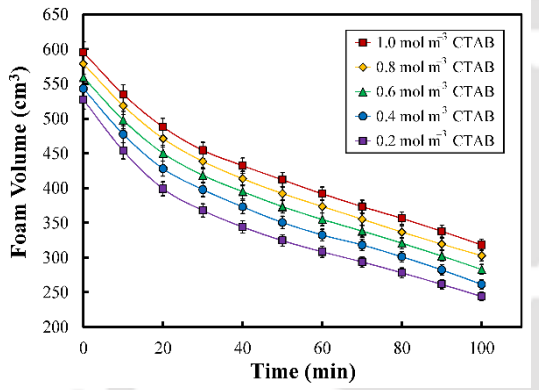

(e) 1.8 mol m^{-3} DDAPS and no salt

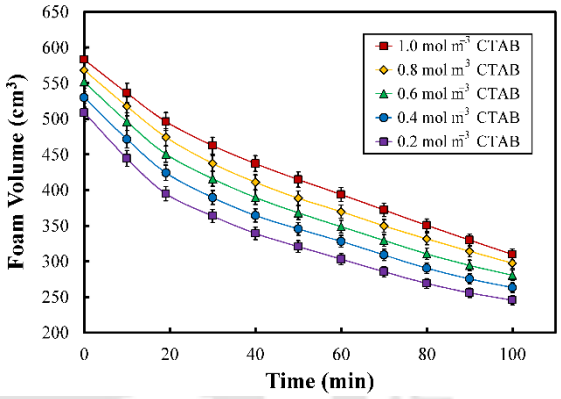

(f) 1.8 mol m^{-3} DDAPS and 10 mol m^{-3} NaCl

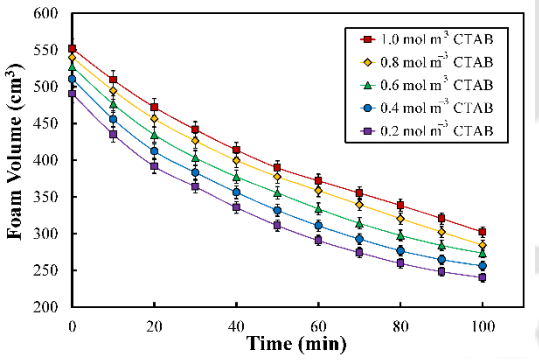

(g) 1.8 mol m^{-3} DDAPS and 50 mol m^{-3} NaCl

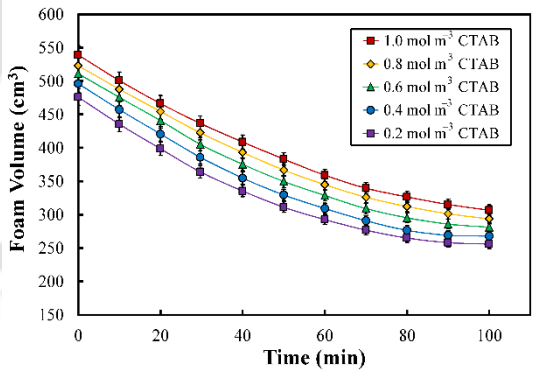

(h) 1.8 mol m^{-3} DDAPS and 100 mol m^{-3} NaCl

Figure 5.9. Effect of NaCl on foam volume at fixed concentrations of DDAPS (i.e., at 0.6 and 1.8 mol m^{-3}) at different concentrations of CTAB.

In addition, electrostatic repulsion is likely to occur between the ammonium head-groups of these surfactants. Therefore, the sodium ions adjust themselves near the negatively-charged sulfonate groups. However, the chloride ions do not produce any substantial effect at the interface.[33] Addition of NaCl enhances the screening efficiency of the charges of the sulfonate and quaternary ammonium groups, and the effectiveness of electrostatic screening depends on the ionic strength of the solution. The salt helps to increase the adsorption of the DDAPS and CTAB molecules, which increases the foam stability. The increased adsorption of the surfactant molecules helps to heal the weak spots in the foam film produced by the random perturbations.[34] These phenomena are influenced by the interfacial packing density of the surfactant molecules.[35]

5.2.3 Zeta potential at the air–water interface in mixed surfactant systems

The zeta potential is an important electrical property of the air–water interface. It helps in visualizing the ionic environment in the vicinity of the interface. The ionic environment near the interface has special properties, which distinguish it from the continuous phases surrounding it. For the charged air–water interface, a balancing counter-charge is present in the adjoining aqueous phase. This charge, although scattered throughout the liquid phase, is concentrated in the proximity of the interface, forming an electrostatic double layer (EDL). The zeta potential depends on the EDL developed near the interface.[36] The EDL consists of an immediate layer adjacent to the interface termed as *Stern layer* (which holds a few ions that are specifically adsorbed on the interface) followed by a diffuse double layer.[37] The zeta potential is the potential at the slipping plane, and the location of this plane varies with the surface morphology. A considerable amount of difference may be observed between the zeta potential and the surface potential (which is the potential at the surface). The latter can be described by the Grahame equation given in

Section 3.2.4 (Chapter 3). Figure 5.10 depicts a schematic diagram of the orientation of the surfactant molecules and the sodium ions around a spherical air–water interface at various concentrations of NaCl.

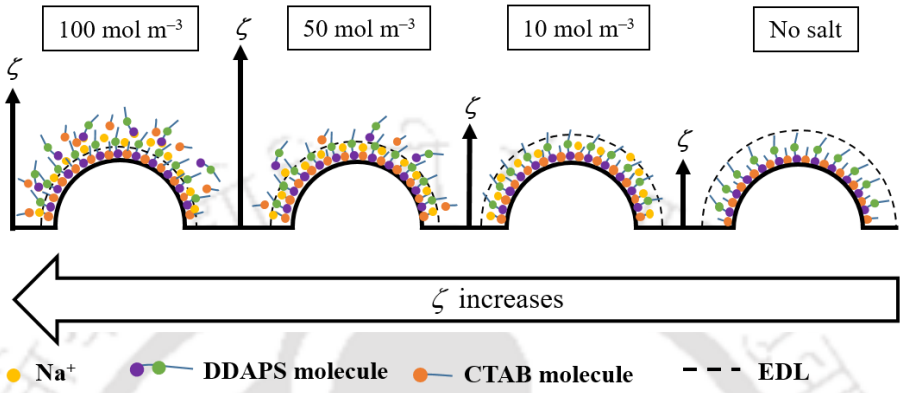

Figure 5.10. Schematic diagram of the orientation of the surfactant molecules and Na^+ around a spherical air–water interface (represented by the semicircle) in the absence of salt, and at 10, 50, and 100 mol m^{-3} NaCl. The figure also depicts the shrinkage of EDL with increasing salt concentration which is shown by the dotted line.

The zeta potential measured at different concentrations of DDAPS and CTAB with and without NaCl is depicted in Figure 5.11. In the mixed systems, a competition between CTAB and DDAPS takes place for adsorbing at the air–water interface. The competition to adsorb on the interface is governed by the speed of diffusion of the surfactant molecules, and the interaction (e.g., electrostatic and steric) between them. Addition of salt to the surfactant solution had a significant impact on zeta potential. The presence of salt enhanced the adsorption of the surfactant molecules by the reduction of the EDL repulsion among the head-groups (see Section 5.2.1). This reduction allowed the surfactant molecules to pack more densely at the interface. A substantial reduction in surface tension in the presence of salt corroborates this fact (Figure 5.3). However, at the

high salt concentration, the zeta potential decreased, as predicted by the Grahame equation (see Section 3.2.4, Chapter 3).

The zeta potential for the mixed surfactant system showed remarkable characteristics, which are shown in Figure 5.11. The pH of the surfactant solution varied between 5.9 and 6.9. The zeta potential in the aqueous CTAB system was positive.[38] For DDAPS, the isoelectric point was 3.2.[39] Therefore, the zeta potential was positive at the lower pH and negative at a higher pH. The zeta potential in the mixed surfactant system depends on the competitive adsorption of the surfactant molecules at the interface. For the mixed surfactant system containing 1.2 mol m^{-3} DDAPS and 0.2 – 1.0 mol m^{-3} CTAB, the zeta potential showed an increasing trend. The negative charge of the interface in the presence of DDAPS got neutralized by the adsorption of the CTAB molecules, and hence the zeta potential changed to positive values. For the mixed surfactant system containing 1.2 mol m^{-3} DDAPS and 0.5 mol m^{-3} CTAB, the value of zeta potential was 21 mV in the absence of salt. However, the zeta potential was 40.3 mV in the presence of 10 mol m^{-3} NaCl. The values of β^{σ} and β^{M} for the 10 mol m^{-3} NaCl system were –2.17 and –1.54, respectively. For the 2.4 mol m^{-3} DDAPS and 0.5 mol m^{-3} CTAB system, the zeta potential was 35 mV in the absence of salt. For the same surfactant composition but in the presence of 10 mol m^{-3} NaCl, the zeta potential was 63 mV. The values of β^{σ} and β^{M} for the 10 mol m^{-3} NaCl system were –5.95 and –4.56, respectively. Thus, it is concluded that the interaction parameters increased when the total surfactant concentration was increased, as a result of the decrease in the interaction between CTAB and DDAPS. The zeta potential increased with increasing NaCl concentration until 50 mol m^{-3}. However, it decreased when the NaCl concentration was increased to 100 mol m^{-3}, which qualitatively agrees with the trend predicted by the Grahame equation (see

Section 3.2.4, Chapter 3).

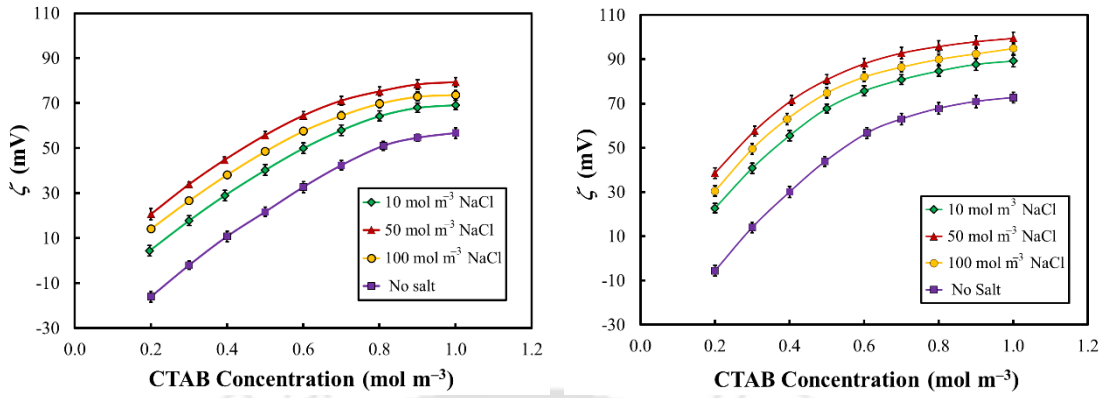

(a) (b)

Figure 5.11. Variation of the zeta potential at the air–water interface in mixed surfactant systems at (a) 1.2 and (b) 2.4 mol m^{-3} DDAPS at different concentrations of NaCl.

5.3 Conclusion

Type I synergism was observed in the DDAPS–CTAB mixed surfactant systems. For these systems, the surface tension decreased more effectively than the single-surfactant systems. The CMC was attained at a lower concentration of CTAB. With increasing NaCl concentration, the γ_{CMC} decreased progressively inasmuch as the adsorption of the surfactant molecules at the air–water interface increased. This occurred as a result of the reduction in the electrostatic repulsion among the surfactant head-groups. The values of β^{σ} and β^{M} indicate that the interaction in the mixed monolayer was more robust than that in the mixed micelle. Addition of NaCl decreased the electrostatic repulsion between the CTAB and DDAPS head-groups and hence increased the interaction parameters.

The synergism was clearly observed in the foaming of the mixed surfactant systems. The initial foam volume, in general, was higher for the mixed surfactant systems than the single surfactant systems. The number of surfactant molecules adsorbed at the

air–water interface was increased upon increasing the surfactant concentration, which increased the foam volume. The EDL repulsion played a major role in foaming. Upon addition of salt, the initial foam volume was reduced due to the increased electrostatic screening, which decreased the EDL repulsion in the foam film leading to the coalescence of bubbles. In the absence of salt (and at low salt concentration), the foam collapsed rapidly in the initial period (i.e., 50 min after the foam formation). In the second half of the experiment, the extent of foam collapse was rather less.

The competitive interaction between the CTAB and DDAPS molecules at the air–water interface had a strong influence on the zeta potential. The zeta potential showed an increasing trend in the mixed surfactant system. The zeta potential increased with increasing NaCl concentration up to 50 mol m^{-3}. However, it decreased upon a further increase in the NaCl concentration to 100 mol m^{-3}, which agrees with the Grahame equation.

References

[1] Holland, P. M.; Rubingh, D. N., *Mixed Surfactant Systems*; American Chemical Society: Washington, 1992.

[2] Wang, X.; Wang, J.; Wang, Y.; Ye, J.; Yan, H.; Thomas, R. K. Properties of mixed micelles of cationic gemini surfactants and nonionic surfactant triton X-100: Effects of the surfactant composition and the spacer length. *J. Colloid Interface Sci.* **2005,** 286, 739–746.

[3] Khan, A.; Marques, E. F. Synergism and polymorphism in mixed surfactant systems. *Curr. Opin. Colloid Interface Sci.* **1999,** 4, 402–410.

[4] Scamehorn, J., *Phenomena in Mixed Surfactant Systems*, ACS Symposium Series, American Chemical Society, Washington DC, 1985.

[5] Ghosh, S.; Moulik, S. Interfacial and micellization behaviors of binary and ternary mixtures of amphiphiles (Tween–20, Brij–35, and sodium dodecyl sulfate) in aqueous medium. *J. Colloid Interface Sci.* **1998,** 208, 357-366.

[6] Haque, M. E.; Das, A. R.; Moulik, S. P. Behaviors of sodium deoxycholate (NaDC) and polyoxyethylene tert-octylphenyl ether (Triton X–100) at the air/water interface and in the bulk. *J. Phys. Chem.* **1995,** 99, 14032–14038.

[7] Jana, P. K.; Moulik, S. P. Interaction of bile salts with hexadecyltrimethylammonium bromide and sodium dodecyl sulfate. *J. Phys. Chem.* **1991,** 95, 9525–9532.

[8] Moulik, S. P.; Haque, M. E.; Jana, P. K.; Das, A. R. Micellar properties of cationic surfactants in pure and mixed states. *J. Phys. Chem.* **1996,** 100, 701–708.

[9] Sharma, K. S.; Patil, S. R.; Rakshit, A. K.; Glenn, K.; Doiron, M.; Palepu, R. M.; Hassan, P. Self-aggregation of a cationic–nonionic surfactant mixture in aqueous media: Tensiometric, conductometric, density, light scattering, potentiometric, and fluorometric studies. *J. Phys. Chem. B* **2004,** 108, 12804–12812.

[10] Goddard, E.; Ananthapadmanabhan, K.; Kwak, J., *Polymer–Surfactant Systems*, Surfactant Science Series, (77) Marcel Dekker, New York, 1998.

[11] Ogino, K.; Abe, M., *Mixed Surfactant Systems*, Surfactant Science Series, (46) Marcel Dekker, New York, 1993.

[12] Bakshi, M. S.; Singh, K. Synergistic interactions in the mixed micelles of cationic gemini with zwitterionic surfactants: Fluorescence and Krafft temperature studies. *J. Colloid Interface Sci.* **2005,** 287, 288–297.

[13] Rosen, M. J., *Surfactants and Interfacial Phenomena*; John Wiley & Sons: New York, 2004.

[14] Lu, T.; Huang, J.; Liang, D. Salt effect on microstructures in cationic gemini surfactant solutions as studied by dynamic light scattering. *Langmuir* **2008,** 24, 1740–1744.

[15] Mu, J.-H.; Li, G.-Z.; Jia, X.-L.; Wang, H.-X.; Zhang, G.-Y. Rheological properties and microstructures of anionic micellar solutions in the presence of different inorganic salts. *J. Phys. Chem. B* **2002,** 106, 11685−11693.

[16] Shi, L.; Tummala, N. R.; Striolo, A. $C_{12}E_6$ and SDS surfactants simulated at the vacuum−water interface. *Langmuir* **2010,** 26, 5462–5474.

[17] Gurkov, T. D.; Dimitrova, D. T.; Marinova, K. G.; Bilke-Crause, C.; Gerber, C.; Ivanov, I. B. Ionic surfactants on fluid interfaces: Determination of the adsorption; role of the salt and the type of the hydrophobic phase. *Colloids Surf. A* **2005,** 261, 29–38.

[18] Bommaganti, P.; Kumar, M. V.; Ghosh, P. Effects of binding of counterions on adsorption and coalescence. *Chem. Eng. Res. Des.* **2009,** 87, 728–738.

[19] Suryanarayana, G.; Ghosh, P. Adsorption and coalescence in mixed-surfactant systems: Air-water interface. *Ind. Eng. Chem. Res.* **2010,** 49, 1711–1724.

[20] Reddy, S.; Ghosh, P. Adsorption and coalescence in mixed surfactant systems: Water−hydrocarbon interface. *Chem. Eng. Sci.* **2010,** 65, 4141–4153.

[21] Guo, W.; Guzman, E.; Heavin, S.; Li, Z.; Fung, B.; Christian, S. Mixed surfactant systems of sodium perfluorooctanoate with nonionic, zwitterionic, and cationic hydrocarbon surfactants. *Langmuir* **1992,** 8, 2368–2375.

[22] Misselyn-Bauduin, A.-M.; Thibaut, A.; Grandjean, J.; Broze, G.; Jérôme, R. Mixed micelles of anionic–nonionic and anionic−zwitterionic surfactants analyzed by pulsed field gradient NMR. *Langmuir* **2000,** 16, 4430–4435.

[23] Hines, J.; Thomas, R.; Garrett, P., Rennie; Rennie, G.; Penfold, J. Investigation of mixing in binary surfactant solutions by surface tension and neutron reflection: Anionic/nonionic and zwitterionic/nonionic mixtures. *J. Phys. Chem. B* **1997,** 101, 9215–9223.

[24] Mullally, M. K.; Marangoni, D. G. Micellar properties of zwitterionic surfactant-alkoxyethanol mixed micelles. *Can. J. Chem.* **2004,** 82, 1223–1229.

[25] Wu, C.; Jim, T. F.; Gan, Z.; Zhao, Y.; Wang, S. A heterogeneous catalytic kinetics for enzymatic biodegradation of poly(ϵ-caprolactone) nanoparticles in aqueous solution. *Polymer* **2000,** 41, 3593–3597.

[26] Rosen, M. J. Synergism in mixtures containing zwitterionic surfactants. *Langmuir* **1991,** 7, 885–888.

[27] Marinova, K. G.; Basheva, E. S.; Nenova, B.; Temelska, M.; Mirarefi, A. Y.; Campbell, B.; Ivanov, I. B. Physico-chemical factors controlling the foamability and foam stability of milk proteins: Sodium caseinate and whey protein concentrates. *Food Hydrocolloids* **2009,** 23, 1864–1876.

[28] Behera, M. R.; Varade, S. R.; Ghosh, P.; Paul, P.; Negi, A. S. Foaming in micellar Solutions: Effects of surfactant, salt, and oil concentrations. *Ind. Eng. Chem. Res.* **2014,** 53, 18497–18507.

[29] Exerowa, D.; Kruglyakov, P. M., *Foam and Foam Films: Theory, Experiment, Application*; Elsevier: Amsterdam, 1997.

[30] Bhakta, A.; Ruckenstein, E. Decay of standing foams: Drainage, coalescence and collapse. *Adv. Colloid Interface Sci.* **1997,** 70, 1–124.

[31] Ruckenstein, E.; Bhakta, A. Effect of surfactant and salt concentrations on the drainage and collapse of foams involving ionic surfactants. *Langmuir* **1996,** 12, 4134–4144.

[32] Rao, A. A.; Wasan, D. T.; Manev, E. D. Foam stability-effect of surfactant composition on the drainage of microscopic aqueous films. *Chem. Eng. Commun.* **1982,** 15, 63–81.

[33] Cummings, S.; Enderby, J.; Neilson, G.; Newsome, J.; Howe, R.; Howells, W.; Soper, A. Chloride ions in aqueous solutions. *Nature* **1980,** 287, 714–715.

[34] Adamson, A. W.; Gast, A. P. The solid–liquid interface-contact angle. *Phy. Chem. Surf.* **1997,** 4, 333–361.

[35] Prud'homme, R., *Foams: Theory, Measurements, and Applications*; Marcel Dekker, Inc.: New York, 2017.

[36] Berg, J. C., *An Introduction to Interfaces & Colloids: The Bridge to Nanoscience*; World Scientific: Singapore, 2010.

[37] Scholz, F., *Electroanalytical Methods: Guide to Experiments and Applications*; Springer: New York, 2010.

[38] Banik, M.; Ghosh, P. The electroviscous effect at fluid–fluid interfaces. *Ind. Eng.*

Chem. Res. **2013,** 52, 1581–1590.

[39] Varade, S. R.; Ghosh, P. Foaming in aqueous solutions of zwitterionic surfactant: Effects of oil and salts. *J. Dispersion Sci. Technol.* **2017,** 38, 1–15.

CHAPTER 6

SUMMARY AND SCOPE FOR FUTURE WORK

6.1 Summary of the work

This thesis has presented a comprehensive study on the stability of foams prepared from the aqueous solution of a zwitterionic surfactant (i.e., DDAPS) in the presence of salts. The ion specific effect and synergism (with a cationic surfactant, i.e., CTAB) in the presence of salts were investigated with respect to foamability and foam stability.

The concentration of DDAPS and salts (i.e., NaCl, $CaCl_2$, and $AlCl_3$) were varied to understand the adsorption of the zwitterionic surfactant. The surface tension decreased with the increasing concentration of DDAPS, thereby indicating an increase in the concentration of surfactant at the air–water interface. Addition of salt further reduced the surface tension indicating enhanced adsorption of the surfactant molecules at the air–water interface. The quantity of salt required for reducing the surface tension and CMC followed the sequence: NaCl > $CaCl_2$ > $AlCl_3$. The efficiency of the 1:1 salts in decreasing the surface and interfacial tension followed the order: CsCl > NaCl > LiCl.

The mechanism of the stability of foams was investigated in the presence and absence of salts. The initial foam volume increased with increasing DDAPS concertation and reduced in the presence of salt. The number of DDAPS molecules at the air–water interface increased upon increasing the surfactant concentration, which resulted in the increase in foam volume. The foam collapse rate was higher during the initial period after foam formation in the absence of salt and at low salt concentration. The foam collapse rate was less afterwards. The electrostatic repulsion between the adsorbed surfactant molecules and the stability of the thin foam film play important roles in these phenomena.

The specific ion effect was distinctly manifested in the foaming of the aqueous DDAPS solutions. The smaller size of Cs^+ caused more DDAPS molecules to adsorb at the air–water interface, whereas the larger size of Li^+ allowed a lesser number of surfactant molecules to adsorb at the interface. The increased adsorption resulted in a

more rigid film, which reduced the flow of water. The higher concentration of the surfactant molecules at the interfaces increased the charge density, and hence a stronger electrostatic double layer repulsion between the interfaces. Both these factors provided more stability to the foams. The efficiency of the counterions in decreasing the foam stability followed the order: $Cs^+ > Na^+ > Li^+$.

A Type I synergism was observed in the DDAPS–CTAB mixed surfactant systems. The values of the interaction parameters indicate that the interaction in the mixed monolayer was more robust than that in the mixed micelle. The effect of this synergism was clearly manifested in the foaming of the mixed surfactant systems.

When *n*-hexane was solubilized in the surfactant solution, the initial foam volume decreased. At the low salt (i.e., NaCl, $CaCl_2$, and $AlCl_3$) concentrations, the foam collapse rate was high during the initial period. However, at the high salt concentrations, the foam collapse rate was less. The entering, spreading, and bridging coefficients were positive. These coefficients decreased with increasing salt concentration. The effectiveness of the salts in increasing the foam stability followed the sequence: $AlCl_3 > CaCl_2 > NaCl$.

The zeta potential at the oil–water interface increased (i.e., ζ became more negative) with the increasing concentration of DDAPS up to the CMC. Addition of a small quantity of salt increased the zeta potential. However, the zeta potential decreased at the high salt concentration. The effectiveness of salts in reducing the zeta potential was in the sequence: $AlCl_3 > CaCl_2 > NaCl$. The efficiency of the 1:1 salts in making the zeta potential more negative followed the order: CsCl > NaCl > LiCl. For the mixed surfactant system, the interaction between the CTAB and DDAPS molecules at the air–water interface had a strong influence on the zeta potential.

The analysis of the effects of salts on the foaming properties of the zwitterionic surfactant has resulted in a better understanding of the fundamental phenomena in colloid

and interface science. These findings have a significant impact on numerous applications such as enhanced oil recovery, firefighting, food processing, development of personnel care products, and froth floatation, to name a few.

6.2 Scope for future work

Based on the present studies, the following works may be carried out in the future to extend our understanding on the behavior of foams:

- Adsorption of surfactants at the air–water and oil–water interfaces in the mixed surfactant systems may be studied in the presence of salts. A mathematical model may be developed for the adsorption.
- Foamability and foam stability may be studied in the presence of nanoparticles (e.g., titanium dioxide, silica, cellulose, lignin, starch, and proteins). The nanoparticles can strongly influence the foaming characteristics of the surfactant solutions. The effects of the experimental parameters (e.g., temperature, pH, and ionic strength) on the foamability and foam stability may be studied.
- Synergism in the zwitterionic–anionic and zwitterionic–nonionic surfactant systems in the presence of salts containing mono-, di-, and trivalent ions may be studied.
- The interaction of zwitterionic surfactants with polar and nonionic molecules like alcohols would be significantly different and interesting study to carry out.
- The synergism studies may be extended to the ternary systems. Ternary and quaternary systems are often encountered in the industry. Although complex, a study of such systems is very important.
- The ion specific effect may be studied in the presence of the divalent ions.

Research output

Referred journals

[1] Varade, S. R.; Ghosh, P. Foaming in aqueous solutions of zwitterionic surfactant: Effects of oil and salts. *J. Dispersion Sci. Technol.* **2017**, 38, 1–15.

[2] Varade, S. R.; Ghosh, P. Foaming in aqueous solutions of mixtures of a zwitterionic and a cationic surfactant in presence of an electrolyte. J. Dispersion Sci. Technol. 2019, (Accepted for publication, May 2019). DOI: 10.1080/01932691.2019.1614944.

[3] Varade, S. R.; Ghosh, P. Foaming in aqueous solutions of zwitterionic surfactant in presence of monovalent salts: the specific ion effect. Chem. Eng. Commun. (Revision submitted in April 2019).

Conferences

[1] Varade, S. R.; Ghosh, P., International conference CompFlu@Hyd 2016, International Institute of Information Technology, Hyderabad, 12–14 December, 2016 (*Poster presented*).

[2] Varade, S. R.; Ghosh, P., Research Conclave '17, Indian Institute of Technology Guwahati, 16–19 March, 2017 (*Poster presented*).

[3] Varade, S. R.; Ghosh, P., International Conference on 'Sophisticated Instruments in Modern Research', Indian Institute of Technology Guwahati, 30 June – 1 July, 2017 (*Poster presented*).

[4] Varade, S. R.; Ghosh, P., 7th Asian Conference in Colloid and Interface Science, Kuala Lumpur, 8–11 August, 2017 (*Poster presented*).

APPENDICES

Appendix A1

Ion 1: charge = $z_1 e$ (A1.1)

Ion 2: charge = $z_2 e$ (A1.2)

From the Debye–Hückel theory, the electrostatic potential due to Ion 1 at the position of Ion 2 located at a distance r is given by

$$\psi_1 = \left(\frac{z_1 e}{4\pi\varepsilon\varepsilon_0 r}\right)\left[\frac{\exp(\kappa a)}{1+\kappa a}\right]\left[\exp(-\kappa r)\right] \quad \text{(A1.3)}$$

The electrostatic energy of interaction between the two ions is given by

$$\phi = \psi_1 \times z_2 e = \left(\frac{z_1 z_2 e^2}{4\pi\varepsilon\varepsilon_0 r}\right)\left[\frac{\exp(\kappa a)}{1+\kappa a}\right]\left[\exp(-\kappa r)\right] \quad \text{(A1.4)}$$

If $\kappa a \to 0$, Eq. (A1.4) becomes

$$\phi = \left(\frac{z_1 z_2 e^2}{4\pi\varepsilon\varepsilon_0 r}\right)\left[\exp(-\kappa r)\right] \quad \text{(A1.5)}$$

If $z_1 = z_2 = z$, Eq. (A1.5) becomes

$$\phi = \left(\frac{z^2 e^2}{4\pi\varepsilon\varepsilon_0 r}\right)\left[\exp(-\kappa r)\right] \quad \text{(A1.6)}$$

Appendix A2

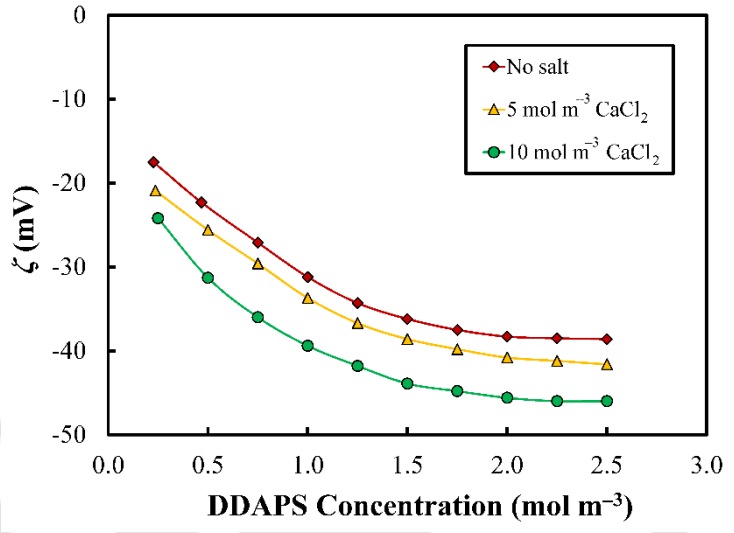

Figure A2. Variation of the zeta potential at the hexane–water interface with the concentration of DDAPS at different concentrations of $CaCl_2$.

Appendix A3

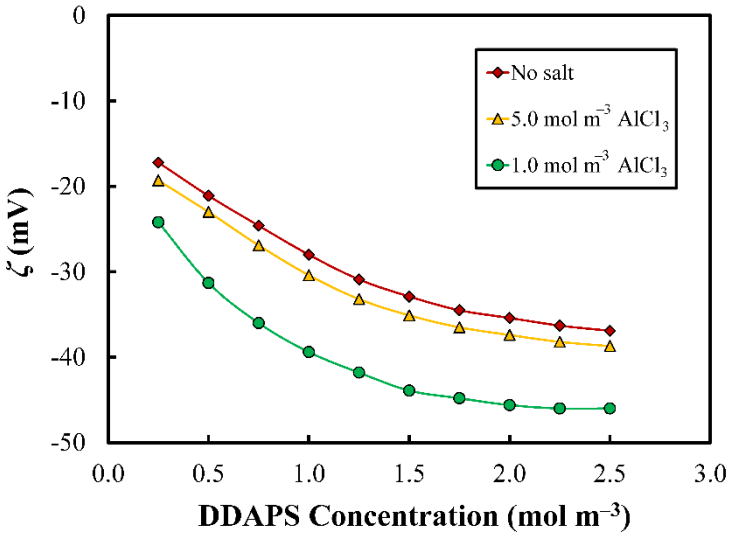

Figure A3. Variation of the zeta potential at the hexane–water interface with the concentration of DDAPS at different concentrations of $AlCl_3$.

Appendix A4

Calculation of the values of Entering (E), Spreading (S), and Bridging (B) coefficients.

$$E = \gamma_{A/W} + \gamma_{O/W} - \gamma_{A/O} \quad \text{(A4.1)}$$

$$S = \gamma_{A/W} - \gamma_{O/W} - \gamma_{A/O} \quad \text{(A4.2)}$$

$$B = \gamma_{A/W}^2 + \gamma_{O/W}^2 - \gamma_{A/O}^2 \quad \text{(A4.3)}$$

At 1.2 mol m^{-3} DDAPS, in the absence of any salt,

$\gamma_{A/W}$ = 44.5 mN m^{-1}, $\gamma_{O/W}$ = 32.8 mN m^{-1}, and $\gamma_{A/O}$ = 47.2 mN m^{-1}

Substituting these values of in equations (A4.1), (A4.2), and (A4.3), we obtain,

$$E = 44.5 + 32.8 - 47.2 = 30.1 \text{ mN m}^{-1}$$

$$S = 44.5 - 32.8 - 47.2 = -75.5 \text{ mN m}^{-1}$$

$$B = 44.5^2 + 32.8^2 - 47.2^2 = 828.25 \text{ mN}^2 \text{ m}^{-2}$$

Therefore, $E = 30.1$ mN m^{-1}, $S = -75.5$ mN m^{-1}, and $B = 828.25$ mN^2 m^{-2}

Appendix B1

Calculation of Γ from the equation 4.1.

$$\Gamma = -\frac{1}{RT}\frac{d\gamma}{d\ln c} \qquad \text{(B1.1)}$$

The surface tension data are plotted as shown in Figure 4.1 (in Section 4.2.1) as γ versus $\ln c$ profiles. A fourth-order least squares polynomial is fitted through these data.

$$\gamma = 0.7001(\ln c)^4 + 1.9187(\ln c)^3 - 0.5866(\ln c)^2 - 10.889(\ln c) + 47.448$$

Therefore, $\frac{d\gamma}{d\ln c} = 2.8004(\ln c)^3 + 5.7561(\ln c)^2 - 1.1732(\ln c) - 10.889$

At $c = 1.0$ mol m^{-3}, we get

$$\frac{d\gamma}{d\ln c} = 2.8004[\ln(1)]^3 + 5.7561[\ln(1)]^2 - 1.1732[\ln(1)] - 10.889 = -10.889$$

Therefore,

$$\Gamma = \frac{10.889}{2\times 8.314\times 298} = 2.19\times 10^{-3} \text{ mmol m}^{-2} = 2.19\times 10^{-6} \text{ mol m}^{-2}$$

The minimum area (A_m) occupied by a surfactant molecule at the air–water interface is calculated as

$$A_m = \frac{1}{\Gamma N_A}$$

$$A_m = \frac{1}{2.19\times 10^{-6}\times 6.023\times 10^{23}} = 0.758 \text{ nm}^2$$

Appendix B2

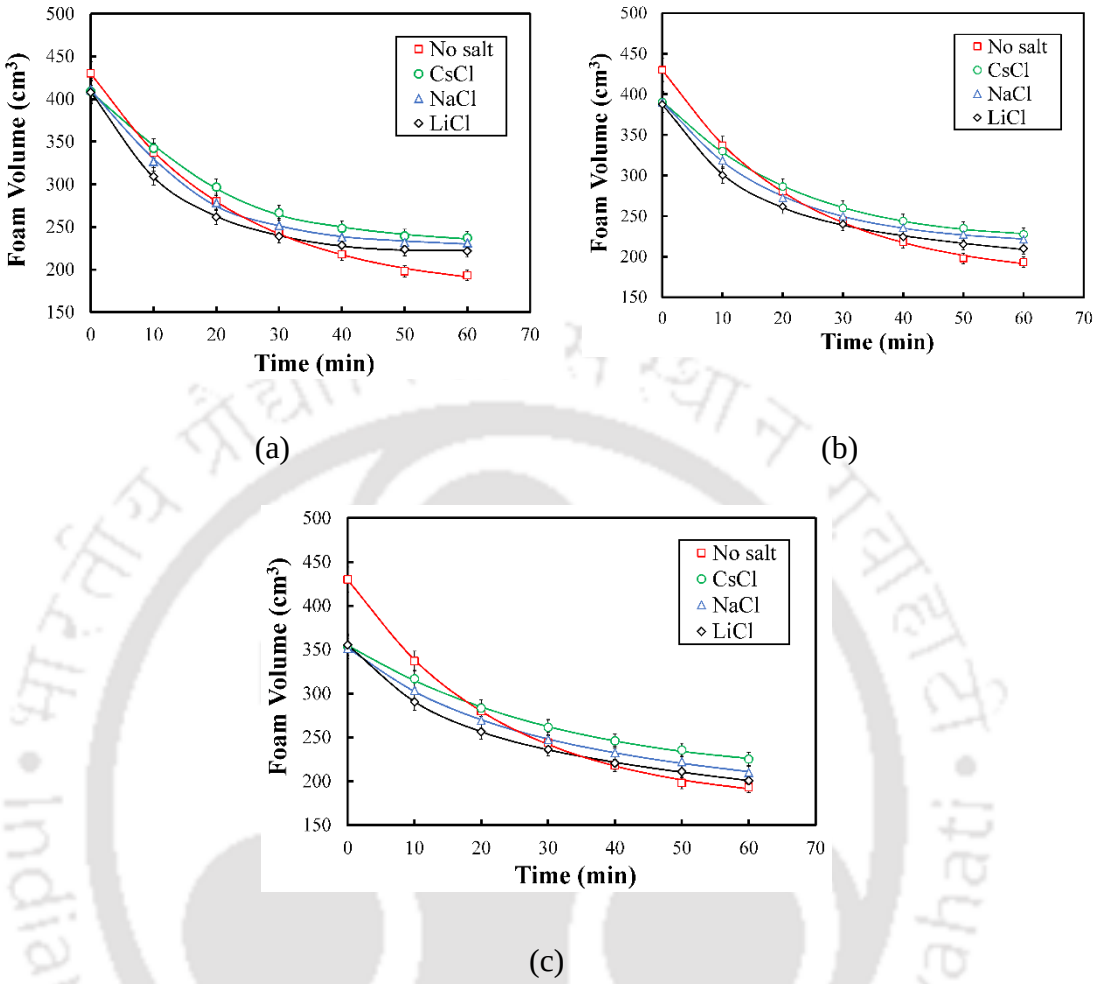

Figure B2.1. A comparative study of the lifetime of foams at 0.6 mol m^{-3} DDAPS at (a) 10, (b) 50, and (c) 100 mol m^{-3} CsCl, NaCl, and LiCl. The solid lines indicate the bi-exponential fits.

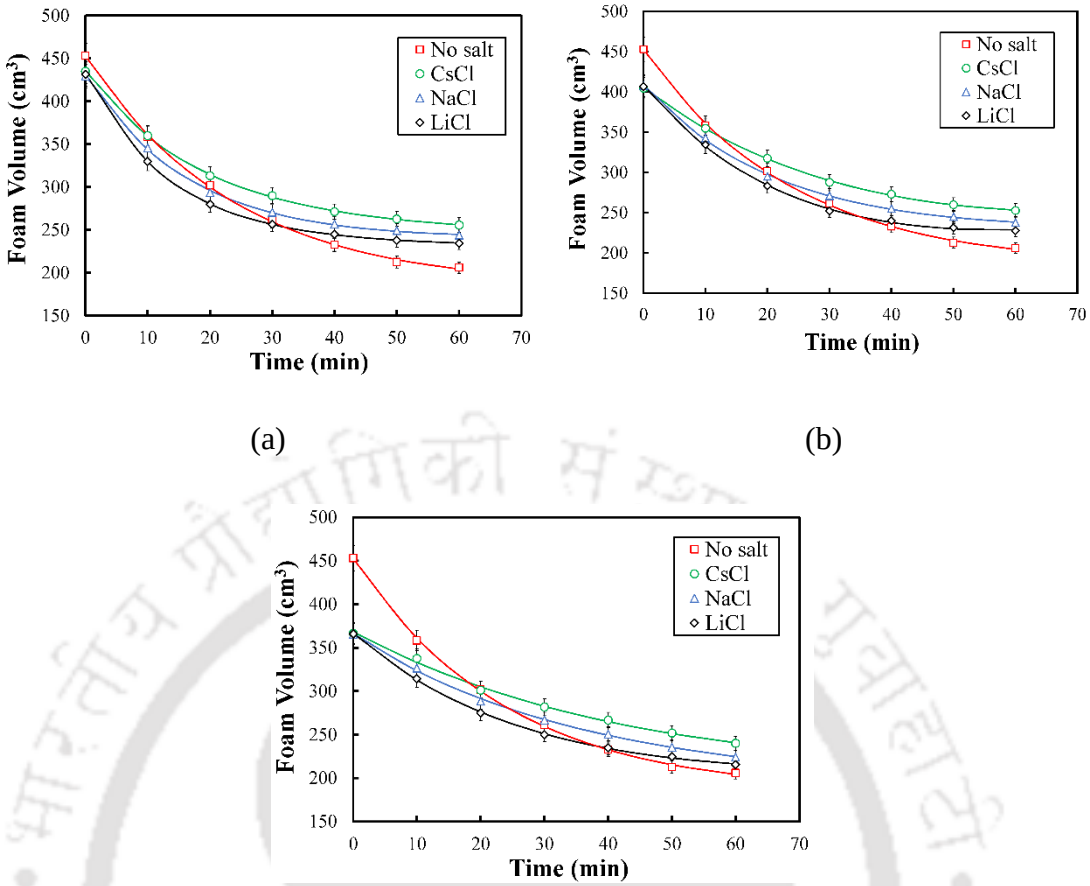

Figure B2.2. A comparative study of the lifetime of foams at 1.2 mol m^{-3} DDAPS at (a) 10, (b) 50, and (c) 100 mol m^{-3} CsCl, NaCl, and LiCl. The solid lines indicate the bi-exponential fits.

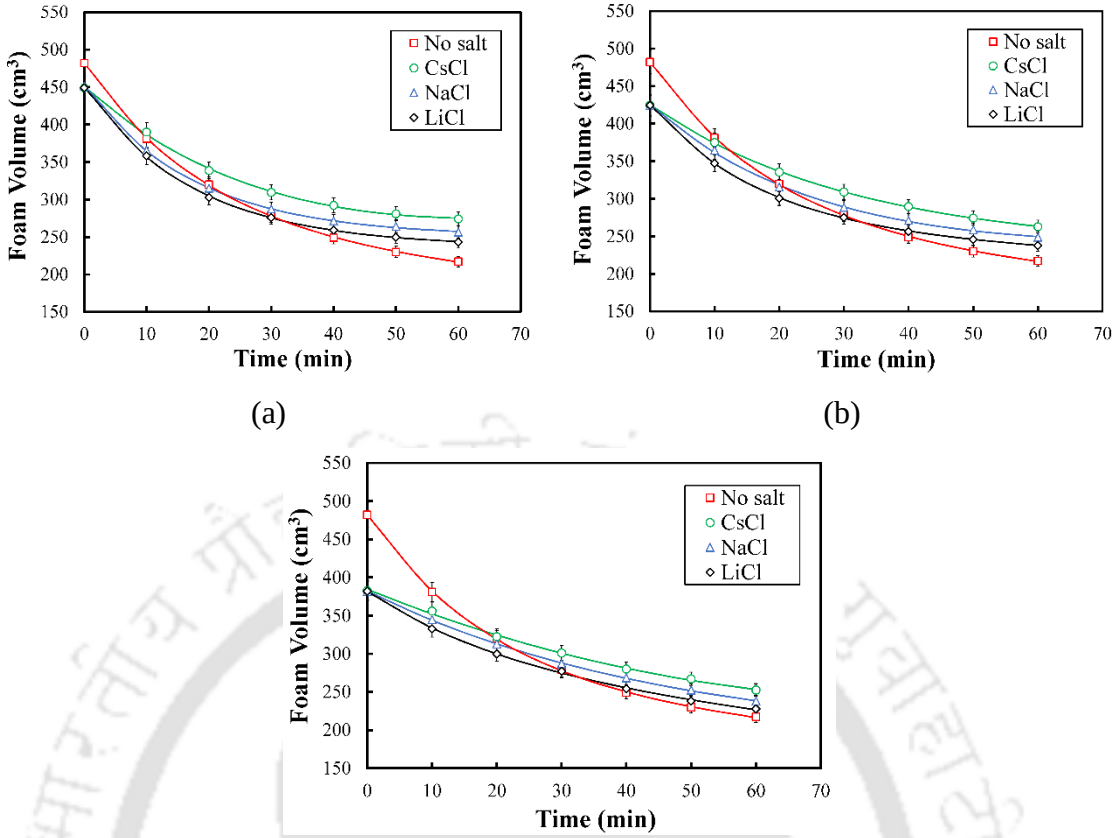

Figure B2.3. A comparative study of the lifetime of foams at 1.8 mol m^{-3} DDAPS at (a) 10, (b) 50, and (c) 100 mol m^{-3} CsCl, NaCl, and LiCl. The solid lines indicate the bi-exponential fits.

Appendix C1

The Gibbs adsorption equation is given by

$$d\gamma = -\sum_i \Gamma_i d\mu_i \qquad \text{(C1.1)}$$

The Gibbs adsorption equation for two surface active solutes in dilute solution is given by

$$d\gamma = RT\left(\Gamma_1 d\ln a_1 + \Gamma_2 d\ln a_2\right) \qquad \text{(C1.2)}$$

where Γ_1 and Γ_2 are the surface excess concentrations of the two solutes at the interface. a_1 and a_2 are the respective activities in the solution phase. For a dilute solution, the activity can be replaced by concentration. Therefore, we have

$$\Gamma_1 = \frac{1}{RT}\left(\frac{-\partial\gamma}{\partial\ln c_1}\right)_{c_2} = \frac{1}{2.303}\left(\frac{-\partial\gamma}{\partial\log c_1}\right)_{c_2} \qquad \text{(C1.3)}$$

$$\Gamma_2 = \frac{1}{RT}\left(\frac{-\partial\gamma}{\partial\ln c_2}\right)_{c_1} = \frac{1}{2.303}\left(\frac{-\partial\gamma}{\partial\log c_2}\right)_{c_1} \qquad \text{(C1.4)}$$

The concentration of each surfactant at the interface can be calculated from the slope of the $\gamma - \log c$ $(\text{or } \ln c)$ plot of each surfactant holding the solution concentration of the other surfactant constant. The molar concentrations of the two surfactants in the solution phase are given by the expression, $c_1 = c_1^0 f_1 x_1$ and $c_2 = c_2^0 f_2 x_2$, where f_1 and f_1 are the activity coefficients, respectively, x_1 is the mole fraction of surfactant 1 in the total surfactant at the interface, and $x_1 = 1 - x_2$. c_1^0 is the molar concentration required to attain a given surface tension in a solution of pure surfactant 1. c_2^0 is the molar concentration required to attain a given surface tension in a solution of pure surfactant 2.

From the non-ideal solution theory, the activity coefficient at the interface is given

by

$$\ln f_1 = \beta^{\sigma} \left(1 - x_1\right)^2 \tag{C1.5}$$

$$\ln f_2 = \beta^{\sigma} \left(x_1\right)^2 \tag{C1.6}$$

where β^{σ} is a parameter related to the interaction between two surfactants at the interface.

Now, $f_1 = \dfrac{c_1}{c_1^0 x_1}$ and $f_2 = \dfrac{c_2}{c_2^0 x_2}$

Therefore, Equations (C1.5) and (C1.6) can be written as

$$\ln\left(c_1 / c_1^0 x_1\right) = \beta^{\sigma} \left(1 - x_1\right)^2 \tag{C1.7}$$

$$\ln\left(c_2 / c_2^0 x_2\right) = \beta^{\sigma} \left(x_1\right)^2 \tag{C1.8}$$

Solving equations (C1.7) and (C1.8), we get

$$\ln\left[c_2 / c_2^0 \left(1 - x_1\right)\right] = \beta^{\sigma} \left(x_1\right)^2 \tag{C1.9}$$

Therefore, $\beta^{\sigma} = \dfrac{\ln\left(c_1 / c_1^0 x_1\right)}{\left(1 - x_1\right)^2}$ (C1.10)

Also, $\beta^{\sigma} = \dfrac{\ln\left(c_2 / c_2^0 \left(1 - x_1\right)\right)}{\left(x_1\right)^2}$ (C1.11)

Thus, from equations (C1.10) and (C1.11)

$$\frac{\ln\left(c_1 / c_1^0 x_1\right)}{\left(1 - x_1\right)^2} = \frac{\ln\left(c_2 / c_2^0 \left(1 - x_1\right)\right)}{\left(x_1\right)^2} \tag{C1.12}$$

Therefore, $\dfrac{x_1^2 \ln\left(c_1 / c_1^0 x_1\right)}{\ln\left(c_1 / c_1^0 \left(1 - x_1\right)\right)\left(1 - x_1\right)^2} = 1$ (C1.13)